



Deliverable No. D2.2

Scenario based user needs and requirements

Grant Agreement No.: 600841
 Deliverable No.: D2.2
 Deliverable Name: Scenario based user needs and requirements
 Contractual Submission Date: 30/11/2013
 Actual Submission Date: 12/01/2014

Dissemination Level		
PU	Public	X
PP	Restricted to other programme participants (including the Commission Services)	
RE	Restricted to a group specified by the consortium (including the Commission Services)	
CO	Confidential, only for members of the consortium (including the Commission Services)	

COVER AND CONTROL PAGE OF DOCUMENT	
Project Acronym:	CHIC
Project Full Name:	Computational Horizons In Cancer (CHIC): Developing Meta- and Hyper-Multiscale Models and Repositories for In Silico Oncology
Deliverable No.:	D2.2
Document name:	Scenario based user needs and requirements
Nature (R, P, D, O) ¹	R
Dissemination Level (PU, PP, RE, CO) ²	PU
Version:	1.0
Actual Submission Date:	12/01/2014
Editor: Institution: E-Mail:	Norbert Graf USAAR graf@uks.eu

ABSTRACT:

This deliverable describes the initial versions of the use cases and scenarios that will be developed for the different cancer domains of the project. These scenarios and use cases are clinically driven to guarantee their translation and usage in clinical care. According to results of previous projects they are categorized according to different levels of usage. The lowest level contains basic scenarios and use cases that can be integrated in different other and more complex scenarios, e.g. roles and rights, pseudonymization, etc. Many of these basic scenarios are already described and corresponding tools are available. This deliverable list such tools and analyses them for their usability in CHIC. On the higher levels all scenarios are composed of basic scenarios. This approach is already part of p-medicine and will be adapted to this project. In summary all developed models and tools will be as granular and modular as possible and provide standardized, open interfaces and functionality descriptions (e.g. via something similar to WSDL (Web Services Description Language)), so that a user can easily build new models as a composition of existing hypomodels. Such an approach guarantees the re-use of already developed tools and models and avoids rebuilding of tools and models from scratch. This will be cost and time effective.

KEYWORD LIST:

User needs, requirements, scenarios, use cases, granularity, modularity, standardization, models, tools

¹ R=Report, P=Prototype, D=Demonstrator, O=Other

² PU=Public, PP=Restricted to other programme participants (including the Commission Services), RE=Restricted to a group specified by the consortium (including the Commission Services), CO=Confidential, only for members of the consortium (including the Commission Services)

The research leading to these results has received funding from the European Community's Seventh Framework Programme (FP7/2007-2013) under grant agreement n° 600841.

The author is solely responsible for its content, it does not represent the opinion of the European Community and the Community is not responsible for any use that might be made of data appearing therein.

MODIFICATION CONTROL			
Version	Date	Status	Author
0.1	16/09/2013	Draft	Norbert Graf
0.2	29/09/2013	Draft	Norbert Graf
0.3	11/10/2013	Draft	Norbert Graf
0.4	24/10/2013	Draft	Norbert Graf
0.5	03/11/2013	Draft	Norbert Graf
0.6	07/11/2013	Draft	Norbert Graf
0.7	21/11/2013	Draft	Norbert Graf
0.8	01/12/2013	Draft	Norbert Graf
0.9	03/12/2013	Draft	Norbert Graf
1.0	12/01/2014	Final	Norbert Graf

List of contributors

- Norbert Graf, USAAR
- Eckart Meese, USAAR
- Rainer Bohle, USAAR
- Georgios Stamatakos, ICCS
- Marco Viceconti, USFD
- Kostas Marias, FORTH
- Caterina Guiot, Unito
- Domenico Gabriele, Unito
- Stefaan van Gool, Leuven
- Lien Solie, Leuven
- Sofie van Cauter, Leuven
- Joost Dejaegher, Leuven
- Elias Neri, Custodix
- Bernard de Bono, UCL
- Helen Byrne, Oxford

Contents

1	EXECUTIVE SUMMARY	7
	PERSPECTIVES ON USER NEEDS AND REQUIREMENTS	8
2	INTRODUCTION	9
2.1	PURPOSE OF THIS DOCUMENT.....	9
2.2	DEFINITIONS AND CONVENTIONS USED IN CHIC	13
2.3	THE HALLMARKS OF CANCER.....	14
2.4	INTRACELLULAR SIGNALLING NETWORKS	16
2.5	THE HETEROGENEITY OF A TUMOUR.....	17
3	REPRESENTATIVE CANCER MODELS SPANNING ALL MAJOR SPATIOTEMPORAL SCALES OF BIOLOGICAL COMPLEXITY.....	18
3.1	INTRODUCTION TO REPRESENTATIVE CANCER MODELS	18
4	SCENARIOS LEADING TO HYPERMODELS – GENERAL ASPECTS	19
4.1	INTRODUCTION.....	19
4.2	IT MODELS	20
4.3	SECURITY MODELS.....	20
4.4	MODELS DEALING WITH SEMANTIC INTEROPERABILITY	24
4.5	STANDARDIZATION OF INTERFACES	24
5	SCENARIOS FOR NEPHROBLASTOMA	25
5.1	INTRODUCTION AND DESCRIPTION OF THE SCENARIO	25
5.2	AVAILABLE DATA AND POST-PROCESSING OF DATA	25
5.3	GRANULAR DISSECTION OF THE NEPHROBLASTOMA SCENARIO.....	39
5.4	HYPERMODEL FOR NEPHROBLASTOMA	41
5.5	ADVANCED NEPHROBLASTOMA SCENARIO	41
6	SCENARIOS FOR GLIOBLASTOMA	46
6.1	INTRODUCTION AND DESCRIPTION OF THE SCENARIO	46
6.2	INTRODUCTION AND DESCRIPTION OF THE SCENARIO	46
6.3	AVAILABLE DATA AND POST-PROCESSING OF DATA	47
6.4	GRANULAR DISSECTION OF THE GLIOBLASTOMA SCENARIO.....	54
6.5	HYPERMODEL FOR GLIOBLASTOMA	57
7	SCENARIOS FOR NON-SMALL-CELL LUNG CANCER (NSCLC).....	58
7.1	INTRODUCTION AND DESCRIPTION OF THE SCENARIO	58
7.2	AVAILABLE DATA AND POST-PROCESSING OF DATA	58
7.3	GRANULAR DISSECTION OF THE SCENARIO	60
7.4	HYPERMODEL FOR NSCLC.....	61
8	SCENARIOS FOR PROSTATE CANCER	62
8.1	INTRODUCTION AND DESCRIPTION OF THE SCENARIO	62
8.2	AVAILABLE DATA AND POST-PROCESSING OF DATA	63
8.3	GRANULAR DISSECTION OF THE SCENARIO	67
8.4	HYPERMODEL FOR PROSTATE CANCER	69
9	A BRIEF OUTLINE OF THE HYPERMODELS FOR NEPHROBLASTOMA, LUNG CANCER AND GLIOBLASTOMA MULTIFORME TO BE DEVELOPED BY CHIC.....	71
10	STRATEGY OF THE CHIC PROJECT FROM THE CLINICAL PERSPECTIVE: BRIDGING CLINICAL FEATURES TO MOLECULAR MECHANISMS	74
11	CONCLUSION	76
12	REFERENCES	77
	APPENDIX 1 – ABBREVIATIONS AND ACRONYMS	85
	APPENDIX 2 – ETHICAL APPROVALS	88
	NEPHROBLASTOMA AND NON-SMALL CELL LUNG CANCER SCENARIO	88

GLIOBLASTOMA SCENARIO	89
PROSTATE CANCER SCENARIO	90
APPENDIX 3 - REPRESENTATIVE CANCER MODELS SPANNING ALL MAJOR SPATIOTEMPORAL SCALES OF BIOLOGICAL COMPLEXITY	92
CANCER MODELS THAT DO EXIST	92
CANCER MODELS THAT DO NOT EXIST.....	129

1 Executive Summary

The main objective of this deliverable is to elaborate the user needs and requirements for the proposed CHIC's infrastructure. By concluding that understanding the end users is the key to success, 'D2.2 Scenario based user needs and requirements' appears to be one of the most important topics of the CHIC project. It will have a deep impact on the proposed activities and research strategies during the runtime of the project. In order to ensure clinical relevance and foster clinical acceptance of hypermodelling in the future, the whole endeavor is driven by the clinical partners of the consortium and compatibility with VPH theme is guaranteed.

The CHIC infrastructure aims to deliver a state of the art technological platform in order to facilitate the development of a suite of tools, services and a secure infrastructure that will support accessibility and reusability of VPH mathematical and computational hypermodels. Developing robust, producible, interoperable and collaborative hypermodels of diseases and normal physiology is a sine qua non necessity if rational, coherent and comprehensive exploitation of the invaluable information hidden within human multiscale biological data is envisaged. The project's technical solution is to embrace the current and future web and its technologies and build its architecture under the tenets of the Service Oriented design. The advantages/requirements, mentioned in the project description, are:

- **Ubiquitous availability** (“anywhere, anytime, any device”) enables mobility, easiness of use, and low cost access and use of the platform;
- **Collaboration** - social networking and other “Web2.0” features are inherent qualities of the proposed solution to allow the building of virtual communities of users to promote interactivity, research, and education;
- **Software as a Service (SaaS)** - central registration and on demand availability of software tools to healthcare professionals and researchers enable the provision of software as a commodity while strengthening interoperability and standardisation of the shared code base.

Cancer hypermodels to be collaboratively developed by the consortium cancer modelers will provide the framework for the development of the CHIC technologies. Clinical adaptation and partial clinical validation of hypermodels and hypermodel oncosimulators will be undertaken in an iterative way. Everything is based on three different layers:

- A multiscale biology layer
- An engineering layer or design layer
- A software layer

The proposed/envisaged CHIC technological platform features are a hypermodelling infrastructure consisting primarily of:

- A hypermodelling editor and a hypermodelling execution environment
- An infrastructure for semantic metadata management
- A hypermodel repository
- A hypermodel-driven clinical data repository
- A distributed metadata repository
- An in silico trial repository for the storage of executed simulation scenarios
- Semantically annotated multiscale models and data generated by using ontological and annotation tools
- An image processing and visualization toolkit and
- Cloud and virtualization services

The CHIC tools, services, infrastructure and repositories will provide the community with a collaborative interface for exchanging knowledge and sharing work in an effective and standardized way. A number of open source features and tools will enhance usability and accessibility. State-of-the-art security and data protection are regarded as a sine qua non.

Perspectives on user needs and requirements

The CHIC platform has different and complex user needs and requirements and in order to overcome the complexity of the proposed project's goals. All scenario based user needs and requirements have been aligned according to three main pillars:

- A technological perspective;
- An end users' perspective;
- A clinical/medical perspective.

The technological perspective on user needs and requirements will have an important impact on the requirements of the CHIC project. Nevertheless it needs to be flexible enough to deal with the 'End users needs and requirements' perspective as well as the 'Clinical/Medical' perspective.

This deliverable will focus exclusively on the perspectives of End Users and the Clinical/Medical perspective. The linkage to the Technological perspectives is underlined and described whenever needed.

2 Introduction

2.1 Purpose of this document

This document defines and describes the scenario based user needs and requirements for the CHIC project. This challenging task of the CHIC project will be executed in an iterative way. From a technological perspective the project is based on three layers. These are:

- A multiscale biology layer
- An engineering layer
- A software layer

The multiscale biology layer forms the biological basis for the models and hypermodels starting from the molecular level, to the cellular, to the tissue, to the organ, to the body up to the epidemiological level taking into account the biological time constraints. The engineering layer is concerned with the interaction between different models. It can also be called a design layer. All models or components are simple and basic. From these models or components more complex hypermodels are built. The software layer is where the models are programmed. The software development process and progress will follow the following steps:

- Requirements
- Design
- Implementation
- Verification
- Maintenance

In practice there is feedback between the three layers, such feedback being needed to optimize the hypermodels in an iterative manner as depicted in the following figure.

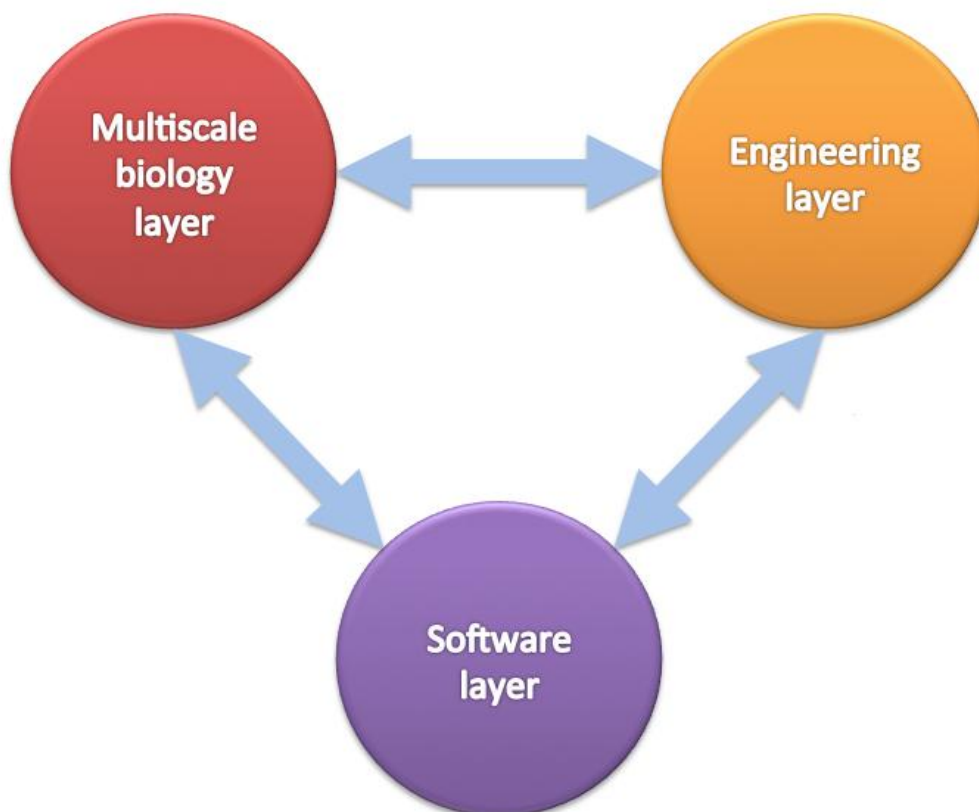


Fig 2.1: Interaction between the different layers as part of an iterative process to optimize the hypermodels

The implementation requirements proposed below are designed to assure the development of a functional and state-of-the art system:

- Software as a Service (SaaS)
- Interoperability
- Flexibility
- Modularity
- Security and granular access for end users
- Social networking frames

Conceptually, requirements analysis involves three types of activity:

- **Requirements gathering:** the task of communicating with users to determine what their requirements are.
- **Analysing requirements:** determining whether the stated requirements are complete, implementable, ambiguous, or contradictory, and then resolving these issues.
- **Recording requirements:** Requirements might be documented in various forms, such as natural-language documents, use cases/scenario, user stories, or process specifications.

Requirements analysis in the frames of the CHIC project is a continuous and iterative process due to the complexity of the technological platform and its modular infrastructure. Nevertheless, the main focus will be on recording scenarios and user needs and user requirements. Project contributors will employ several techniques to elicit the requirements and user needs. In general, this included activities as holding interviews, or requirements workshops, meetings and telephone conferences and creating requirements lists in the form of 'use cases/scenario' as well as continuous scientific literature reviews. At later stages and according to the elaborated 'use cases/scenario' project activities will focus on prototyping.

As already described in p-medicine most important for the architecture is the mentioned modularity of the system. All developed software, tools and services should be as granular and modular as possible and provide standardized, open interfaces and functionality descriptions (e.g. via something similar to WSDL (Web Services Description Language)), so that a user can easily build new models as a composition of existing granular tools. As an example one needs only once to develop a tool that will link gene expression data of a tumour with the KEGG database. If this tool is as generic as possible and if the interface between the gene expression data and the KEGG database is standardized one will be able to use this tool in different settings and models, independent of the underlying tumour or disease. Such an approach needs to standardize interfaces between different tools and between tools and data. A description of such specifications needs to be done, so that the different research groups can standardize their data and establish what preconditions are needed to run such composed models. It is important that for each granular tool a standardized interface to data be defined. The developed models will then be able to be used in scenarios.

The development of the architecture for CHIC needs to take interoperability issues into account. This includes also semantic interoperability of data. A model will process input data to produce a result. Such a result with its output data might be input data for another model thus going from simple models to hypermodels. For that purpose a categorization of models into four different levels as already proposed in p-medicine is helpful:

1. Level for fundamental tools
2. Level for basic tools
3. Level for modular tools
4. Level for domain specific tools

Fundamental tools are those that are fundamental for the architecture. This level includes mainly IT-tools that can be used in all models. The basic level will contain only such tools that are domain and scenario unspecific, e.g. pseudonymization tool, curation tool for data. Modular tools are scenario specific but not domain specific, e.g. a tool for patient empowerment. At a higher level, tools, models and services are domain specific. Fundamental and basic tools can be re-used in different scenarios and domains. For this purpose interoperability and standardization is of utmost importance to avoid building each tool again and again from scratch.

According to the classification of tools, scenarios will be classified in the following levels (fig. 2.2):

1. Technical scenarios
2. Basic scenarios
3. Domain unspecific scenarios
4. Domain specific scenarios
5. Hypermodel scenarios

Technical scenarios are part of other scenarios including basic scenarios. Domain unspecific scenarios can be composed of basic scenarios and will be able to be used in domain specific scenarios. By doing so, scenarios do not need to be developed from scratch and it will foster the development of standards and interoperability. If interoperability and standards are developed the integration of external scenarios into the CHIC framework is possible.

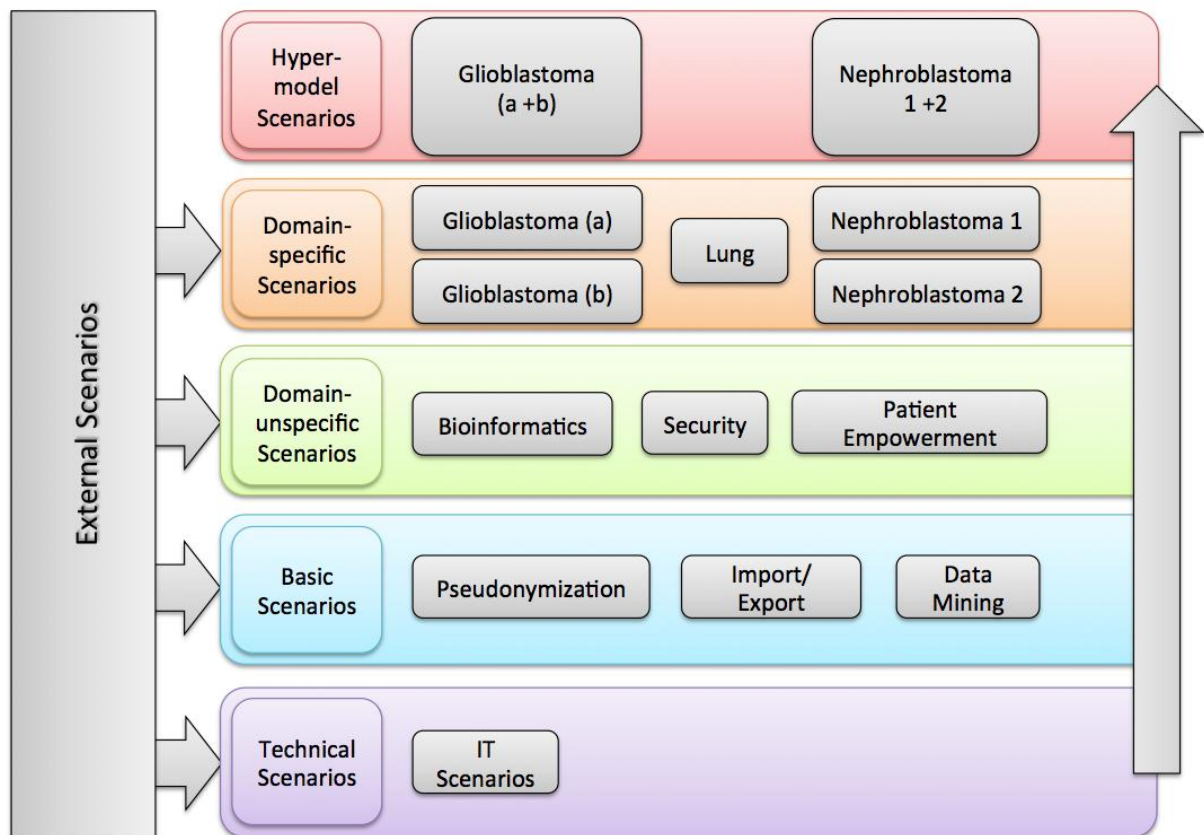


Fig. 2.2: Levels of scenarios giving examples on all levels. Interoperability and standards will allow the integration of external scenarios

Each scenario needs to be translated into a use case via iteration between clinicians and all other stakeholders involved in the project. This needs to be an iterative process and should include the search for re-usable tools that are already available. The construction of such a modular architecture, with tools and models categorized into different levels, is a major factor contributing to the sustainability of the architecture beyond the funding period of CHIC.

The development of tools and models has to be done in several steps. The backbone of all tools, models and services is a systems biology approach. Therefore, in a first step, end-user driven use cases must be defined in terms of clinically driven scenarios. These use cases form the basis for tool development. Before the programming of a tool, a mock-up will be made and evaluated by end-users using fake data (fig. 2.3). In order to evaluate a tool a test bed needs to be set up where retrospective data will be used. This test bed (including tools and data) will be fixed to allow repeated runs of the tools. If the tools are used in clinical settings with prospective data a test bed with the legal framework for prospective data will be set up allowing the curation and update of the data. This test bed will be named “clinbed”. The tools used in this clinbed are validated and will be certified. This approach to development is in accordance with the extremely successful procedures developed within p-medicine.

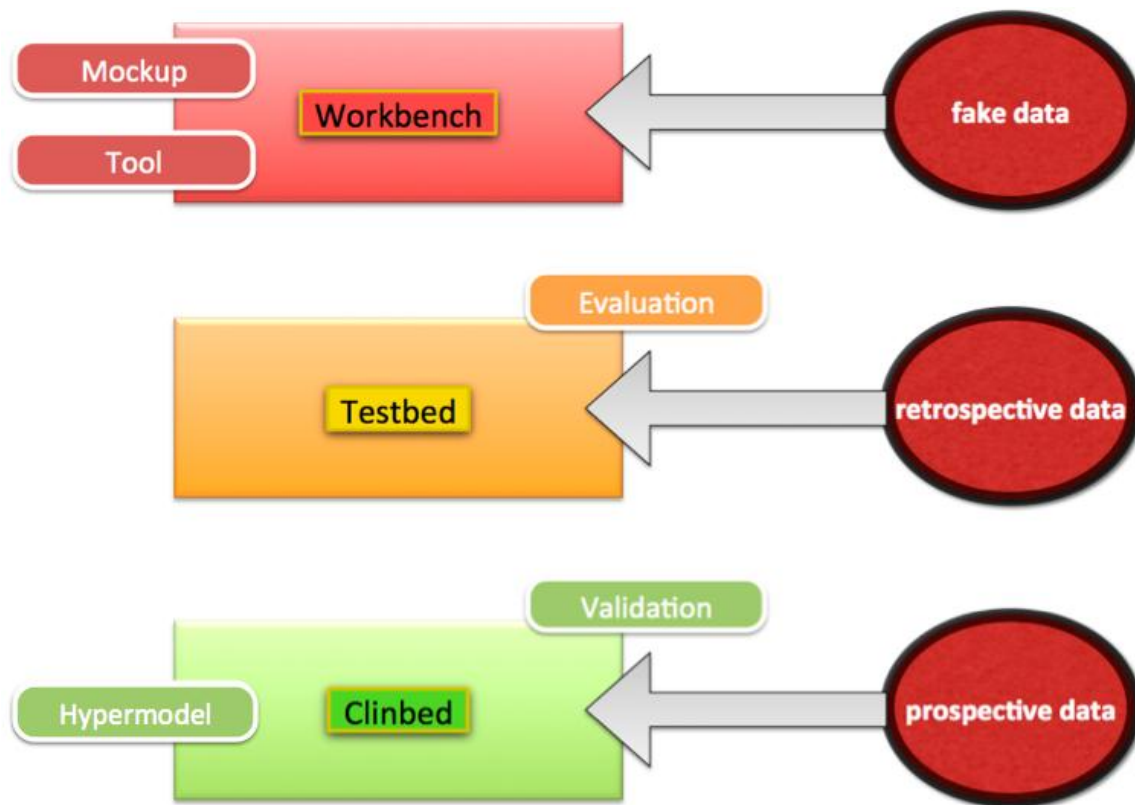


Fig. 2.3: The hierarchy of the architecture for developing tools from workbench, to testbed to clinbed.

The roles and rights management system regulates those data and tools, services and models an end-user can access and use.

Of high importance for the architecture of the CHIC platform is to facilitate data exchange with other health care systems in accordance with the legal framework. Otherwise it will become an “information island” that contains different patients’ data sets, isolated from other information about the patients, with limited access and value. As a result, the CHIC platform should interoperate with other systems throughout the entire health and clinical studies information environment.

At a minimum, CHIC should export anonymized data to, and import-export data from other systems in a standardized (and interoperable) way. To provide interoperability, the CHIC platform should support from its inception communications, messaging, and content encoding standards as other health information systems (HIS) like EHR.

2.2 Definitions and conventions used in CHIC

In the following chapter several definitions are given that the CHIC consortium has agreed upon. These definitions are important for the different stakeholders within the project to understand each other.

Atomic and other scale models: The term atomic is used in CHIC only for atomic scale models that means for models that deal with the interactions of atoms such as during drug-protein interactions. They include basically Newtonian interactions (mass attraction) and Coulomb charges attraction or repulsion and are frequently simulated using Molecular Dynamics (MD) (like the (Drug) Binding Affinity Calculator (BAC)). The potential energy used in MD is a set of force field functions and parameters derived from both experimental work and high-level quantum mechanical calculations. Therefore, an atomic scale model could be either a hypomodel if it is used as a component of e.g. a molecular network model or even (in a purely theoretical context) as a hypermodel if it is viewed as composed of subatomic level models such as quark models. This is an extreme case for biological modeling. Here the quantum mechanical approach, or QM/MM (for which the 2013 Nobel prize in Chemistry was awarded), should be preferable as a hypermodel, or even better "multiscale models for complex chemical systems", as stated in the Nobel Prize 2013 citation.

Atomic or other scale models are not to be used as generic terms as are the terms hypomodel (or component model) or hypermodel (or composite model). An atomic model is seen as a model on the atomic scale. This leads to the definition of molecular models, cellular models, tissue models and body models or even epidemiological models. Such models are representing the different scales of models of space and/or time. Here different scales of space are used to define atomic or molecular models. The same can be done using different time scales. An atomic model simulating Newtonian interactions will run in another time scale than a cellular model, where e.g. mitosis is simulated.

Elementary Model: An elementary model in CHIC is any model that has been designed, implemented (and possibly tested) to work as a single unit, regardless if it is a single-scale, single biological process or multi-scale/biological process model.

Hypomodel or Component Model: This is a generic term for a model that is not composed of other models. Several hypomodels or component models can be linked to form a hypermodel.

Hypermodel or Composite Model: A hypermodel is a composition of component models. It can be defined as an orchestration of Remote Procedure Calls (RPCs).

In the CHIC project we assume that every atomic model can be exposed as a Remote Procedure Call (RPC); the most common type of RPC nowadays are Web Services, but this term is specifically associated with given implementation details, such as the use of SOAP for messaging, and the use of WSDL for machine-readable description of the service. Since in some particular cases the computational constraints might impose alternative implementation choices we use this term as more generic.

In general it is possible that each RPC is associated to a uniform resource identifier (URI), which can be annotated with a large and complex set of metadata. When we compose component models into a hypermodel, it is possible to imagine that some of these metadata are used to provide machine-readable instructions on the composition of such component models, for example checking that the

inputs types of the second models are compatible with the output types of the first. It is also possible to imagine that an automated registry is maintained, where all available component models are listed.

However, specific implementation details might prevent to realize this hypermodelling architecture by using exclusively Web Services (and all associated paraphernalia of standards such as WSDL and UDDI) and Software-As-A-Service (SaaS) approaches (that imply a completely cloudified implementation). Two concrete examples coming from experiences in past projects that practically prevent a complete cloudification of the hypermodelling infrastructure are:

1. the difficulty of transporting large binary objects with SOAP, and
2. the ties of software and hardware (related to execution specs or trivially to licensing mechanisms for commercial software)

In this sense terms such as WSDL and SaaS used in this deliverable should not be intended literally, but as conceptual paradigms that will be implemented whenever possible with widely accepted industrial standards such as WSDL, but that in some cases might impose non-standard implementations dictated by the computational constraints that multiscale models frequently impose. In certain cases coupling models (hardwiring them together) makes much more sense than integrating them through a linking tool (e.g. an electromechanical heart tissue model).

2.3 The Hallmarks of Cancer

Hanahan and Weinberg [1] proposed in 2000 that the diversity of cancer and its underlying molecular mechanisms can be explained by six biological processes:

1. sustaining proliferative signalling,
2. evading growth suppressors,
3. resisting cell death,
4. enabling replicative immortality,
5. inducing angiogenesis and
6. activating invasion and metastasis,

To these processes, four biological processes were added in 2011 [2]:

7. genome instability and mutation,
8. tumour-promoting inflammation,
9. deregulating cellular energetics and
10. avoiding immune destruction [2].

Together these molecular and cellular changes may explain the development of cancer from normal cells and are called the ‘Hallmarks of Cancer’. Figure 2.4 gives a graphical description of these hallmarks [2]. The concept of ‘Hallmarks of cancer’ is a powerful guide for translational research not only for drug development but also for early detection and the development of new and more targeted therapies that have fewer side effects and enhance the quality of life of cancer patients.

The following main bullets underline the complex molecular nature of cancer [3]:

1. Cancer cells must acquire modifications in most of the 10 hallmarks if they are to develop and evolve towards a malignant, invasive state. This requires functional changes in multiple pathways.
2. Only stem and progenitor cells with a high plasticity may be able to sustain a coordinated perturbation of these different hallmarks.

3. Only a fraction of cells within a lesion can progress towards invasion and metastasis.
4. Cancer development involves interactions between cancer cells and their microenvironment, including inflammation and immune responses.

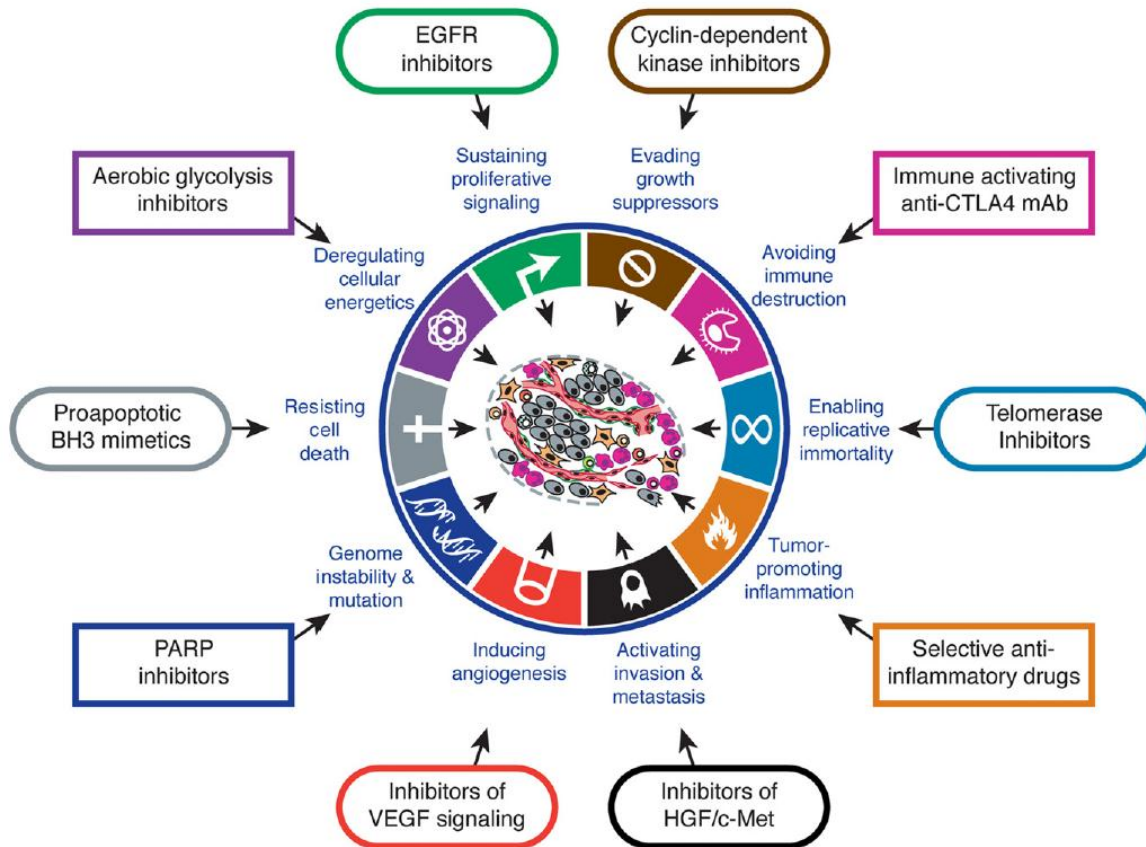


Fig. 2.4: The Hallmarks of Cancer (copied from [2]).

To gain success with better treatments one needs to take these hallmarks into consideration. All 10 hallmarks can be addressed by different treatment options as depicted in figure 2.4 and summarised in the following list:

- | | |
|--|--------------------------------------|
| 1. sustaining proliferative signalling | → EGFR inhibitors |
| 2. evading growth suppressors | → Cyclin-dependent kinase inhibitors |
| 3. resisting cell death, | → Proapoptotic BH3 mimetics |
| 4. enabling replicative immortality | → Telomerase inhibitors |
| 5. inducing angiogenesis | → Inhibitors of VEGF signaling |
| 6. activating invasion and metastasis | → Inhibitors of HGF/c-Met |
| 7. genome instability and mutation | → PARP inhibitors |
| 8. tumour-promoting inflammation | → Selective anti-inflammatory drugs |
| 9. deregulating cellular energetics | → Aerobic glycolysis inhibitors |
| 10. avoiding immune destruction | → Immune activating anti-CTLA4 mAb |

These 10 hallmarks underline the need to build granular models that can be linked to hypermodels. Each hallmark involves multiple steps that occur across diverse spatiotemporal scales. Equally

different hallmarks have steps occurring at the same spatiotemporal scale. For each step or spatiotemporal scale a model might be developed resulting in hypermodels related to these hallmarks. Combining all these hypermodels to a new hypermodel and getting input data from a single patient to all the different hypomodels one might be able to best describe the cancer of this patient, as such a hypermodel would simulate all biological processes that are thought to be of relevance for cancer development and treatment.

2.4 Intracellular Signalling Networks

Intracellular signalling networks regulate the operations of normal cells as well as of cancer cells. These integrated circuits are reprogrammed and affect the regulation of those hallmarks described in cancer cells [2]. The orchestration of separate sub-circuits, depicted in differently colored fields [2], is different compared to normal cells changing the crosstalk between sub-circuits. In addition signals from the microenvironment including different cell types do interact with the cancer cell and do influence the way these subunits perform [2].

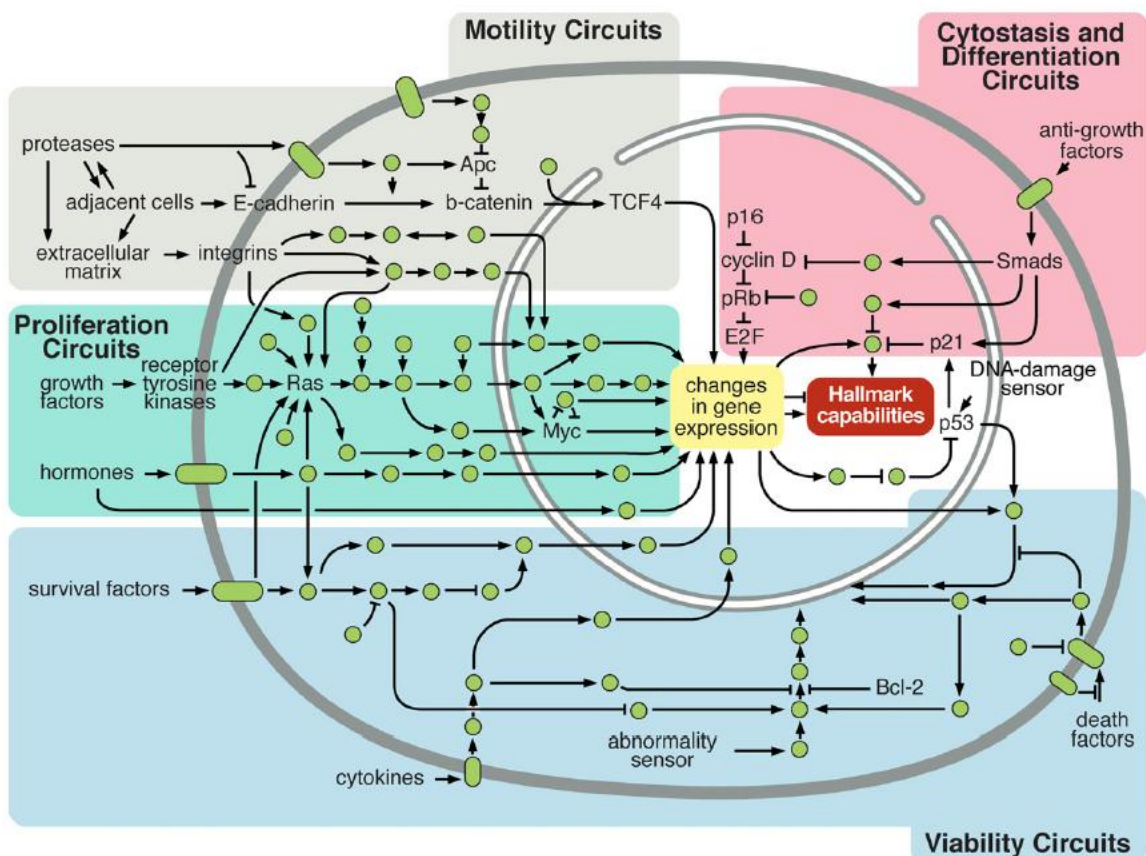


Fig. 2.5: Intracellular signalling networks in cancer cells (copied from [2]).

To simulate the behaviour of cancer cells the intracellular signalling network and the interaction of cancer cells with the microenvironment needs to be modelled. Each of the sub-circuits as well as the interaction with the microenvironment can serve as a component model that is regarded as a model on the molecular scale. A hypermodel of a cancer cell build from these component models will be up-scaled to the cellular level. Such a hypermodel, representing one cancer cell, can serve again as a component model, as many of these component models will build a hypermodel of a tumor on the tissue scale. Modelling the interaction of the tumor with body components like the immune or

endocrine system will put such a hypermodel on the body scale. One can even start modelling at the atomic level, if the interaction of a drug with a cellular receptor is simulated on the drug protein level, where basically Newtonian interactions (mass attraction) and Coulomb charges attraction are simulated. As such a component model will have impact on the molecular sub-circuit of a cell a sub-circuit can be regarded as a hypermodel if several atomic models are linked together simulating their influence on the sub-circuit. In conclusion, depending on the granularity of scenarios a model can serve as a component model as well as a hypermodel.

2.5 The heterogeneity of a tumour

In addition to the above-described hallmarks of cancer the heterogeneity of a single cancer in a single patients is a further challenge in the research area. By collecting biological specimen from a tumour, one can question how representative a tiny piece of biomaterial that is taken for research is for the whole tumor to be analysed. Missing representation will produce non-reproducible data. If they are entered into a model, the output of the model cannot be correct. This is enhanced by different analytical methods if one collects data from different laboratories or if different analytical systems are used for molecular biological methods. The reproducibility of experiments and resulting data for input in models is of utmost importance in this context. Figure 2.6 highlights different areas of reproducibility.

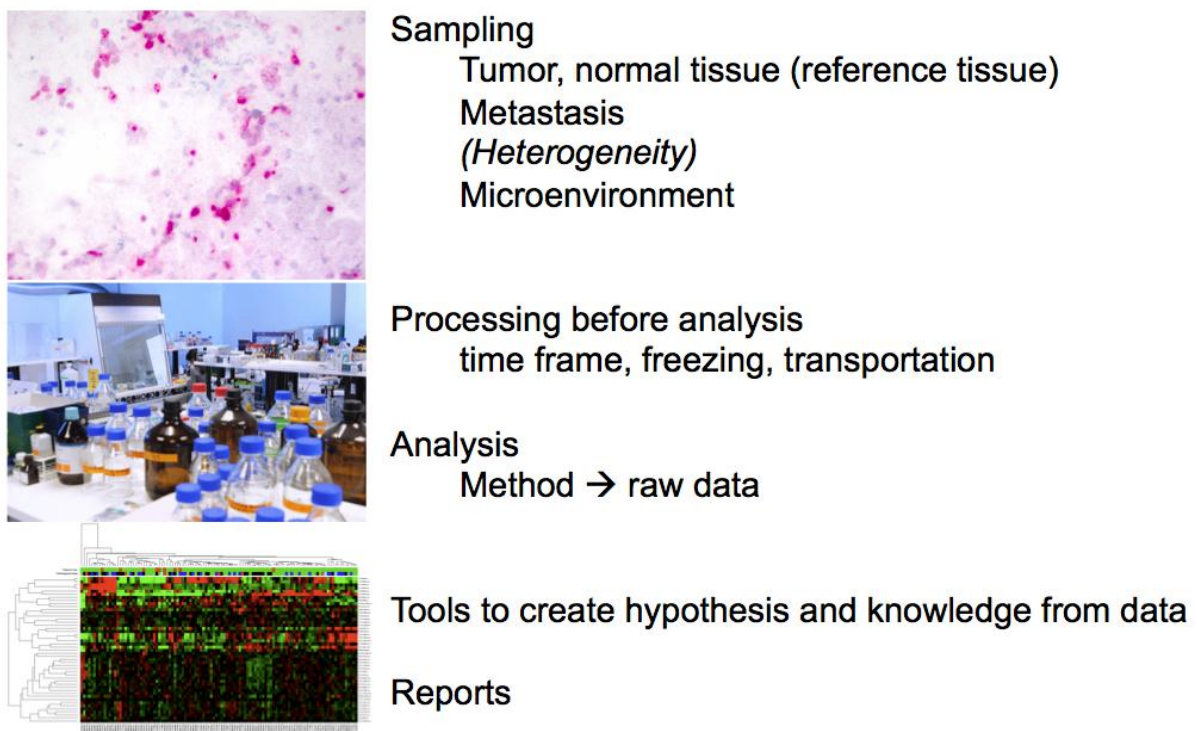


Fig. 2.6: Factors that influence the reproducibility of molecular genetic data.

3 Representative cancer models spanning all major spatiotemporal scales of biological complexity

3.1 Introduction to representative cancer models

Technical partners of the CHIC project collected representative cancer models within WP6. This section lists these models and ranks them according to clinical relevance. The technical details of these models (input parameters, output parameters, software requirements and hardware requirements) are described in detail in Deliverable 6.1 (Cancer hypomodelling and hypermodelling strategies and initial component models). Part of this deliverable is also to select those models that can be reused in the clinical scenarios that are described for the different cancer domains in this deliverable. This will also influence the ranking of these models. According to availability of the models they can be classified in two groups:

1. those that already exist and
2. those that need to be developed within the CHIC project.

Appendix 3 lists these representative cancer models. In the 2 tables the colour in the first row indicates the clinical relevance of the model. Three different categories are defined:

1. Implement in first phase as test case (highly relevant)
2. Implement later in the project (relevant)
3. Implement only if time permits (less relevant)

Category 1 is indicated in green, 2 in yellow and 3 is not highlighted.

4 Scenarios leading to hypermodels – General aspects

4.1 Introduction

This section describes from a clinical perspective how hypermodels will be developed within CHIC. Each scenario starts with a question that is relevant for clinicians. These questions need to be as easy as possible but also addressing a complicated or complex phenomenon that cannot be answered by current medical practice. The goal of a hypermodel will be to give a validated answer to clinicians that will provide them with better treatment options for individual patients.

To be successful in the development of hypermodels many iterative steps need to be done during the developmental process. It is important to understand that from an architectural perspective a hypermodel is always a composition of different component models. Even hypermodels themselves can serve as component models for other hypermodels as shown in fig. 4.1. Each model needs input data for processing resulting in output data that will get input data for other models. In that way hypermodels are composed. At the end the hypermodel will give a result, which is the answer of the initial asked question.

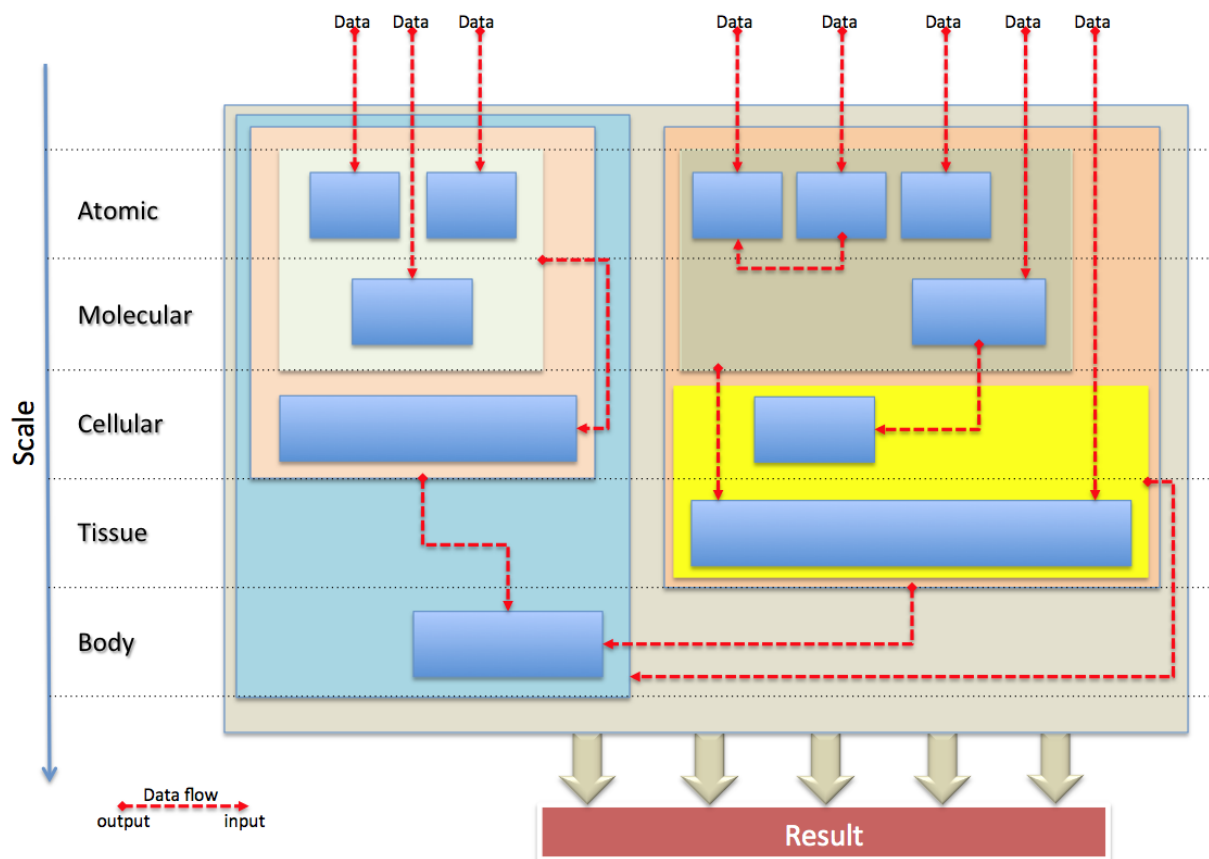


Fig. 4.1: Schematic representation of a hypermodel, composed of different models. Component models can be linked to composite models that by themselves can serve as component models for other hypermodels.

It is agreed that for each cancer domain, a single question will be answered by a hypermodel composed of different models including hypermodels themselves.

The steps during the developmental process are:

1. Description of the question as a scenario that is understood by the whole consortium
2. Dissection of the scenario into granular components that will be described as single use cases and be categorized into those levels described in chapter 2.1 in this document
3. Each use case will form the basis of a component model
4. Search for re-usable and existing models
5. The composition/linkage of all component models will build the hypermodel
6. For each existing (component) model testing of usability needs to be done
7. For each non-existing component model a mock-up will be build in an iterative way by starting an interactive evaluation process regarding usability, robustness and reproducibility
8. Definition of the data that are needed for each component model. This includes:
 - a. Data security and safety according to the legal and ethical framework of CHIC
 - b. Data availability
9. Evaluation of the hypermodel regarding usability, robustness and reproducibility
10. Validation of the hypermodel with prospective data
11. Certification of the hypermodel. This step is not part of the CHIC project.

In Appendix 3 relevant, existing cancer models are listed and ranked according to relevance. In addition in chapter 3.2 models are listed that are under development and of relevance for the CHIC project. All models of chapter 3 are categorized according to the scale at which they act: the atomic, molecular, cellular and whole body scales. In addition tools are needed that serve as component models and fulfil the general functionalities needed for (hyper-)models. These are IT tools that define the architecture, security tools like pseudonymization and/or anonymization tools and tools dealing with semantic interoperability. All these tools are needed for each (hyper-)model and they should be generalized and reusable for all developed (hyper-)models within the CHIC project. Last but not least the question of standardization of interfaces needs to be addressed to simplify the linkage of component models to build a hypermodel.

4.2 IT models

At a basic level IT tools are part of all hypermodels. These include tools for setting up an IT infrastructure, to store and share heterogeneous data and to process these data. In this setting tools for security and interoperability are also needed.

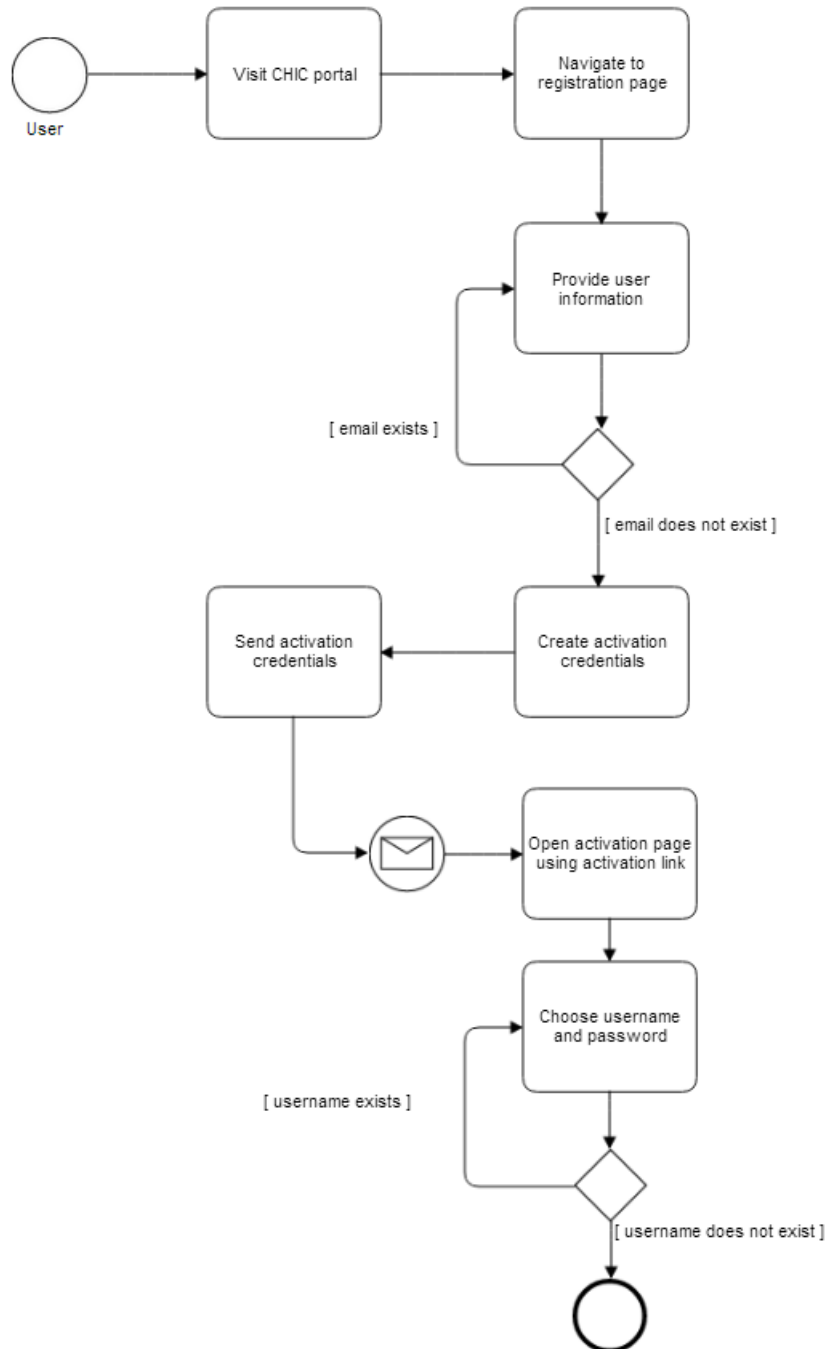
4.3 Security models

All human users, including patients, physicians, researchers and administrators, need a registered account before access can be granted to tools or data within the CHIC platform. Based on the identity (authentication) of a user, the security framework should evaluate the access control policies governing the CHIC resources (authorization). In other words, a user must prove their identity to the platform before they can access the CHIC tools and data.

The CHIC Identity or Token Provider is the entry point on which the user authenticates by proving his/her identity through username/password credentials. Once authenticated, the identity provider issues an identity assertion that can then be used by the end user to proof his identity to all services within CHIC. Based on this assertion, identity decisions can then be taken by the security framework whether the identified user has access to the requested resource.

4.3.1 CHIC Authentication & SSO Scenario

This scenario describes the flow in which a user is able to access a CHIC service through e.g. the CHIC portal.

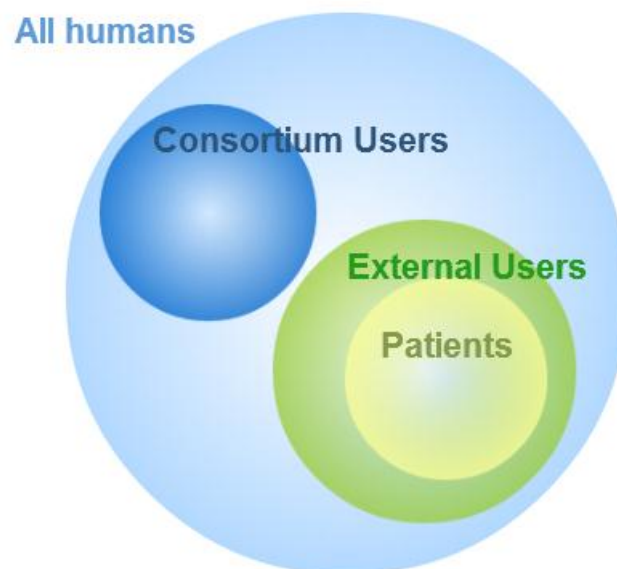


1. User A surfs to the CHIC portal. Since the user is not authenticated yet, the user is redirected to the CHIC identity provider (IDP).
2. The IDP shows an authentication form in which a user can enter its username and password.
3. The username and password are checked against the username and password in the identity store.

4. If username and password are correct the IDP queries the identity store for identity attributes, and other attribute providers for extra information on the authenticated user. The IDP creates an identity token.
5. The user is redirected back to the portal providing the identity token. User A has access to the portal and all accessible portlets and links.
6. User A is still authenticated on the portal but wished to access another CHIC service (Service B) in a second browser tab. The user visits Service B where he is not yet authenticated.
7. The user is redirected to the IdP.
8. As the user has an open session with the IdP, not authentication credentials are requested, but instead the user is immediately redirected to service B passing the user’s identity token.
9. The user is now authenticated on service B.

4.3.2 User Registration

Users registering on the CHIC framework can be subdivided into two or three main classes: consortium users, external users and possibly patients. Each of these user classes have different registration, authentication and authorization flows.



1. **Consortium users** are part of an organization which is a registered partner of CHIC e.g. USAAR, UCL ... Each partner organization is responsible for the registration and management of their users. A user administrator is thus assigned to each organization. User management is done through the CHIC Identity Management Portal.
2. **External users**, users that are not within one of the consortium partners, might also need access to some of CHIC’s tools or results. External users must register using a public CHIC registration link. Since there is no trust between an unknown user and the CHIC framework, publicly registered users have limited access. Afterwards a CHIC user administrator can grant the user more access, given that the administrator trusts the user’s identity.
3. **Patients** are a “special” kind of external user as patients could get access to their own sensitive data. No decision has yet been taken though on whether patients would directly get access to the CHIC platform.

4.3.2.1 External User Registration Scenario

External users register themselves by going to the CHIC public registration page (1). Once the registration form has been submitted (2) the user will receive an activation mail (3). Through the activation link in this email the user can activate his account by choosing a username, password (4). Through the activation the user's email address is confirmed. During the activation process the user should also validate his account details and choose a security question and answer. These can then later be used for account recovery.

Note that a user will only have limited access until a CHIC user administrator approves the user and gives him access rights.

4.3.2.2 Consortium User Registration Scenario

Consortium users on the other hand do not register themselves, but are instead registered by their consortium's organization administrators. After registration they also receive an activation mail.

As organization administrators know their personnel, new consortium users are implicitly approved during registration.

4.3.2.3 Credential recovery

When a user loses or forgets his/her username and/or password the credential must be recovered.

4.3.2.3.1 Username recovery

1. On the CHIC portal there is a link "Forgot Username". Clicking this link takes the user to the username recovery page.
2. There the user must provide the email address the user was registered with.
3. If the email address exists in the identity store, all the active usernames linked to this email address are sent.

4.3.2.3.2 Password recovery

1. On the CHIC portal there is a link "Forgot Password". Clicking this link takes the user to the password recovery page of the IDM.
2. The user must provide his/her active username.
3. If the username exists the user will be posed the security question. If the submitted answer is correct a recovery link is sent to the user.
4. Using the received recovery mail, the user can open the recovery page in which the user can choose a new password.

4.3.2.4 Integration with Third Party Identity Providers

From a user point of view, one of the biggest disadvantages to username-password credentials is the need to remember yet another username and secure (preferably random) password. Although the credential recovery flow is user friendly and quite straightforward, new users may be reluctant to participate because they need yet another set of username and password.

A user friendly solution to this would be to integrate the CHIC security framework with large third-party identity providers such as Gmail, Facebook ... CHIC accounts could thus be linked to the accounts of other identity systems, which would allow a user to authenticate making use of the username and password they use daily.

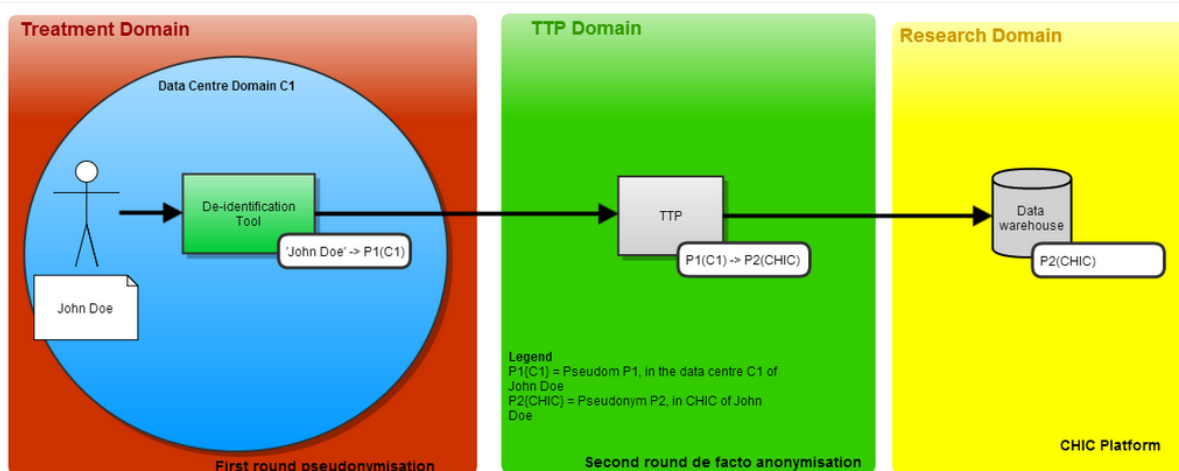
Many of those public identity providers though allow for easy password recovery. It is for example quite easy to take over the Facebook account of someone you know through password recovery. This

poses potential security breaches. This risk must be further investigated and evaluated during the CHIC project.

4.3.3 De-Identification and Upload of data into the CHIC platform

As described in D4.1 “Initial analysis of the ethical and legal requirements for sharing of data” data exporters are responsible for de-identifying their data before uploading it to the CHIC research domain. To achieve this, data exporters should export their data locally in a transferrable format such as CSV, XML, DICOM. Once exported, the data can be de-identified locally at the data source through a de-identification tool. CHIC will provide a standard compliant implementation. Once de-identified the data should be uploaded through the CHIC Trusted Third Party (TTP) into the CHIC Data Warehouse.

The TTP is responsible for a second round pseudonymisation so that it is not possible anymore to go back from the CHIC patient pseudonym to the original patient without intervention of the TTP.



4.4 Models dealing with semantic interoperability

This task is elaborated in WP8 and WP10 of the CHIXC project and will be described in detail in the corresponding deliverables

4.5 Standardization of interfaces

Standardization of interfaces is essential to build hypermodels. Mainly WPs 8, 9 and 10 address this issue. Details are given in corresponding deliverables of these WPs.

5 Scenarios for Nephroblastoma

5.1 Introduction and description of the scenario

The most important question to be answered by the hypermodel for nephroblastoma is the following:

Will the nephroblastoma of a patient shrink in response to preoperative chemotherapy?

The answer to this question should be 'yes' or 'no'. Shrinkage is determined by using imaging studies to measure the change in tumor volume. If the tumor volume is less than 75% of the initial tumor volume then the answer to the question is 'yes'. If there is an increase of more than 25 % in tumor volume after preoperative chemotherapy then the answer will be 'no'. If the tumor volume is between 75% and 125% of the volume before preoperative chemotherapy then the tumor volume is regarded as unchanged and therefore the answer is 'no' as well.

This question is of importance as all patients diagnosed with a kidney tumor between the ages of 6 months and 16 years will receive preoperative chemotherapy within the SIOP (International Society of Paediatric Oncology) protocol, if imaging studies suggest nephroblastoma as the most probable diagnosis. Chemotherapeutic treatment is currently based solely on imaging studies without histologically proven diagnosis. The reason to start with preoperative chemotherapy is the fact that 90% of tumors do shrink, making surgical removal of the nephroblastoma easier and resulting in downstaging of the tumor with less postoperative treatment. However in about 10% of patients the tumor will not shrink but increase in size. Such behaviour results in a worse situation for the patient that should be avoided. At present it is not possible to predict which tumors will shrink and which will not. By collecting all available data of a patient with nephroblastoma at the time of diagnosis the response to preoperative chemotherapy can hopefully be simulated with these data. If the developed model will predict the correct answer to the above described question patients will benefit from such an approach by applying them the best treatment right from the time of diagnosis. Physicians will only believe such a model if the results of the simulations are validated. Therefore this model needs to be developed with retrospective data and validated with prospective data in an iterative process.

The hypermodel for nephroblastoma will be an advanced oncosimulator simulating the response of chemotherapy on nephroblastoma in the computer (in silico).

5.2 Available data and post-processing of data

5.2.1 Available data

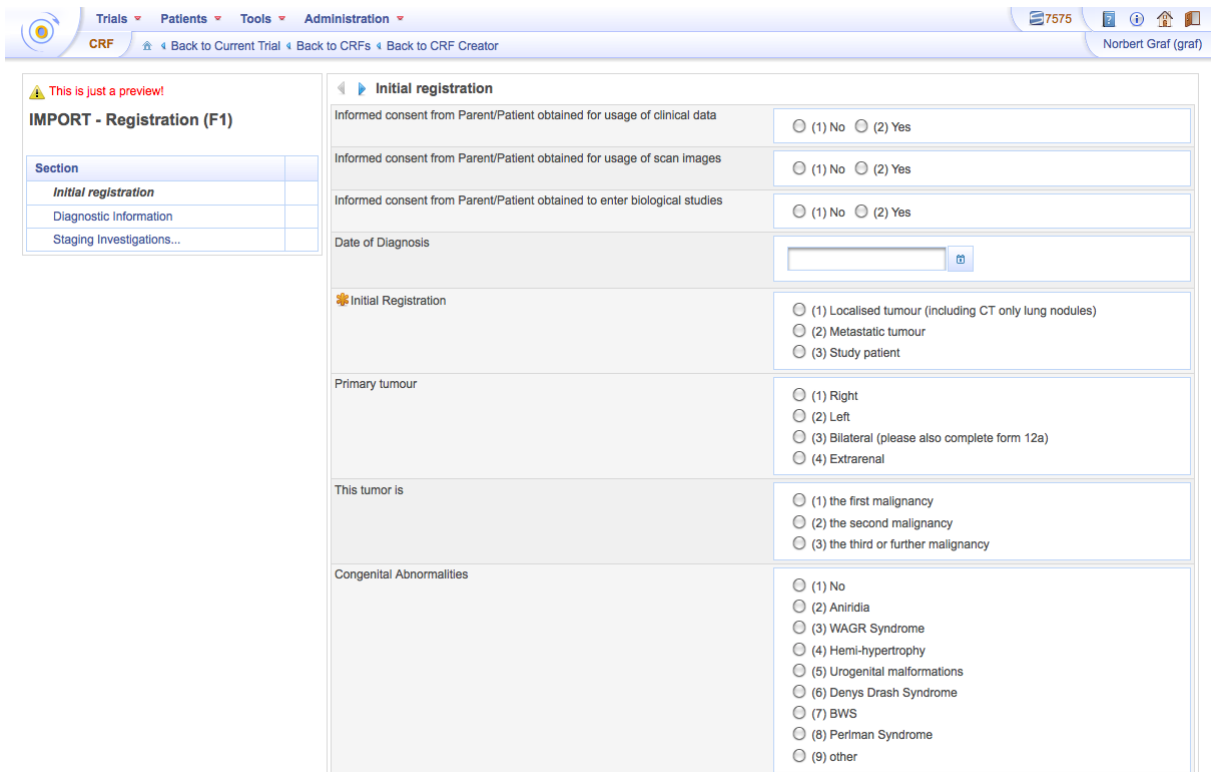
There will be retrospective and prospective data available for the nephroblastoma scenario. The retrospective data are data that are collected within the SIOP 2001/GPOH trial. For these data ethical approval is already available (Ethik-Kommission der Ärztekammer des Saarlandes Kenn-Nr.: 104/10 from 19th of August 2013; see also Appendix 2). The prospective data will be collected within the next prospective SIOP trial for nephroblastoma that is just under development. For this trial new informed consents including the usage of data within the CHIC project will be written and ethical approval obtained. In CHIC we will only use data of patients with unilateral nephroblastoma without metastasis who received pre-operative chemotherapy. All data will only be shared and used according to the legal framework of CHIC. Within this framework the data can be regarded as de-facto anonymous data.

All data besides the imaging data will be collected within ObTiMA³ that is further developed in the CHIC project. ObTiMA is a data management application for clinical trials that is GCP compliant. The imaging data will be available from a DICOM server that is established in the p-medicine project.

The following data will be available for the nephroblastoma scenario:

Clinical data:

The clinical data include data as age, gender, date of diagnosis, date of chemotherapy, date of surgery, date of irradiation, date of end of treatment, dates of follow-up visits, date of relapse, kind of relapse, date of death, reason for death, kind of treatment (including chemotherapeutic drugs, irradiation, surgery), symptoms, genetic predisposition syndromes (like Beckwith-Wiedemann syndrome, WAGR syndrome (**W**ilms Tumor, **A**niridia, **U**rogenital malformations, **R**etardation), Perlman syndrome, etc.), Tumor size at the time of diagnosis, tumor size after preoperative chemotherapy. These data are primarily stored in CRFs of ObTiMA of the corresponding trials. They are stored in ObTiMA in an encrypted way and all personal data pseudonymized. Before usage is possible in CHIC a second pseudonymization is done via a trusted third party (legal and ethical framework of CHIC). Figure 5.1 shows a CRF in ObTiMA of the nephroblastoma trial.



The screenshot shows the 'Initial registration' section of a CRF. It contains several form fields with radio button options:

- Informed consent from Parent/Patient obtained for usage of clinical data:** (1) No, (2) Yes
- Informed consent from Parent/Patient obtained for usage of scan images:** (1) No, (2) Yes
- Informed consent from Parent/Patient obtained to enter biological studies:** (1) No, (2) Yes
- Date of Diagnosis:** A date input field with a calendar icon.
- Initial Registration:** (1) Localised tumour (including CT only lung nodules), (2) Metastatic tumour, (3) Study patient
- Primary tumour:** (1) Right, (2) Left, (3) Bilateral (please also complete form 12a), (4) Extrarenal
- This tumor is:** (1) the first malignancy, (2) the second malignancy, (3) the third or further malignancy
- Congenital Abnormalities:** (1) No, (2) Aniridia, (3) WAGR Syndrome, (4) Hemi-hypertrophy, (5) Urogenital malformations, (6) Denys Drash Syndrome, (7) BWS, (8) Perlman Syndrome, (9) other

Fig. 5.1: CRF of clinical data within ObTiMA

Data from ObTiMA can be downloaded into the CHIC platform for further usage. During the download process a second pseudonymization via a trusted third party (TTP) is done. The exported data format is according CDISC-ODM⁴. Figure 5.2 shows the download module within ObTiMA.

³ ObTiMA: Ontology based trial management application; <http://obtima.org>

⁴ <http://www.cdisc.org/odm-certification>

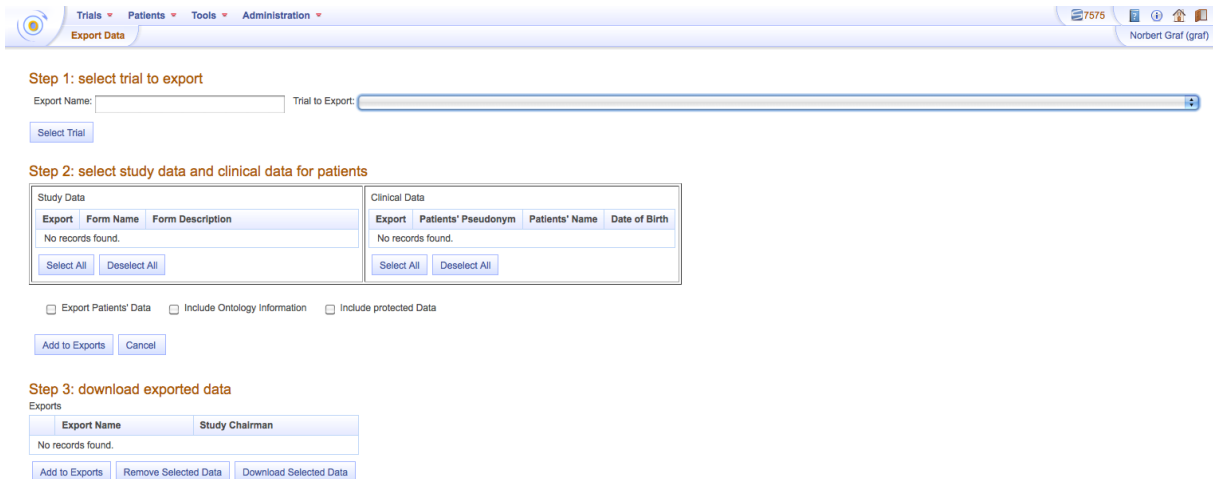


Fig. 5.2: The download module within ObTiMA

Pathological data:

Within SIOP trials patients are primarily treated with pre-operative chemotherapy before they are operated (tumornephrectomy). Pre-operative chemotherapy results in tumor volume shrinkage in about 90% of patients resulting in a so-called down-staging of the tumours. Around 60 % of tumors will be local stage I tumors and the histological subtypes can be used as in vivo response criteria for actinomycin-D and vincristine as the pre-operative given chemotherapeutics. The histological classification is done according to the Stockholm Classification System [4] and shown in figure 5.3.

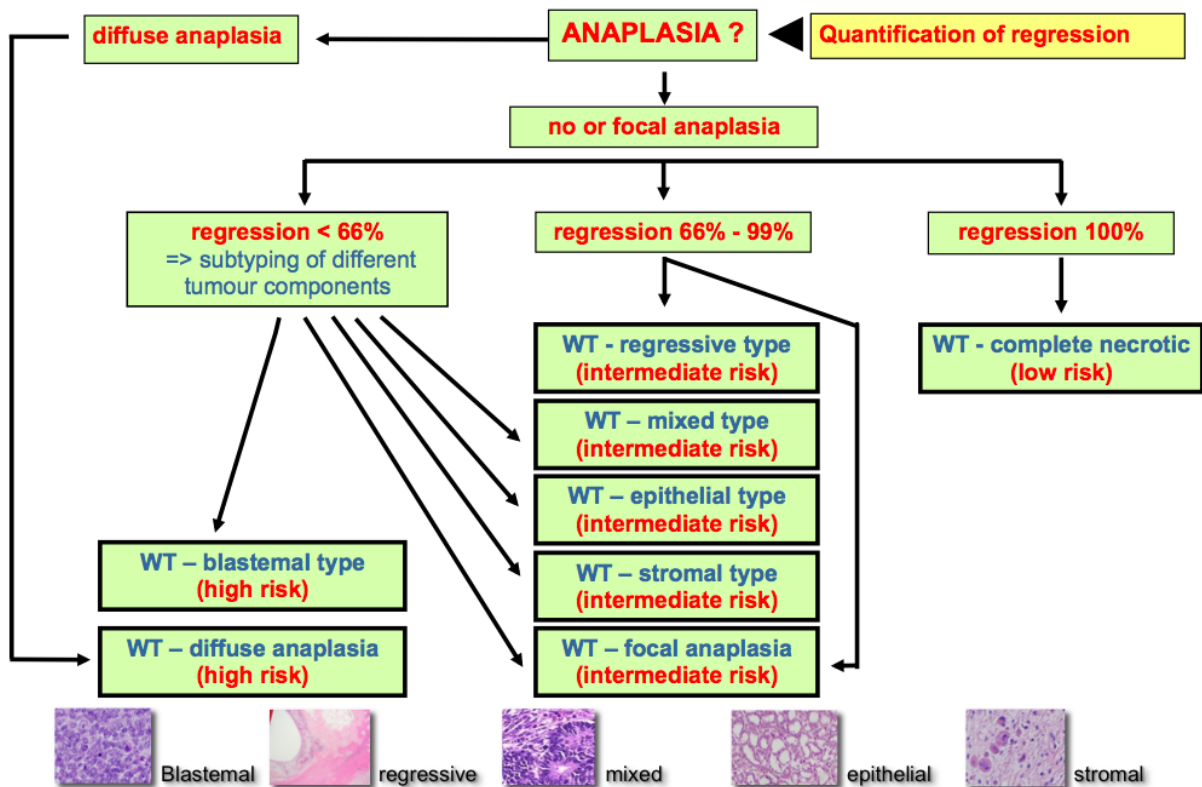


Fig. 5.3: Histological classification of nephroblastoma

Pre-treatment with actinomycin-D and vincristine results in about 5% of completely necrotic tumors showing the optimal response to chemotherapy. If more than 1/3 of the tumor is surviving the tumor is classified according to the most relevant histological component. In case of at least 2/3 of the surviving tumor is blastemal the tumor is recognized as a blastemal subtype with a poor outcome, as the surviving blastemal cells are chemotherapeutic resistant. Besides the blastemal subtype diffuse anaplasia in the tumor is also related with poor outcome. Correlations between histological subtypes of nephroblastoma and specific molecular biological findings are not completely understood. Figure 5.4 shows the current knowledge between histology and molecular biology. There are still 25% of tumors where a corresponding molecular background is unknown. Especially for the blastemal subtype after preoperative chemotherapy a molecular marker needs to be detected. In most of the tumors a single molecular finding is unable to explain the malignant aetiology and behaviour of the tumor.

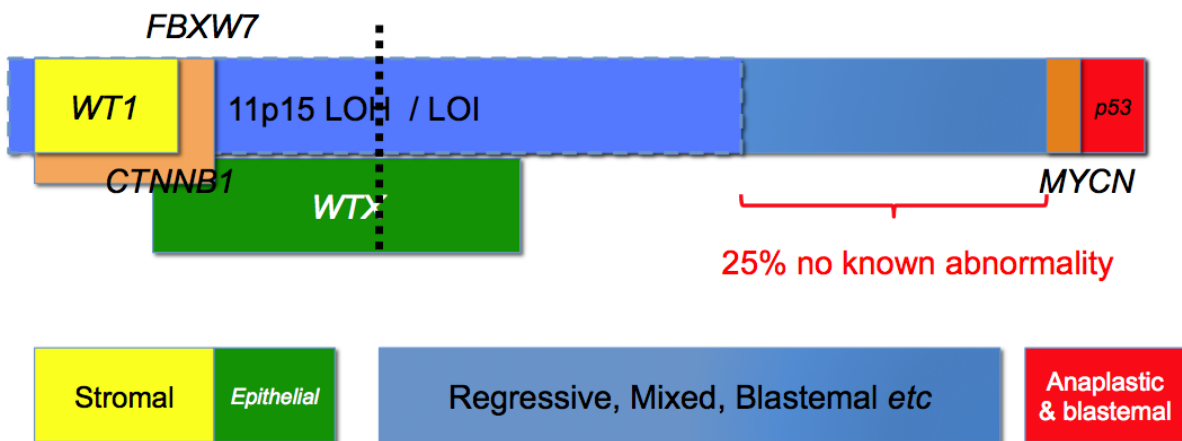


Fig. 5.4: Current knowledge between the histological subtypes of nephroblastoma and molecular biology

Local tumor stage after surgery is an important stratification parameter for postoperative treatment. The local tumor stage is defined as given in Table 5.1. All data that are needed to define the local tumor stage are collected within all SIOP nephroblastoma trials.

Local Stage	Description
I	<ul style="list-style-type: none"> The tumor is limited to the kidney or surrounded with a fibrous pseudocapsule, if outside of the normal contours of the kidney. The renal capsule or pseudocapsule may be infiltrated with the tumor but the tumor does not reach the outer surface, and the tumor is completely resected (resection margins 'clear'). The tumor may be protruding ('bulging') into the pelvic system and 'dipping' into the ureter (but it is not infiltrating their walls). The vessels of the renal sinus are not involved.

	<ul style="list-style-type: none"> • Intrarenal vessel involvement may be present. <ul style="list-style-type: none"> • <i>Fine needle aspiration or percutaneous core needle biopsy ('tru-cut') do not upstage the tumour. The presence of necrotic tumor or chemotherapy induced changes in the renal sinus/hilus fat and/or outside of the kidney should not be regarded as a reason for upstaging a tumour.</i>
II	<ul style="list-style-type: none"> • The tumor extends beyond the kidney or penetrates through the renal capsule and/or fibrous pseudocapsule into perirenal fat but is completely resected (resection margins 'clear'). • The tumor infiltrates the renal sinus and/or invades blood and lymphatic vessels outside the renal parenchyma but is completely resected. • The tumor infiltrates adjacent organs or vena cava but is completely resected.
III	<ul style="list-style-type: none"> • Incomplete excision of the tumor, which extends beyond resection margins (gross or microscopical tumor remains postoperatively). • Any abdominal lymph nodes are involved. • Tumor rupture before or intra-operatively (irrespective of other criteria for staging). • The tumor has penetrated through the peritoneal surface. • Tumor implants are found on the peritoneal surface. • The tumor thrombi present at resection margins of vessels or ureter, transected or removed piecemeal by surgeon. • The tumor has been surgically biopsied (wedge biopsy) prior to preoperative chemotherapy or surgery <ul style="list-style-type: none"> • <i>The presence of necrotic tumor or chemotherapy-induced changes in a lymph node or at the resection margins should be regarded as stage III.</i>

Imaging data:

Imaging studies are done at the time of diagnosis and after preoperative chemotherapy before surgery. These data are pseudonymized and uploaded on a DICOM server that was developed within p-medicine and is used within the nephroblastoma trials of SIOP. Within CHIC MRI images are further deployed. From patients the following modalities are requested: T1, T1 with contrast enhancement, T2 and t2 flair. A typical nephroblastoma of the right kidney is shown in figure 5.5. in MRI (T1 modality) in coronary view.

In addition diffusion weighted images (DWI) and perfusion images will be collected from those patients where these DICOM files are available. They are not routinely done. From all patients the tumor will be rendered and the volume calculated. Further post-processing of data is explained in chapter 5.2.2.



Fig. 5.5: MRI of a typical right sided nephroblastoma. (T1 modality)

Molecular data:

Molecular data will be collected at different time points. At the time of diagnosis and after pre-operative chemotherapy serum and blood from patients with nephroblastoma treated within SIOP trials will be collected and analysed for nephroblastoma autoantibodies and miRNA. From retrospective samples these data are currently analysed to find a pattern of miRNA and autoantibodies that are correlated to the blastemal subtype and/or outcome. This pattern can then prospectively used to correlate the findings of these markers from individual patients with the risk of relapse or the probability of having a blastemal subtype tumor. As the histological diagnosis is only available after tumornephrectomy the knowledge about the possible histology in a single patient at the time of diagnosis would be of utmost importance as this would help to stratify treatment according to the individual outcome as early as possible.

The molecular data of patients will be provided by ObTiMA and the biobanking module that is currently under development in p-medicine. Figure 5.6 shows a part of the CRF of the biobanking module.

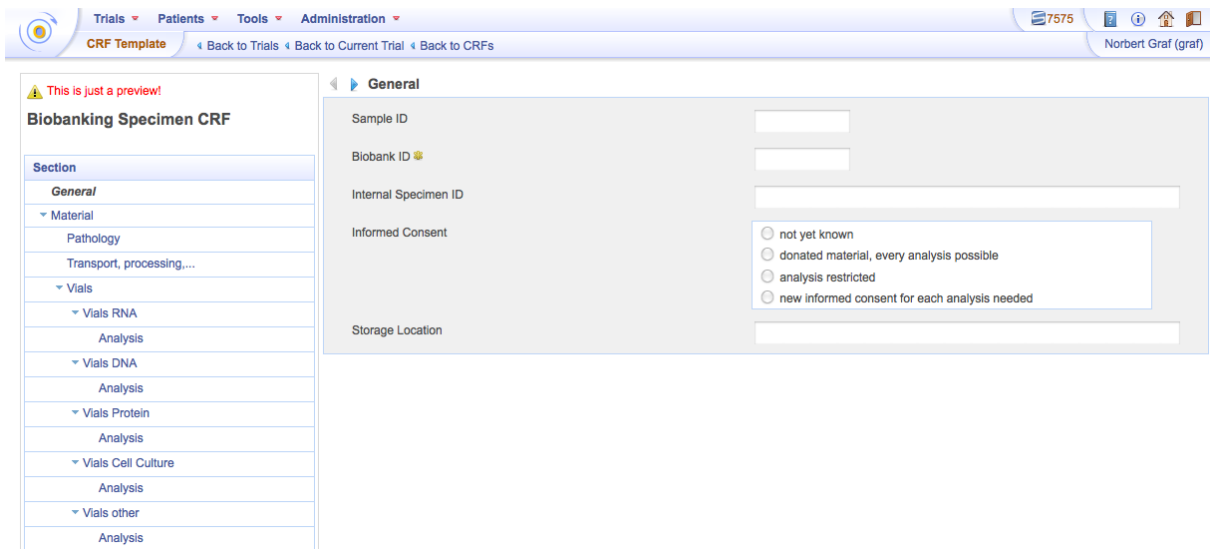


Fig. 5.6: Part of the CRF of the biobanking module of CHIC

Commonly occurring somatic gene mutations in Wilms' tumor are those of *WT1*, *WTX*, *CTNNB1* and *TP53*. Although they may occur single or in combination they are only involved in one third of tumours [5]. *CTNNB1* and *TP53* are a well-established oncogene and a tumour suppressor gene (TSG), respectively, and accumulating data suggest that *WTX* also functions as a TSG [6]. *IGF2* has been mapped to the short arm of chromosome 11p15, which also harbours *WT* susceptible genes, like *WT1*. *WT1* conforms to a TSG label: patients heterozygous for *WT1* germline mutations are predisposed to Wilms' tumor and *WT1* is inactivated in tumours. The WAGR syndrome is caused by a complete deletion of one copy of the Wilms' tumor gene, *WT1* and the adjacent aniridia gene, *PAX6* on chromosome 11p13 [7]. In patients with aniridia this information helps to identify those patients, who are at risk for developing Wilms' tumor, by screening them for the combined deletion of *WT1* and *PAX6*. *WT1* is also involved in the Denys-Drash syndrome (glomerulosclerosis, Wilms' tumor, and ambiguous genitalia) [8] caused by dominant-negative germ line point mutations. A similar constitutional *WT1* splice-site mutation underlies the Frasier syndrome (intersex, nephropathy and gonadal tumors) [9]. It is of interest that in only 5% of Wilms' tumors a constitutional, and in further 10% a sporadic, *WT1* mutation can be found [10]. In those with germ line mutations bilateral Wilms' tumors are more frequent [11]. The *WT1* protein functions as a transcription factor that is clearly critical for normal kidney development. There is a close correlation between *WT1* mutations and the histology of stromal predominant tumors with rhabdomyomatous features [12]. There is also an association between anaplasia in *WT* and *TP53* mutations.

In familial Wilms' tumors, accounting for approximately 1% of patients, there is usually no associated congenital abnormality or predisposition to other tumor types [13, 14, 15]. Genetic linkage studies in different families have localized one gene for familial Wilms' tumor, *FWT1*, to chromosome 17q [16] and another, *FWT2*, to 19q. Further *FWT* genes are waiting for identification, for there are other families known clearly unlinked to any currently identified Wilms' tumor locus [17]. Up to now there is only one genome wide association study ongoing that includes genetic predisposition of *WT* [18].

The latter studies illustrate that a variety of germ line (epi-)genetic aberrations are involved in the development of Wilms tumors. Although a genetic predisposition is described in 9%-17% of the Wilms tumor patients, most Wilms tumors occur sporadically [11, 19, 20]. Today's knowledge about the etiology of Wilms Tumor is given in Figure 5.4 in a schematic overview.

In sporadic Wilms tumors, however, the driving somatic genetic aberrations need to be further unraveled. The CHIC proposal aims to elucidate molecular aberrations by high throughput sequencing and expression analysis as well as by further *in vivo* validation. So far, **genome wide screening for novel molecular aberrations of renal tumours in children using high throughput methods**, which requires joined international forces, **has not been performed on a large scale**. In adult renal tumour studies these efforts have already proven to be successful [21, 22, 23, 24, 25].

In order to ensure clinical relevance, the molecular data will be collected in a way to allow correlation with histological subtypes and / or clinical outcome. For Wilms tumors, pattern of miRNA will be generated and correlated to the blastemal subtype, which in turn is related to the clinical outcome. To ensure comparability between the molecular data of the three selected tumor types, we will generate miRNA pattern for Wilms tumors, lung cancer and glioblastoma using a standardized protocol [26, 27, 28]. This protocol has already been established and tested on various tumor types. The protocol described in detail here, is the same used for lung cancer and glioblastoma. It will not be repeated in the corresponding section of these tumor domains. It includes an experimental and an *in silico* pipeline.

miRNA RNA isolation and microarrays

In detail, the miRNA will be isolated according to the following protocol. Total RNA from tumor tissues will be isolated after phenol/guanidine-based lysis of tumor tissues by silicamembrane-based purification with the miRNeasy Mini Kit (Qiagen). Total RNA from blood will be isolated using our protocol from Leidinger et al. [29], eluted in nuclease-free water and stored at -80 °C. RNA concentration will be measured using NanoDrop 2000 (ThermoScientific) and RNA integrity using the Small RNA kit (Agilent) on a Bioanalyzer 2100. The expression profile of human miRNAs will be determined using SurePrint miRNA microarrays (Agilent) as described by [29]. Hybridization of Cyanine3-labeled miRNA samples to the high-definition arrays will be carried out at 55°C for 20h. Array-chips will be scanned in a high-resolution microarray scanner from Agilent Technologies. Signal intensity values will be extracted from the raw data file using feature extraction software (Agilent Technologies).

Data analysis and classifications

The microarray expression values will be background corrected, log transformed and quantile normalized to account for inter-array effects. Identification of differentially expressed miRNAs will be performed via an unpaired two-tailed t-test. Differential expression will be defined by

- i) at least 2-fold increased or decreased mean expression value and by
- ii) a p-value < 0.05 in t-test.

The resulting p-values will be adjusted for multiple testing according to Benjamini-Hochberg adjustment method [30]. Data samples will be classified using different classification scenarios: First, we will include the entire set of analysed mature miRNAs, and second we will only consider features selected in a prior feature subset selection. In both scenarios, the classifier refers to a support vector machine (SVM) with linear kernel and 20 repetitions of 10 fold cross validation. The applied feature subset selection can be defined a filter method as described by Guyon et al. [31]. Features were ranked according to their p-values in t-test. To assess the performance quality of the classifier, we will calculate mean accuracy, sensitivity and specificity. The complete analysis and classification pipeline will utilize the freely available R software (<http://www.r-project.org/>). The SVM classifier will be based on the R package e1071.

miRNA annotation, target prediction, and Pathway analysis

We will use TAM tool [32] to annotate the significant miRNAs. To obtain the most complete list of targets for these significant miRNAs we will use the miRWalk database (<http://www.ma.uni->

heidelberg.de/apps/zmf/mirwalk/) that allows simultaneous searches of several databases including DIANA-mT, miRanda, miRDB, miRWalk, RNAhybrid, PICTAR4, PICTAR5, PITA, RNA22 and TargetScan.

Pathways putatively regulated by significantly deregulated miRNAs, which will be found by over-representation analysis (ORA). The target prediction will be carried out by means of the online analysis-tool GeneTrail [33, 34], which is a web-based application that analyses gene sets for statistically significant accumulations of genes that belong to functional category relying on common databases like KEGG (Kyoto Encyclopedia of Genes and Genomes), Gene Ontology (GO), TRANSPATH, and TRANSFAC. The in silico analysis tool Gene-Trail is available at (<http://genetrail.bioinf.uni-sb.de>). The P-values for the KEGG pathways will be FDR adjusted and considered significant if smaller than 0.05. A second webservice for pathway analysis is MInePath (<http://minepath.org/>).

Figure 5.7 shows the clustering of the 100 most variable miRNAs. The identified pattern will prospectively be correlated with the findings of the individual patients' prognosis. Ultimately the pattern will help to find disrupted pathways in the tumor and thus stratifying treatment according to the individual outcome or even finding of new drugs targeting disrupted pathways. To this end, it is important to emphasize that the molecular data stem from the same patient as the imaging, the histological and the clinical data.

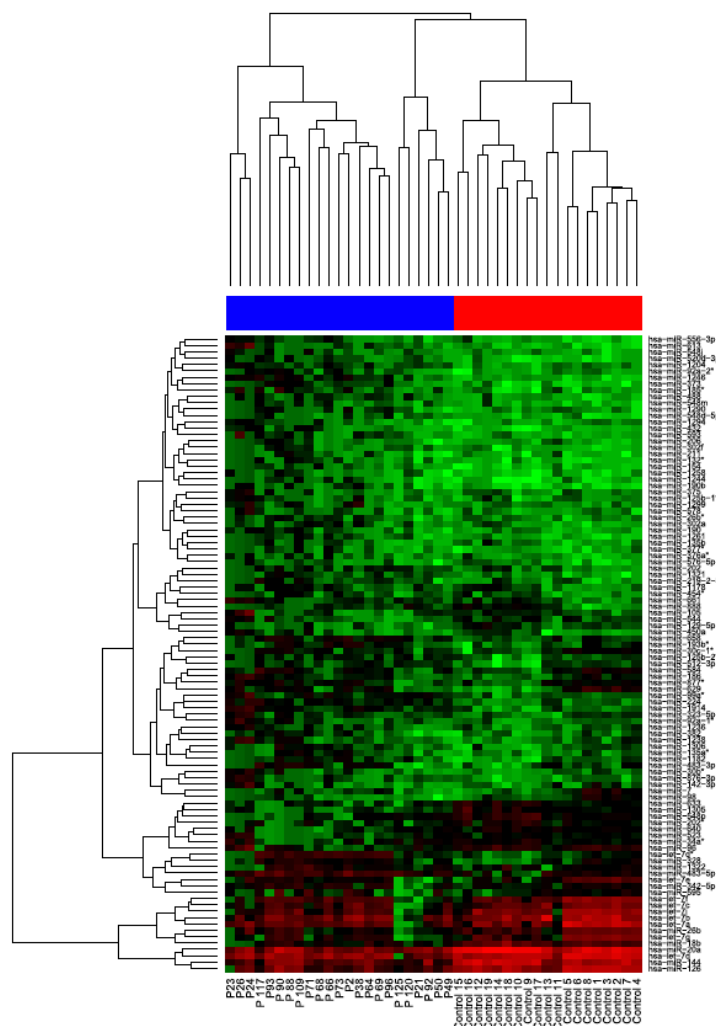


Fig. 5.7: Clustering of the 100 most variable miRNAs in nephroblastoma

5.2.2 Post processing of imaging data

Imaging data will be uploaded on the DICOM server as described above. These images need further processing to calculate the tumor volume, to describe the heterogeneity of the tumor by histograms of signal intensities, to calculate ADC values out of the DWI images and display them on the image of tumor and to calculate the perfusion of different tumor areas. The rendering and segmentation of the tumor, the volume calculation and histograms of signal intensities of the tumor are done with the help of DoctorEye [35] that was developed within the ContraCancrum and the TUMOR projects. Figure 5.8 gives shows the rendering of a nephroblastoma and figure 5.9 the corresponding histogram of the signal intensities.

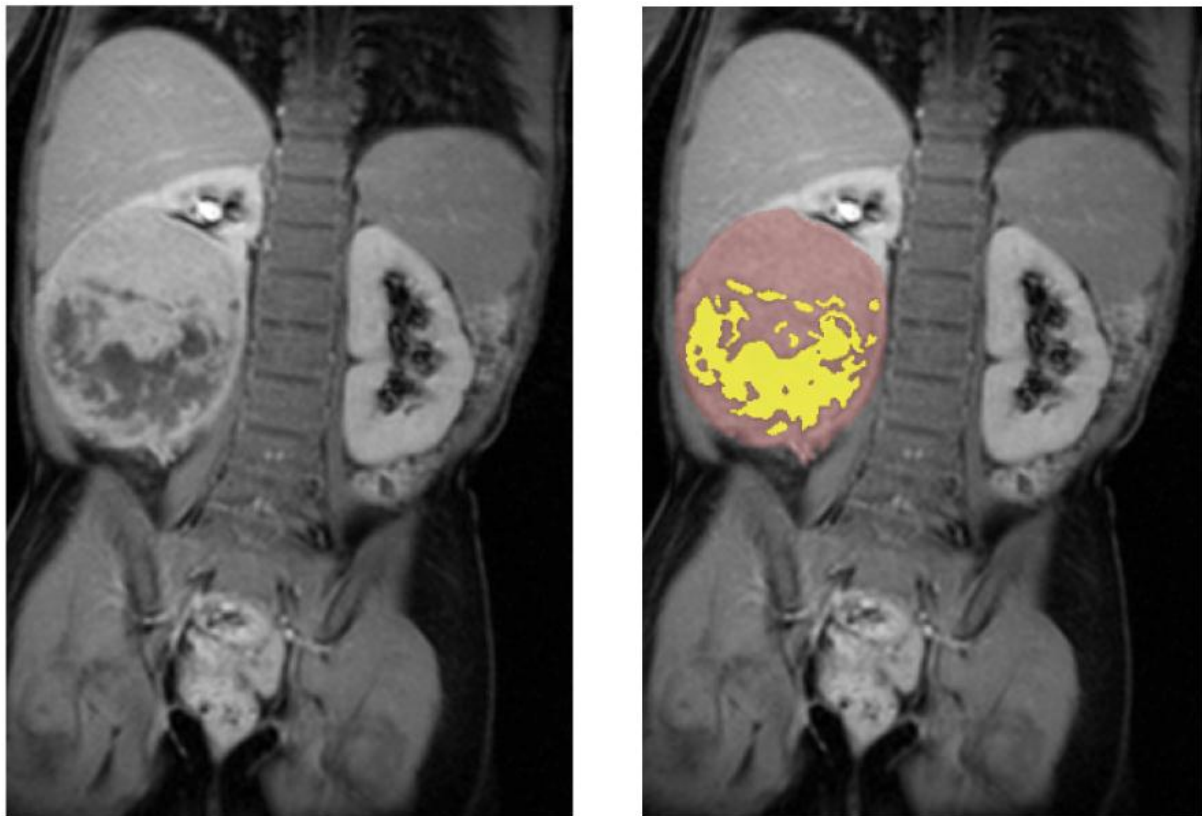


Fig. 5.8: Tumor segmentation and volume calculation using DoctorEye

With the help of DoctorEye the following characteristics of the signal intensity histogram are calculated: Minimum, maximum, mean, median, standard deviation, variance, kurtosis, skewness, harmonic mean and geometric mean.

A high kurtosis distribution (pure leptokurtic distribution) has a sharper *peak* and longer, fatter *tails* than the normal distribution (mesokurtic distribution), while a low kurtosis distribution (pure platykurtic distribution) has a more rounded peak and shorter, thinner tails than a normal distribution. A positive skew indicates that the tail on the right side of the histogram is longer or fatter than on the left side. A negative skew indicates the opposite. A zero value indicates that the tails on both sides of the mean balance out, which is the case in a symmetric distribution of the histogram. Kurtosis and skewness can be used to describe the heterogeneity and the composition of the tumor [36]. The higher the kurtosis value is the tumor can be regarded as more homogeneous. Figure 5.10 is showing this for one patient where the homogeneous area of the tumor is compared with the whole tumor area.

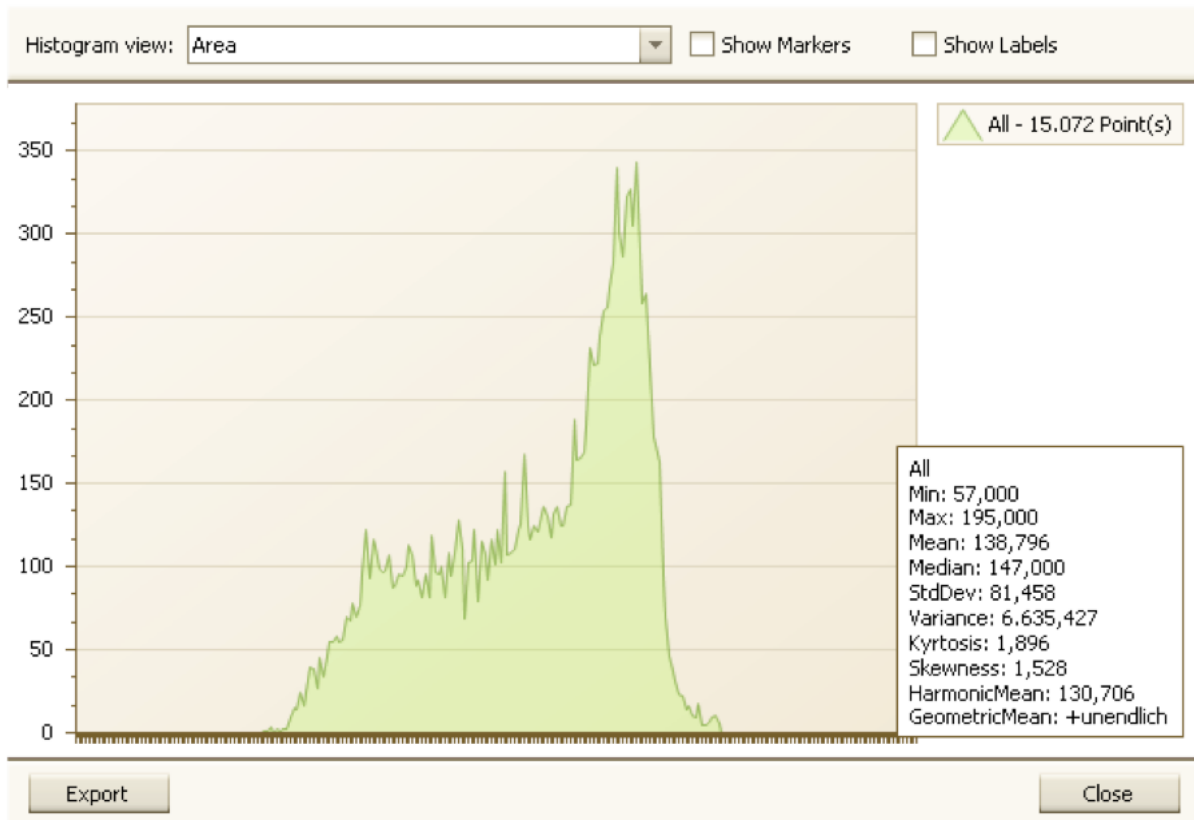


Fig. 5.9: Histogram of signal intensities of the nephroblastoma displayed in figure 5.8. Histogram and calculations are done with DoctorEye.

Skewness in T1 weighted images can be used to describe the composition of the tumor. The more negative a skew is the more high signal intensities are found, the higher a positive skew is the more low signal intensities can be found in the tumor. As low intensities are correlated to necrosis and cysts and high intensities to vital tumor in T1 MRI images skewness is related to the composition of the tumor. In addition the mean and median values as well as the standard deviation of the signal intensities need to be considered to describe the image correctly.

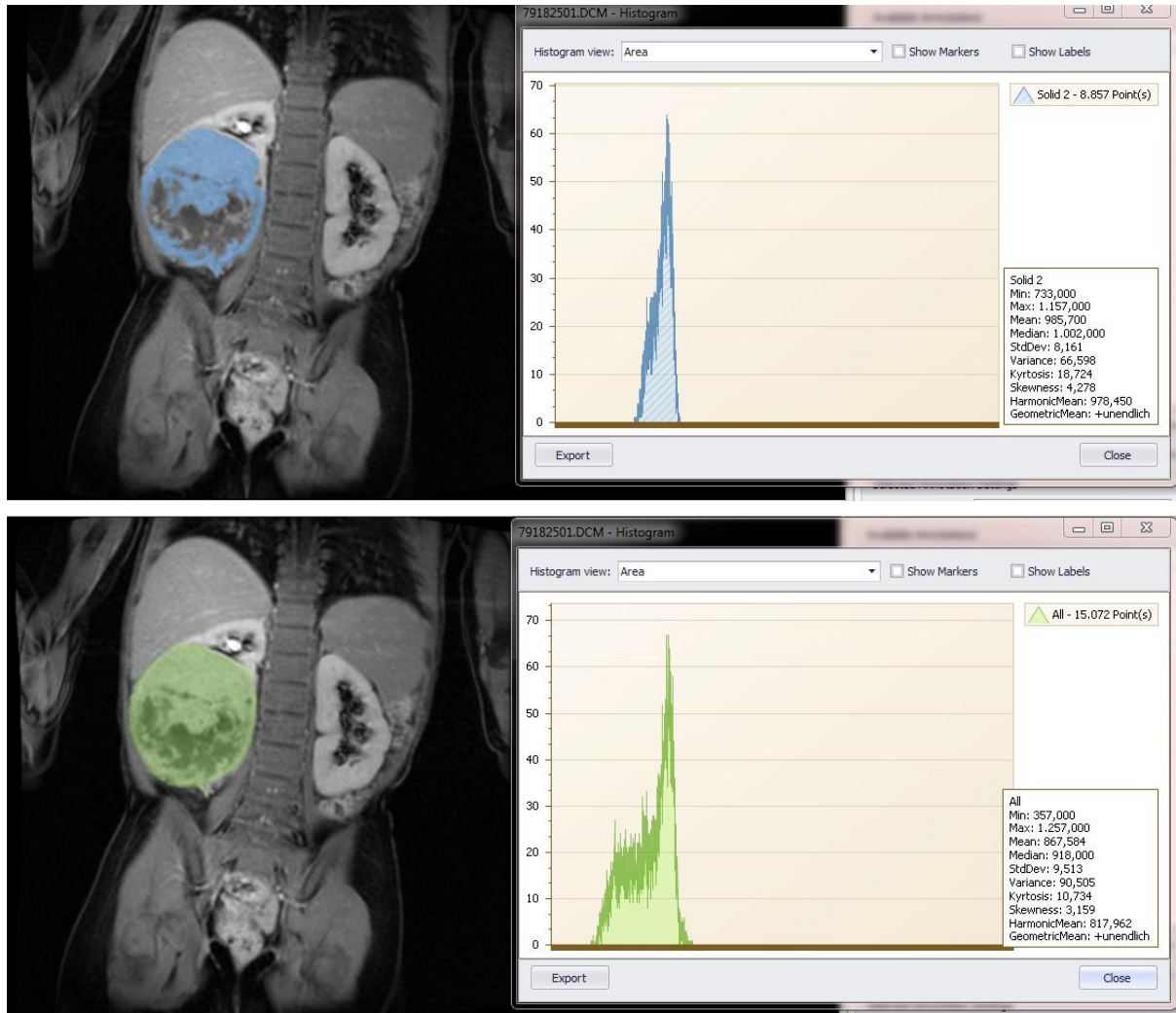


Fig. 5.10: Calculation of kurtosis and other parameters from MRI imaging studies in a patient with nephroblastoma. In the upper image only the area of homogeneous tumor is segmented resulting in a kurtosis value of 18,724 whereas in the second image and segmentation of the whole tumor area the kurtosis value is 10,734.

Diffusion weighted MRI (dMRI) is a magnetic resonance imaging (MRI) method which allows the mapping of the diffusion process of molecules, mainly water, in biological tissues, in vivo and non-invasively. The Apparent Diffusion Coefficient has become an important diagnostic aid to diffusion weighted imaging (DWI). ADC is the post processing of DWI being calculated from DWI. The ADC depends on the degree of restriction of water diffusion [37]. Accordingly, tissues with multiple barriers to diffusion like high cell density have a low ADC [38]. Malignant embryonal tumors like nephroblastoma typically have high cell counts. But as in nephroblastoma the stromal subtype is characterized by a lower cell count it should be possible to distinguish the different subtypes of nephroblastoma with high cellularity (blastemal subtype) and those with low cellularity (stromal subtype or necrotic areas) by corresponding differences in ADC values.

Diffusion-weighted imaging with calculation of ADC maps is feasible in abdominal tumours in childhood. An inverse correlation exists between cellular density and ADC measurements. Preliminary data in nephroblastoma suggest that tissue cellularity is an important determinant of ADC value, which might help in terms of early prediction of therapy response [39, 40]. ADC values changes during chemotherapy and may help to stratify according to treatment response. If the ADC

value increases during chemotherapy the cellularity is going down. This information is helpful selecting the right area for taking tumor material for molecular analysis.

Figure 5.11 shows DWI and the corresponding ADC values in nephroblastoma of different patients at the time of diagnosis and after pre-operative chemotherapy. By calculating the tumor volume in these patients the ADC values will provide further info regarding chemotherapeutic induced response. In figure 5.11 case A shows a decrease in tumor volume and a higher ADC value, which shows a clear response to pre-operative chemotherapy, whereas in case C the tumor volume and the ADC value is increasing not allowing to determine the response. Not only this case histological images need to be superimposed with the DWI and cellularity needs to be correlated with the ADC values to gain new insights into tumor biology. This knowledge will be further enhanced if from specific tumor areas with known histology and ADC values molecular data will be available. Therefore the ADC mapping images are important to discuss with pathologists where to sample tumor tissue for molecular biology.

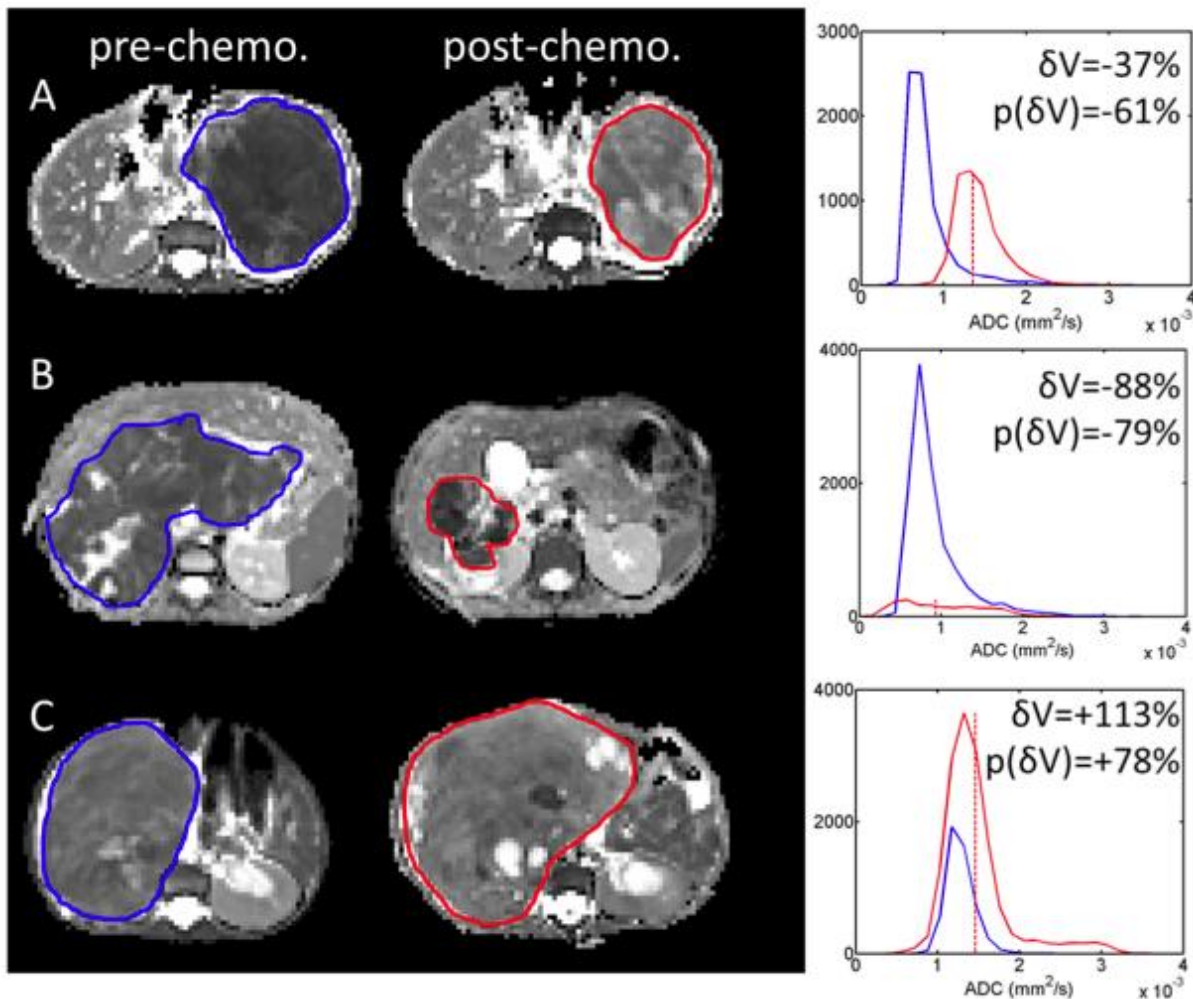


Fig. 5.11: DWI and ADC mapping of nephroblastoma from different patients before and after pre-operative chemotherapy. Presented at the annual meeting of the British Chapter of the ISMRM, September 2012, provided by Prof. Kathy Pritchard-Jones from UCL.

There are different techniques of detecting **perfusion parameters** with the use of MRI, the most common being dynamic susceptibility contrast imaging (DSC-MRI). In DSC-MRI, Gadolinium contrast

agent is injected and a time series of fast T2-weighted images is acquired. As Gadolinium passes through the tissues, it produces a reduction of T2 intensity depending on the local concentration. The acquired data are then post-processed to obtain perfusion maps with different parameters, such as BV (blood volume), BF (blood flow), MTT (mean transit time) and TTP (time to peak). This technology is not yet developed for nephroblastoma. Within the next prospective SIOP trial it will be applied in few centres to gain new knowledge about tumor perfusion before and after pre-operative chemotherapy MRI protocols for these imaging studies are under development.

5.2.3 Knowledge about data correlations

The following correlations between clinical, pathological, imaging and molecular data are known [41, 42, 43]. Correlations described under 14 to 16 are under development during the CHIC project.

1. **Age:** patients younger than 2 years of age are doing better than those with older age
2. **Time of diagnosis:** Tumors detected by routine examinations in patients without symptoms are smaller and maybe more responsive to treatment
3. **Gender:** There is no difference in outcome between boys and girls
4. **Pathology:** Surviving blastema after preoperative chemotherapy is correlated with poor outcome. The absolute volume is most relevant
5. **Pathology:** Anaplasia is correlated with p53 mutation
6. **Pathology:** Stromal subtype is correlated with WT1 mutations, sometimes with germline mutations
7. **Pathology:** Stromal and epithelial subtype do not respond well to chemotherapy
8. **Pathology:** Stromal and epithelial subtype have an excellent prognosis if they are completely resected
9. **Pathology:** Tumor volume after preoperative chemotherapy (> 500ml) has a negative impact on outcome (with the exception of stromal and epithelial subtype)
10. **Pathology:** Local stage I is doing better than stage II and stage III
11. **Imaging:** ADC value is correlated with cell density
12. **Imaging:** Kurtosis of histograms of signal intensities is correlated with tumor heterogeneity
13. **Imaging:** Skewness of histograms of signal intensities is correlated with the composition of the nephroblastoma
14. **miRNA Pattern:** miRNA pattern from serum and blood at the time of diagnosis are under development that correlate with the amount of blastema
15. **miRNA Pattern:** miRNA pattern from serum and blood at the time of diagnosis are under development that correlate with response to treatment and outcome
16. **autoantibody Pattern:** Autoantibody pattern from serum at the time of diagnosis is under development that correlates with histological subtypes and response to treatment

5.3 Granular dissection of the nephroblastoma scenario

The granularity of the scenario is based on the available data as described above and the use cases that are needed to pseudonymize, semantic annotate, upload, share and integrate these data. A whole picture of the scenario is given in figure 5.12. In this figure the granularity of the scenario is shown. Different composition models (hypomodels) are linked to the nephroblastoma hypermodel.

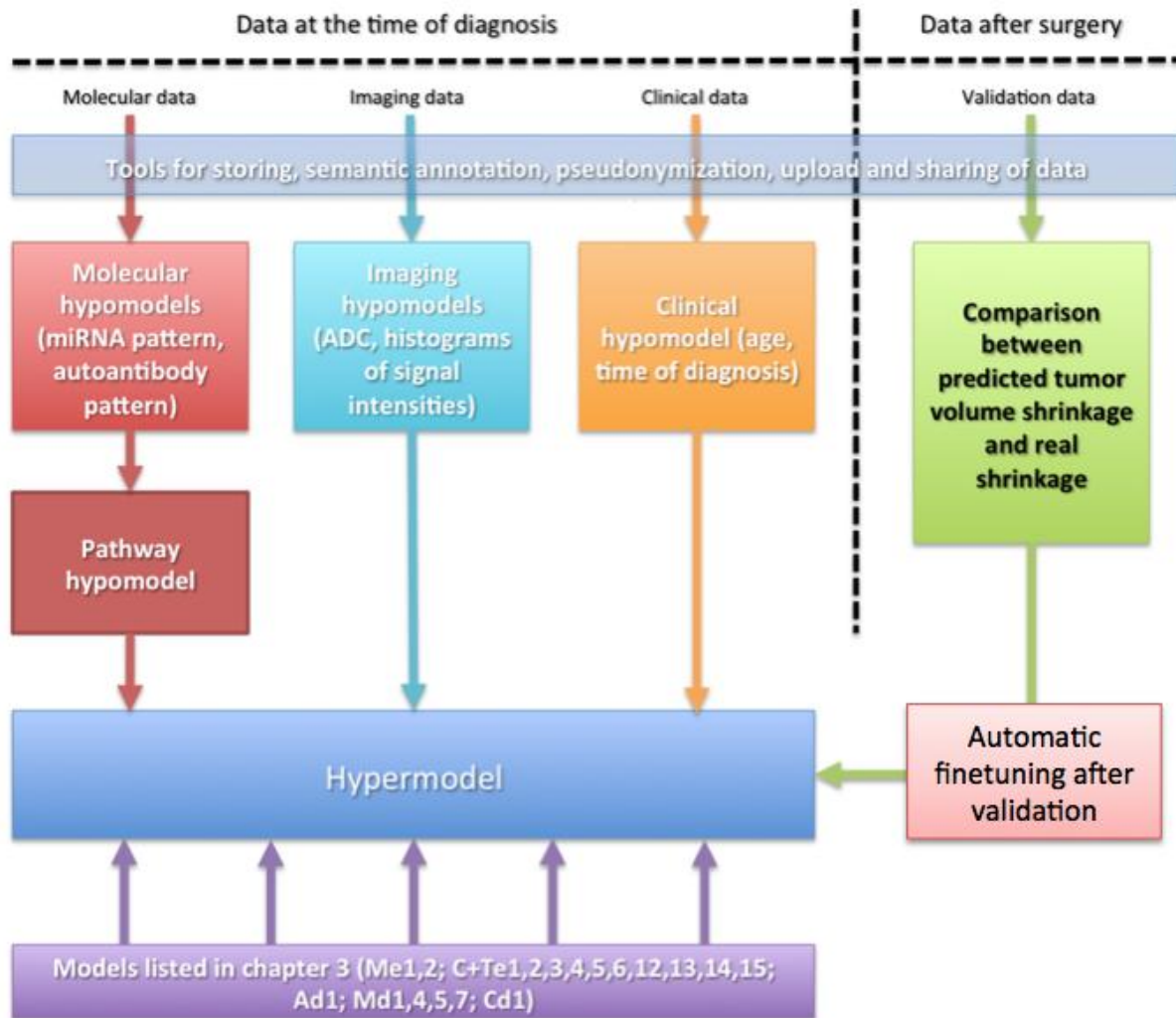


Fig. 5.12: Schematic view of the nephroblastoma scenario described by the linkage of hypomodels composing the nephroblastoma hypermodel

5.3.1 Data integration into the CHIC platform

As for each other model data pseudonymization, semantic annotation, uploading to the CHIC platform for sharing, integrating and usage is a necessity. The corresponding tools are described in chapter 4.2 to 4.5. The data that are needed are described in chapter 5.2 of this deliverable. In summary all data besides the imaging data are stored in ObTiMA. From ObTiMA data will be exported to the CHIC platform according to the legal framework of CHIC. Imaging data are stored on a DICOM server provided by p-medicine. These data need post-processing using DoctorEye and tools for analysing DWI and perfusion. These tools need to be developed within the CHIC project.

5.3.2 Clinical scenario

The clinical scenario will be translated into the clinical hypomodel. Most important are age and the time of diagnosis. The younger the patient and the earlier the diagnosis is done, the better is the outcome of a patient. Other clinical data do not show correlations to tumor shrinkage or outcome.

5.3.3 Imaging scenario

There are different scenarios within the imaging scenario. Each of these scenarios can be seen as a hypomodel. These are:

1. Rendering of the tumor to calculate tumor volume at the time of diagnosis and after pre-operative chemotherapy
2. Histograms of signal intensities of the segmented tumor
3. Diffusion weighted imaging and ADC mapping of the tumor
4. Perfusion weighted imaging and mapping of the tumor

Rendering and segmentation of the tumor will be done with DoctorEye [26]. Pseudonymized imaging data will be downloaded from the DICOM server into DoctorEye where a clinician does the rendering of the tumor. DoctorEye automatically calculates tumor volumes as well as other parameters including the histogram of signal intensities. The rendered tumor is uploaded automatically on the DICOM server and the calculated values are stored in ObTiMA for downloading into the CHIC platform.

Radiologists do the DWI imaging and ADC mapping. They will upload these data on the DICOM server and the calculated values will be stored in ObTiMA for further usage.

To run perfusion-weighted images standardized protocols for MRI are needed. These are under progress by radiologists. To map the perfusion with the images a tool for nephroblastoma needs to be developed within the CHIC project.

As a result of these imaging models data will be created that gives the tumor volume, the heterogeneity of the tumor, cellularity of the tumor and perfusion of the tumor. There are correlations of these parameters to the histology, response to treatment and outcome. These data are needed for the nephroblastoma hypermodel.

The tumor volume after pre-operative chemotherapy is used for validation.

5.3.4 Molecular scenario

The molecular scenario is based on autoantibodies against nephroblastoma and miRNAs at the time of diagnosis. Currently retrospective data are analysed to find a pattern of autoantibodies and miRNAs at the time of diagnosis that do correlate with resistant blastema after preoperative chemotherapy, response to pre-operative chemotherapy and outcome. As soon as these correlations are defined such miRNA data and protein data of a single patients can be compared with the corresponding pattern and a risk assessment is possible to calculate the probability of response to treatment. After surgery the amount of blastema can be correlated with the prediction of resistant blastema by these molecular pattern.

For each patient metabolic pathways will be analysed by linking the miRNA pattern of a patient with the KEGG database. Specific disrupted pathways can be used in the advanced nephroblastoma hypermodel for drug selection that interact with such pathways.

5.3.5 Usage of models as listed in chapter 3 of this deliverable

Within the nephroblastoma hypermodel the following hypomodels from chapter 3 will be used. They are described in detail in deliverable 6.1. Most of them are already developed. The linkage of these models with all other hypomodels of the nephroblastoma hypermodel is the biggest challenge and will be solved by semantic interoperability.

5.3.6 Validation scenario

The validation scenario will compare the real tumor volume shrinkage measured with the help of DoctorEye in the DICOM images after pre-operative chemotherapy with the prediction of the hypermodel. This validation hypomodel will send this comparison automatically to the machine learning hypomodel.

5.3.7 Machine learning scenario

The machine learning hypomodel will fine-tune the hypermodel to improve the prediction. The more often the hypermodel is used in different patients the better the prediction will get.

5.4 Hypermodel for nephroblastoma

The hypermodel for nephroblastoma will predict the tumor volume shrinkage of nephroblastoma in single patients that are treated with preoperative chemotherapy. This hypermodel is composed of different hypomodels as described above and schematically demonstrated in figure 5.10.

5.5 Advanced Nephroblastoma scenario

5.5.1 Introduction

An advanced nephroblastoma hypermodel will answer the question to: What is the best treatment for preoperative chemotherapy to get the most shrinkage of a nephroblastoma. In this case different treatment options need to be compared. This needs the integration of a drug selection component model, the Binding affinity calculator and the models Ae2, 3 and 4 into the nephroblastoma hypermodel. The models Ae2, 3 and 4 are described in chapter 3 and in more detail in deliverable 6.1.

A schematic outline of this advanced hypermodel is shown in figure 5.13.

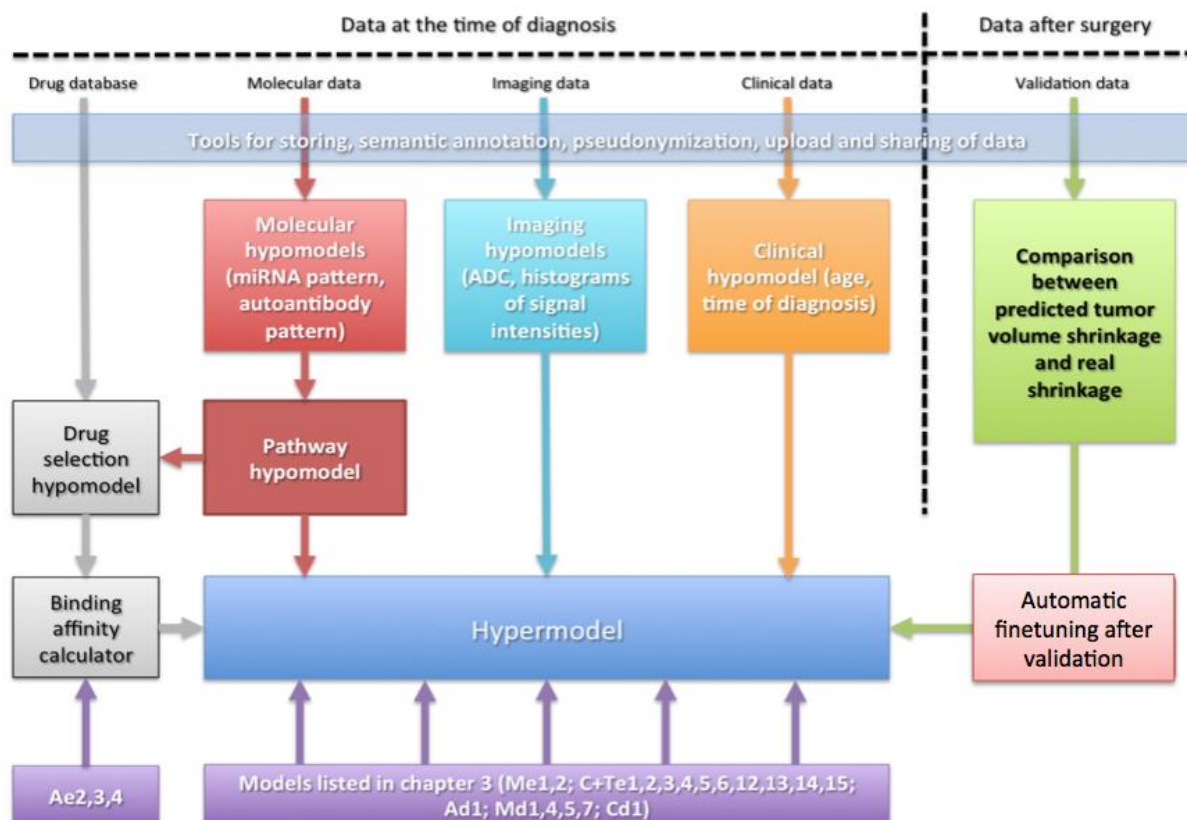


Fig. 5.13: Schematic view of the advanced nephroblastoma scenario described by the linkage of hypomodels composing the advanced nephroblastoma hypermodel

5.5.2 Drug selection scenario

The pathway hypomodel will provide for each single patient the information about those pathways that are disrupted in their nephroblastoma. Using databases about drug information, like DrugBank (<http://www.drugbank.ca/>), one can do data mining to find those drugs that are interaction with the corresponding pathways.

The following Information is provided from the website of DrugBank: “The DrugBank database is a unique bioinformatics and cheminformatics resource that combines detailed drug (i.e. chemical, pharmacological and pharmaceutical) data with comprehensive drug target (i.e. sequence, structure, and pathway) information. The database contains 6811 drug entries including 1528 FDA-approved small molecule drugs, 150 FDA-approved biotech (protein/peptide) drugs, 87 nutraceuticals and 5080 experimental drugs. Additionally, 4294 non-redundant protein (i.e. drug target/enzyme/transporter/carrier) sequences are linked to these drug entries. Each DrugCard entry contains more than 150 data fields with half of the information being devoted to drug/chemical data and the other half devoted to drug target or protein data.” Within this website one can search for specific pathways but also for specific drugs as shown in figures 5.14 and 5.15. This will allow selecting those drugs that are the best candidates for the drug affinity calculator hypomodel that is described in the next chapter.

Other websites with similar information are: The Therapeutic Target Database (TTD) (<http://xin.cz3.nus.edu.sg/group/ttd/ttd.asp>), the PharmGKB database (www.PharmGKB.org), the SuperTarget database (http://bioinf-apache.charite.de/supertarget_v2/) and the 'Search tool for interactions of chemicals' (STITCH) (<http://stitch.embl.de/>).



DRUGBANK
Open Data Drug & Drug Target Database

Home Browse Search Downloads About Help Tools Contact Us

Search: Apoptosis [Help / Advanced](#)

Search Results for "Apoptosis"

Displaying results 1 - 20 of 60 in total

1 2 3 Next › Last »

[DB05773 — ado-trastuzumab emtansine](#) small molecule, approved

...agent, DM1 (a maytansine derivative)--to produce cell cycle arrest and **apoptosis**. Ado-trastuzumab emtansine is marketed under the brand name Kadcyla... ..effects of ado-trastuzumab emtansine are cell cycle arrest and cell death by **apoptosis**. DM1 has a plasma protein binding value of 93%. The route...

[Identification](#) [Taxonomy](#) [Pharmacology](#) [Pharmacoeconomics](#) [Properties](#) [References](#) [Interactions](#) [Comments](#)

[DB03496 — Flavopiridol](#) small molecule, experimental, investigational

...inhibiting cyclin-dependent kinases, arresting cell division and causing **apoptosis** in non-small lung cancer cells. Flavopiridol 131740-09-5 Glycogen... ..N 2.81 Inhibits cyclin-dependent kinases, arresting cell division and causing **apoptosis** in non-small lung cancer cells. 401.84 401.103000462 1C8K...

[Identification](#) [Taxonomy](#) [Pharmacology](#) [Pharmacoeconomics](#) [Properties](#) [References](#) [Interactions](#) [Comments](#)

[DB01169 — Arsenic trioxide](#) small molecule, approved, investigational

...line agents. It is suspected that arsenic trisulfide induces cancer cells to undergo **apoptosis**. Due to the toxic nature of arsenic, this drug carries... ..suspected that arsenic trioxide induces cancer cells to undergo **apoptosis**. The metabolism of arsenic trioxide involves reduction of pentavalent...

[Identification](#) [Taxonomy](#) [Pharmacology](#) [Pharmacoeconomics](#) [Properties](#) [References](#) [Interactions](#) [Comments](#)

[DB08870 — BRENTUXIMAB VEDOTIN](#) small molecule, approved

Brentuximag vedotin or Adcetris® is an antibody-drug conjugate that combines an anti-CD30 antibody and the drug monomethyl auristatin E (MMAE... ..metabolized primarily via oxidation by CYP3A4 and CYP3A5. Brentuximag vedotin causes **apoptosis** of tumor cells by preventing cell cycle progression...

[Identification](#) [Taxonomy](#) [Pharmacology](#) [Pharmacoeconomics](#) [Properties](#) [References](#) [Interactions](#) [Comments](#)

[DB00271 — Diatrizoate](#) small molecule, approved

A commonly used x-ray contrast medium. As diatrizoate meglumine and as Diatrizoate sodium, it is used for gastrointestinal studies, angiography... ..agents like diatrizoate are cytotoxic to renal cells. The toxic effects include **apoptosis**, cellular energy failure, disruption of calcium homeostasis...

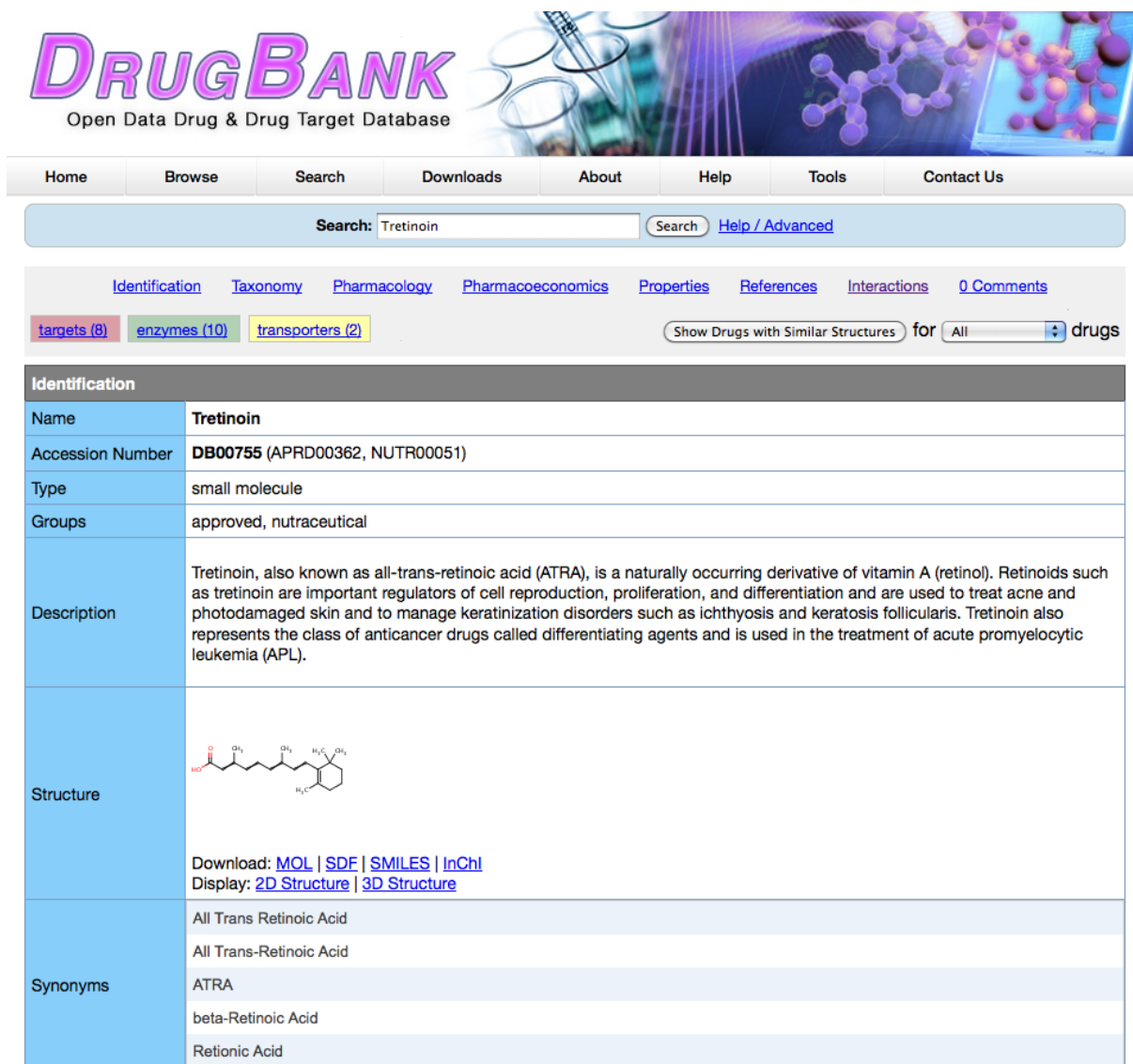
[Identification](#) [Taxonomy](#) [Pharmacology](#) [Pharmacoeconomics](#) [Properties](#) [References](#) [Interactions](#) [Comments](#)

[DB01249 — Iodixanol](#) small molecule, approved

Iodixanol is a nonionic hydrophilic compound commonly used as a contrast agent during coronary angiography, particularly in individuals with renal... ..agents like iodixanol are cytotoxic to renal cells. The toxic effects include **apoptosis**, cellular energy failure, disruption of calcium homeostasis...

[Identification](#) [Taxonomy](#) [Pharmacology](#) [Pharmacoeconomics](#) [Properties](#) [References](#) [Interactions](#) [Comments](#)

Fig. 5.14: DrugBank website showing the results of the search for drugs interacting with the apoptotic pathway



DRUGBANK
Open Data Drug & Drug Target Database

Home Browse Search Downloads About Help Tools Contact Us

Search: Tretinoin [Search] [Help / Advanced](#)

[Identification](#)
[Taxonomy](#)
[Pharmacology](#)
[Pharmacoeconomics](#)
[Properties](#)
[References](#)
[Interactions](#)
[0 Comments](#)

[targets \(8\)](#)
[enzymes \(10\)](#)
[transporters \(2\)](#)

Show Drugs with Similar Structures for drugs

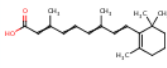
Identification	
Name	Tretinoin
Accession Number	DB00755 (APRD00362, NUTR00051)
Type	small molecule
Groups	approved, nutraceutical
Description	Tretinoin, also known as all-trans-retinoic acid (ATRA), is a naturally occurring derivative of vitamin A (retinol). Retinoids such as tretinoin are important regulators of cell reproduction, proliferation, and differentiation and are used to treat acne and photodamaged skin and to manage keratinization disorders such as ichthyosis and keratosis follicularis. Tretinoin also represents the class of anticancer drugs called differentiating agents and is used in the treatment of acute promyelocytic leukemia (APL).
Structure	 <p>Download: MOL SDF SMILES InChI Display: 2D Structure 3D Structure</p>
Synonyms	All Trans Retinoic Acid All Trans-Retinoic Acid ATRA beta-Retinoic Acid Retionic Acid

Fig. 5.15: DrugBank website showing the results of the search for a specific drug (Tretinoin or ATRA)

5.5.3 Binding Affinity Calculator

Molecular dynamics (MD) techniques can be used to study the interactions between inhibitors and receptors in atomistic detail, and to predict the effect of different receptors/mutations on inhibitor binding affinities using free energy calculations. Several computational approaches exist to estimate ligand binding affinities, with various levels of accuracy and computational expense [44, 45, 46]. The molecular mechanics Poisson-Boltzmann surface area (MM/PBSA) and linear interaction energy (LIE) methods are frequently used approaches to the calculation of binding affinities from simulations of the physical states of a ligand-protein complex. The MM/PBSA and LIE methods post-process a series of snapshots from MD trajectories of the complex. In contrast to more rigorous methods such as thermodynamic integration (TI), the MM/PBSA and LIE approaches are faster by several orders of magnitude.

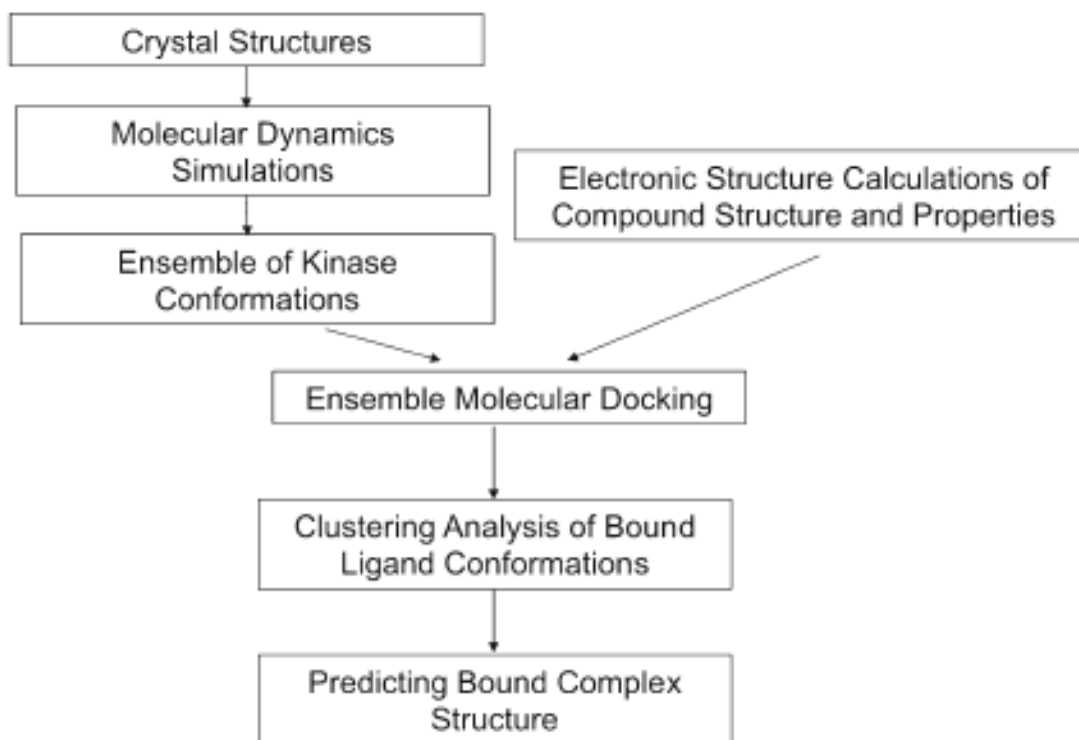


Fig. 5.16: Flow chart how CHIC addresses binding affinity between mutated receptors in cancer and their inhibitors.

6 Scenarios for Glioblastoma

6.1 Introduction and description of the scenario

6.2 Introduction and description of the scenario

The first question that needs to be answered by the Glioblastoma Multiforme (GBM) hypermodel is: Will a specific patient benefit from adding Dendritic Cell vaccination (DC vaccination) to the standard treatment for GBM? The answer should be 'YES' or 'NO' and will be answered by measuring Progression Free Survival (PFS) after 6 months (the confirmatory primary end-point of the phase IIb prospective double blind placebo-controlled randomized clinical trial HGG-2010 trial, EurdraCT 2009-018228-14). In the case of 'YES' there is a benefit of DC vaccination in terms of higher probability of reaching the 6 months PFS point (PFS 6m).

Since there is a more complex design in the study (cfr. below), patients in the placebo group receive vaccination after ± 6 months in case relapse did not occur. A second question will hence be: Will a patient benefit more from early (within the first 6 months of standard treatment) or late (after 6 months of standard treatment) vaccination for overall survival.

A third question to be answered is which immune profile (cfr. below, cluster analysis) will predict good outcome after vaccination.

GBM is the most common primary brain cancer with an incidence of 3-4/100.000/year. Current standard treatment consists of maximal surgical resection, followed by 6 weeks of concomitant radiotherapy (30x2Gy) and Temozolomide, followed by 6 cycli of adjuvant Temozolomide (i.e. Stupp protocol [47]). Despite this multimodal treatment, median PFS is only 6.9 months and median OS 14.6 months. Hence, there is an urgent need for additional, safe and effective therapies.

DC vaccination has been studied for many years as an experimental therapy to treat GBM. After gross total or subtotal removal of the GBM, the tumor itself is processed in the laboratory to make whole tumor lysates. These whole tumor lysates contain multiple antigens expressed by the GBM. After surgery and after weaning of corticosteroids, a leucapheresis is performed to harvest a large amount of monocytes. These monocytes are cultured en differentiated to dendritic cells (DCs) under specific laboratory conditions. The dendritic cells are afterwards loaded/pulsed with tumor lysate, after which maturation is induced with a second cocktail of cytokines. Finally, the autologous mature lysate-loaded DCs (DCm-HGG-L) are injected back in the patient at specified moments (cfr. infra). The activated DCs will present the tumor antigen to specific cytotoxic T-cells, leading to an effective activation of the adaptive immune system and subsequent killing of residual or recurrent intracranial tumor cells.

There have been multiple study reports of DC vaccination for GBM, mainly after recurrence and relapse resection. We have incorporated DC vaccination in the standard therapy (cfr. schedule below) in the HGG-2006 phase I/II trial [48] proving the safety and feasibility of this treatment in newly diagnosed GBM. This study also showed that RPA classification (cfr. infra) stratified patients on pretreatment variables and this was related with outcome. Although the previous clinical trials provide proof of principle and remarkable results in a subset of patients, not all patients benefit from DC vaccination. Defining the patient subgroup likely to benefit from this highly personalized and labor-intensive therapy is thus of clinical and economical importance.

We are currently running the HGG-2010 trial in which patients with newly diagnosed GBM are randomized between DC vaccination and placebo injections. After ± 6 months (after completing adjuvant Temozolomide), there is an unblinding procedure so that placebo-treated patients can start DC vaccination. The primary outcome of the study is PFS at 6 months. OS is a secondary outcome.

Multiscale prospective data are collected (cfr. infra), and probably a combination of parameters can predict if a certain patient will benefit from DC vaccination.

Through hypermodelling within the CHIC environment, we want to explore if a patient with certain patient-, surgery- and tumor-related characteristics will have a response to DC vaccination, and which immune profiles are more likely to predict a good response.

After developing the oncosimulator, it will have to be validated in a next prospective patient cohort.

6.3 Available data and post-processing of data

6.3.1 Available data

All data for the GBM scenario will be collected within the HGG-2010 study; a phase IIb prospective placebo-controlled double blind randomized clinical trial for the treatment of patients with newly diagnosed glioblastoma multiforme with tumor vaccination as “add-on therapy” to standard primary treatment (EudraCT 2009-018228-14). For these data the informed consent is already available and the ethical approval is obtained (Commissie Ethische Ethiek van de Universitaire Ziekenhuizen KU Leuven, kenmerk: ML6285 from 1st of March 2010). All data will be shared and used according to the legal framework of CHIC.

All patient data besides some specific immune therapy related data are stored within KWS (*‘clinical working station’*), the central data management application of the University Hospitals Leuven. The specific immune therapy related data are collected within an in-house managed FileMaker database for all HGG-IMMUNO-trials patients. A new in-house database will be provided where both data management applications are combined to gather all data for CHIC, i.e. data collected within the context of the HGG-2010 trial.

Before usage is possible in CHIC, anonymization and pseudonymization procedures as well as data transfer issues are supervised via a trusted third party (legal and ethical framework of CHIC). Following data will be available for the GBM scenario:

Clinical data:

The clinical data of importance for the HGG-2010 trial are transferred from KWS, where all data are personally identified, to our in-house FileMaker database, where these data are pseudonymized via a unique number, and stored in a CRF. Clinical data of interest are: sex, age of diagnosis, date of diagnosis, weight, RPA classification according EORTC, presenting symptoms, date of resection, extent of resection, progression free survival, overall survival, relapse resection and relapse treatment. These data are gathered by clinical examination and by follow-up of each patient before, during and after treatment in the HGG-2010 protocol.

Imaging data:

Imaging studies in patients with GBM are performed at the time of diagnosis, (before and) after surgery and during adjuvant therapy. Magnetic resonance imaging (MRI) is the most commonly used imaging technique to document this pathology.

Within CHIC, data from two different sources will be used.

Firstly, we will provide data that are obtained in routine clinical setting. At multiple time points during the disease process, patients undergo an MRI scan: at the time of diagnosis, (before and) after surgery and during adjuvant therapy on a three-monthly basis. In the University hospitals of Leuven,

the routine MRI protocol consists of conventional MRI such as T1-weighted images before and after contrast administration, T2-weighted images and FLAIR-images. These imaging techniques provide structural information on the brain and associated pathology: to determine the location of the pathology, the extent of the lesions and its relationship to the surrounding structures. Moreover, the protocol is further elaborated with two functional techniques: diffusion weighted imaging and dynamic susceptibility weighted imaging, which provide information on cellularity and tissue perfusion, respectively.

Secondly, MRI will be provided from a clinical imaging study in which patients with GBM treated with DC therapy undergo monthly an extensive MRI imaging session from the start of immune therapy onwards. Hereby, it is the aim to document the time course and unravel the imaging characteristics on advanced MRI of immune therapy induced inflammatory responses versus tumor relapse. The Medical Ethical Committee of the University Hospitals Leuven approved this study and informed consent is obtained from all volunteers and patients before scanning (study reference number “s53303”). This prospective follow-up study is linked to the clinical trials in the University Hospitals of Leuven, investigating DC therapy for HGG. Both the clinical trials on dendritic cell therapy and the associated longitudinal imaging follow-up study are ongoing studies at the start of the CHIC project. Patients are imaged with an extensive imaging protocol consisting of the conventional MRI techniques as mentioned above combined with functional MRI techniques such as diffusion kurtosis imaging to assess the tumoral micro-environment, two types of perfusion imaging: dynamic susceptibility weighted imaging and dynamic contrast-enhanced imaging in order to assess the vascularity of the lesions and MR spectroscopy to assess metabolic characteristics of the lesions.

From this extensive imaging dataset, only a subset of data will be used within CHIC, namely the type of data and the time points that are also available in the datasets of patients, scanned in routine clinical setting. By doing so, a consistent set of data can be provided. The time points available in both groups (routine clinics and imaging study) are immediately preoperative, immediately post-operative, after induction vaccines and every three months in follow-up.

Within the CHIC framework, the MR images of every patient in the selected time points will be assessed for different criteria: location, volume of the contrast-enhancement, volume of perilesional oedema, cerebral blood volume in the contrast-enhancing lesions (derived from dynamic susceptibility-weighted imaging) and mean diffusivity in the contrast-enhancing lesions (derived from diffusion weighted imaging).

Tumor characteristics:

One of the inclusion criteria for entering the HGG-2010 trial is the confirmation by the reference pathologist of a histologically proven diagnosis of primary GBM WHO grade IV. However, it has become clear that pathological identical tumor can clinically behave different. Further subclassification in GBM is needed: extensive work has been done to unravel different genetic and molecular groups of GBM, with prognostic impact. It was shown that tumors carrying an IDH1 mutation and/or MGMT promotor methylation have a better prognosis. IDH1 mutations can be detected by immunohistochemistry. PTEN deletion was found to have an immunosuppressive effect.

Subclassifications based on gene expression patterns have been developed. Most known are the Phillips and Verhaak classification. The Phillips classification describes 3 (Proneural, Mesenchymal and Proliferative) subtypes [49] the Verhaak classification 4 (Proneural, Mesenchymal, Classical and Neural) distinct profiles [50] Comparison led to the identification of robust Mesenchymal and Proneural profiles.

Moreover, GBM are subclassified on the base methylation patterns in 6 subgroups, as is published by Sturm *et al.* [51] These 6 subgroups were related to the gene expression profiles, providing a comprehensive and integrative summary of subclassification.

It is likely that some tumor subclasses will respond better to DC vaccination, as was already suggested in a small study by Prins [52].

A small part of frozen tumor of all patients (that has not been used to prepare vaccines) and paraffine coupes are stored and available for mutational, transcriptional and methylation analysis to the extent possible. A possible limiting factor will be the small amount of tumor tissue. The protocol for these analyses needs still to be developed.

Data inherent to the HGG-2010 protocol outline:

Figure 6.1 shows the outline of the HGG-2010 trial; the upper line of the study represent the experimental arm (i.e. DC vaccination), the lower line the control arm (placebo vaccination).

After operation, after confirmation of (sub)total resection including reference radiology, and after confirmation of the diagnosis of GBM including reference pathology, the inclusion in the trial is done at the trial centre in Leuven by the principal investigators after evaluation of all the necessary information on the clinical, neurosurgical, radiological and pathological data.

Leucapheresis is performed prior to radiochemotherapy around one week after complete withdrawal of preoperative corticosteroids. At this time point the patient will be randomised and stratified on the preoperative RPA class (table 6.1 [53]). A concealing, random allocation algorithm is used to organize the randomisation. After deblinding at the eighth vaccination the information about randomisation is provided.

RPA CLASS	Age	Pathology	Kamofsky	WHO	MMSE
I	< 50	Grade III			Normal
II	≥ 50	Grade III			
III	< 50 or < 50	Grade IV	90-100	0	
IV	< 50 or ≥ 50	Grade IV		1-2	≥ 27
V	≥ 50 or ≥ 50	Grade IV			< 27
VI		Grade IV	< 70		

Table 6.1: Table for determination of the RPA according to EORTC.

Radiochemotherapy is administered according to the Stupp protocol [47] meaning six weeks daily intake of Temozolomide, 75 mg/m²/day, simultaneous to conventional fractionated irradiation with a total dose of 60 Gy. Data on the schedule and dose of this treatment modality will be provided into the CHIC dataset.

After radiochemotherapy, patients allocated to the *experimental arm* will receive four weekly “DCm-HGG-L” vaccinations. Preparation of the immune therapy starts with differentiation of DC out of PBMC, obtained through leucapheresis. Immature DC are loaded with tumor proteins obtained from tumor lysate. The amount of protein in the lysate will be determined with Coomassi blue staining [54]. After maturation the DC are ready to be administered as a DCm-HGG-L vaccine. Technical details of this preparation are fixed, only variable data per patient will be provided: amount of PBMCs at the start of the procedure, viability and number of viable immature DC and viability and number of viable mature DC. Purity of DC is determined by FACS analysis with the following staining on the total cell population: CD3:CD56, CD14:CD19, CD14+CD83:CD11c, and CD83 for the determination of % CD3+ T cells, % CD14+ monocytes, % CD19+ B cells, % CD56+ NK(T)cells, % CD83-CD14-CD11c+ DCi and %CD83+ DCm. Stainings on the CD11c gate are performed to assess the potency: CD83:CD11c, CD86:CD11c and HLADR:CD11c.

After the four induction (DCm-HGG-L) vaccines, maintenance chemotherapy is started in a 5/28 day schedule according to the Stupp protocol [47] six cycles of 5 days with Temozolomide every 28 day, first cycle 150 mg/m²/day, from the second cycle on 200 mg/m²/day as long as no hematologic toxic effect occurs. Data on the schedule and dose of this treatment modality will be provided, as are the blood counts taken before starting a new cycle of maintenance chemotherapy.

At day 8 of cycle 1, 2, 3 and 6 of the maintenance chemotherapy, boost vaccinations with lysate HGG-L are injected. Further boosts with HGG-L will be injected each 12 weeks depending on the amount of HGG-L available. Although the injected amount of proteins is fixed by protocol, the patient variables protein amount, lysate volume and protein concentration will be provided.

Three weeks after cycle 6, “PFS 6m” will be determined.

Patients allocated to the *placebo control arm* of the HGG-2010 trial, will follow the same schedule as patients in the experimental arm what concerns radiochemotherapy and maintenance chemotherapy. These patients will be injected with vehicle without cells and lysate instead of DCm-HGG-L and HGG-L. Three weeks after cycle 6 debinding takes place and “PFS 6m” will be determined. Afterwards, four weekly DCm-HGG-L injections and 3 HGG-L injections every 28 days will be administered and then further each 12 weeks depending on the amount of HGG-L available, similarly to the experimental treated arm.

Monitoring data:

At indicated time points different kinds of monitoring will take place.

Radiological monitoring includes post-operative MRI, MRI after the four weekly vaccines (DCm-HGG-L or vehicle), after maintenance Temozolomide cycle 3 and 6 and further MRI follow-up at least each 3 months. Data such as volume, contrast enhancement, infiltration-, perfusion-, diffusion- and oedema characteristics are described.

Haematological monitoring is performed by doing blood analysis of standard cell formulas at the same time points as when imaging is done and after at the start of the treatment after radiochemotherapy (regardless which arm of the study). These data will be included as well.

Immunological monitoring is done at the same time points as haematological monitoring. At these fixed time points, blood is taken and PBMC are isolated in the laboratory and frozen. These will be thawed after completing follow-up of patients, and analysed for following parameters:

- FACS will be done to determine the relative mononuclear cell populations (CD8+ T-cells, CD4+ T-cells, CD4+CD25+CD127dim Treg-cells, CD3+CD56+ NK(T)-cells, CD3-CD56+ NK-cells. Also, activation markers as CTLA-4, CD137 and CD69 on CD4+ and CD8+ cells and GARP on Treg-cells will be measured. This protocol is under development. The evolution of these cell populations during treatment will be a marker for the immunological responses or shifts. These evolutions will be correlated with the clinical evolution, and it will be investigated whether certain evolutions can predict good outcome.
- The T-cell response to tumor lysate will be measured as a marker of an effective anti-tumoral T-cell response. Concretely, T-cells will be stimulated with tumor lysate. Afterwards RNA will be isolated from the T-cells and qPCR for IFN- γ response (as surrogate marker for a specific Th1-cell response against the tumor) will be performed. These responses will be correlated with clinical outcome.
- Since single parameters probably are insufficient to detect subtle changes in the immune system, cluster analysis of multiple parameters will be performed, as was already described in two publications [50, 55].

Data on disability, self-reliance and quality of life will be recorded at each vaccination moment using the FMH [56] and Karnofsky index, and the EORTC questionnaire [57, 58, 59, 60]. Every item of each of these questionnaires will be included as well.

The data will be stored in the in-house FileMaker database.

Molecular data:

Molecular analysis will be performed on different levels:

- Tumor characteristics: mutations, gene expression profiles, methylation state.
- Immunological monitoring: PBMC isolation and characterisation with measurement of the anti-tumor response *in vitro*. [61].

We refer to the respective sections above for more detailed information.

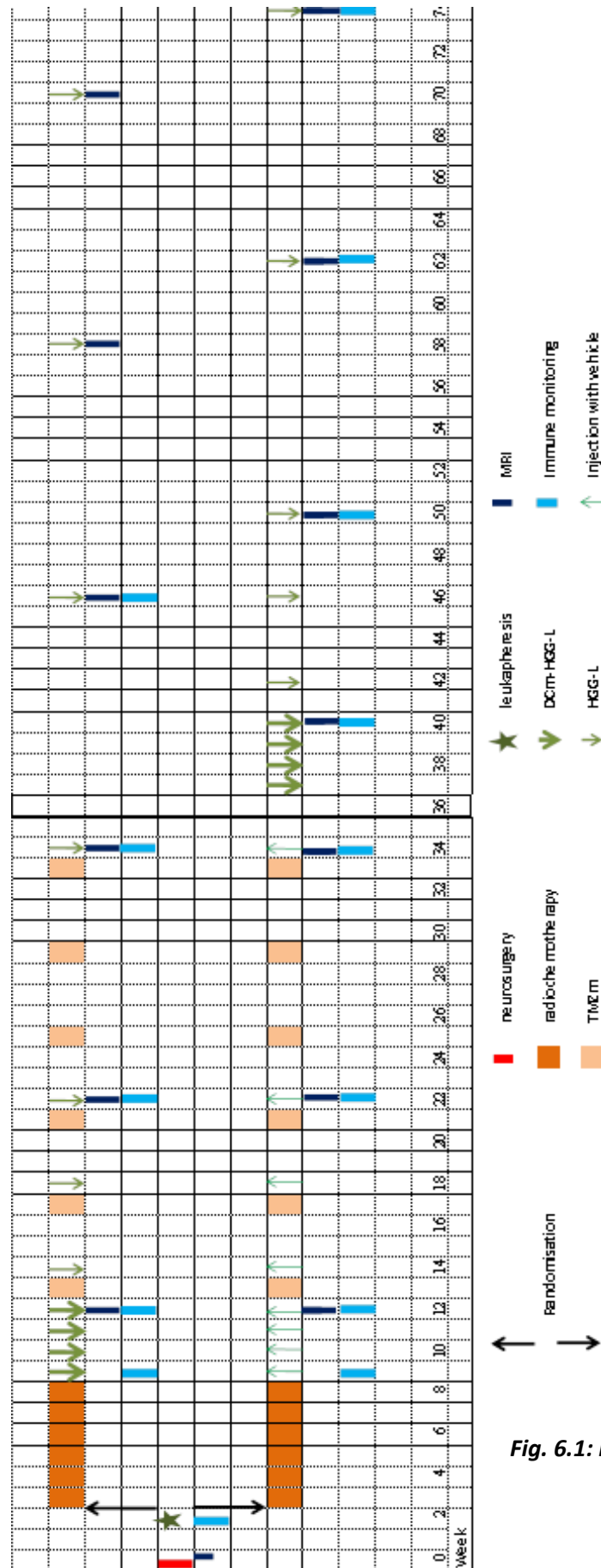


Fig. 6.1: HGG-2010 outline

6.3.2 Post processing of imaging data

Imaging data will be uploaded on the DICOM server.

As previously mentioned (see section 6.2.1), MR images of every patient in the selected time points will be assessed for different criteria. The lesion location will be evaluated by visual inspection. The volume of the contrast-enhancement and the volume of perilesional oedema will be assessed with manual delineation and in a second stage probably by automatic segmentation (see below). Cerebral blood volume in the contrast-enhancing lesions will be derived from gamma variate fitting procedure after correction for leakage and circulation [62]. Mean diffusivity in the contrast-enhancing lesions (derived from diffusion weighted imaging) will be derived from a mono-exponential fitting procedure [63].

Data of the longitudinal imaging study will be furthermore used in collaboration with two CHIC partners.

The group of the University of Bern uses the conventional MRI data to develop automatic segmentation algorithms to define contrast-enhancing tumoral regions, non-contrast enhancing tumoral regions and oedematous tissue defined by regions of increased signal intensity on T2-weighted or FLAIR image. Objective quantification of the tumor is a key indicator in therapy follow-up, as the current guidelines to assess the imaging follow-up in patients with GBM (RANO criteria, [64] are based on the estimation of volume changes of the contrast-enhancing and non-contrast enhancing lesions.

Furthermore, dynamic contrast-enhanced MRI data (DCE MRI) are processed in collaboration with the group of FORTH. DCE-MRI is less widely used than dynamic susceptibility weighted MRI (DSC-MRI) in perfusion imaging of the brain but we believe that this technique holds some promises for future applications, as it overcomes some of the limitations of DSC-MRI. Rupture of the blood-brain barrier (BBB) is non-specific and occurs in different types of lesions. Rupture of the BBB can be exploited with a regular T1-weighted image. However, recent research demonstrated that the dynamics of the signal enhancement in DCE-MRI may yield information of the nature of the lesion. Tumour relapse is characterized by a very rapid increase in the initial phase of the signal intensity-versus time curve compatible with a pronounced vascular phase, whereas radiation necrosis is characterized by a very slow signal increase, compatible with absence of a vascular phase because of the occlusive vasculopathy described in radiation-induced injury [65]. Moreover, DCE-MRI circumvents an important disadvantage of DSC-MRI because the dynamic T1-weighted images used to acquire DCE-MRI, is considerably less prone to susceptibility-artefacts originating from blood products or iron depositions, or in regions situated near the skull base, the sinuses and air-bone tissue interfaces, compared to the GE-EPI sequences used in DSC-MRI.

6.3.3 Knowledge about data correlations

The following correlations between clinical, pathological, surgical, immunological and molecular data are known.

- **RPA classification:** age, KPS and MMSE: Subdivides patients with HGG in 3 categories based on pretreatment variables. In the case of GBM, patients can have class 3, 4 or 5, with a better prognosis in lower classes. The HGG-2006 trial demonstrated that these pretreatment variables are relevant in studies on DC vaccination.
- **Immune state:** Glucocorticoid administration, clinically needed for peritumoral oedema, has a negative effect on DCs and is unwanted when treating with DC vaccination.

- **Gender:** No difference in outcome between men and women is known.
- **Localisation:** No specific localisation is known to be predictive for better response to DC vaccination. However, localisation has an indirect effect on outcome as deep or eloquent located tumors are not suitable for resection. Without extensive resection, DC vaccination is impossible. Moreover, the 6 molecular subtypes of GBM tumors are related with their location and age at diagnosis.
- **Extent of resection:** A more extensive resection is a prognostic parameter for better outcome. Ideally, a gross total resection is performed (no contrast capitation on T1 MRI after surgery). This is an independent prognostic parameter, but has particular importance in the case of DC vaccination as it lowers the need for corticosteroids and diminishes the immunosuppressive properties of the tumor.
- **Mutations:** The presence of IDH1 mutation is associated with a better prognosis, although not specifically for response to DC vaccination
- **Epigenetic silencing** of MGMT by promotor methylation is independently associated with better outcome, especially with better response to Temozolomide. It is unknown whether this predicts good outcome after DC vaccination.
- **PTEN mutation** is associated with increased immunosuppression and might be a negative prognostic factor for DC vaccination, although this has not yet be investigated.
- **Gene expression profile:** The Proneural gene expression profile is associated with younger age and better outcome. The Mesenchymal profile is associated with poor outcome, but data from a small study [49] suggest that this profile is more immunogenic and hence has a better response to DC vaccination.
- **Tumor micro-environment:** A higher number of CD8+ T-cells in the tumor micro-environment is associated with better outcome. A higher number of tumor suppressive regulatory T-cells might be a negative predictor for DC vaccination, but a direct relation with poor outcome has not been proven.
- **Immune monitoring:** Peripheral immune responses are reported in 50% of treated patients, but relations with outcome are less clear. Several explanations were given: the fact that the peripheral immune response does not reflect what is happening in the brain, the inability to detect subtle immune changes by measuring single or few immune parameters or the distortion of the response due to complex laboratory techniques to detect the response. These last 2 can be corrected by developing multi-scale parameter (cluster) analyses, and by developing simple, robust and reproducible laboratory tests.
- **Pseudoprogression:** pseudoprogression is a transient contrast enhancement, which suggests tumor progression, but is in reality a reaction towards the provided radiochemotherapy. Pseudoprogression is a marker of tumor sensitivity to the treatment.
- **rrCBV and overall survival:** preliminary evidence that relative regional cerebral blood volume (rrCBV) values of glioblastoma at the time of diagnosis correlates with overall survival. The higher the rrCBV values, the worse the prognosis [66]. It can be of interest to further explore this in glioblastoma patients treated with immune therapy.

6.4 Granular dissection of the glioblastoma scenario

Figure 6.2 depicts the granularity of the GBM scenario: different hypomodels are linked to the GBM hypermodel. This granularity is the result of the knowledge in the field, collected data in the HGG-2010 trial and already existing models.

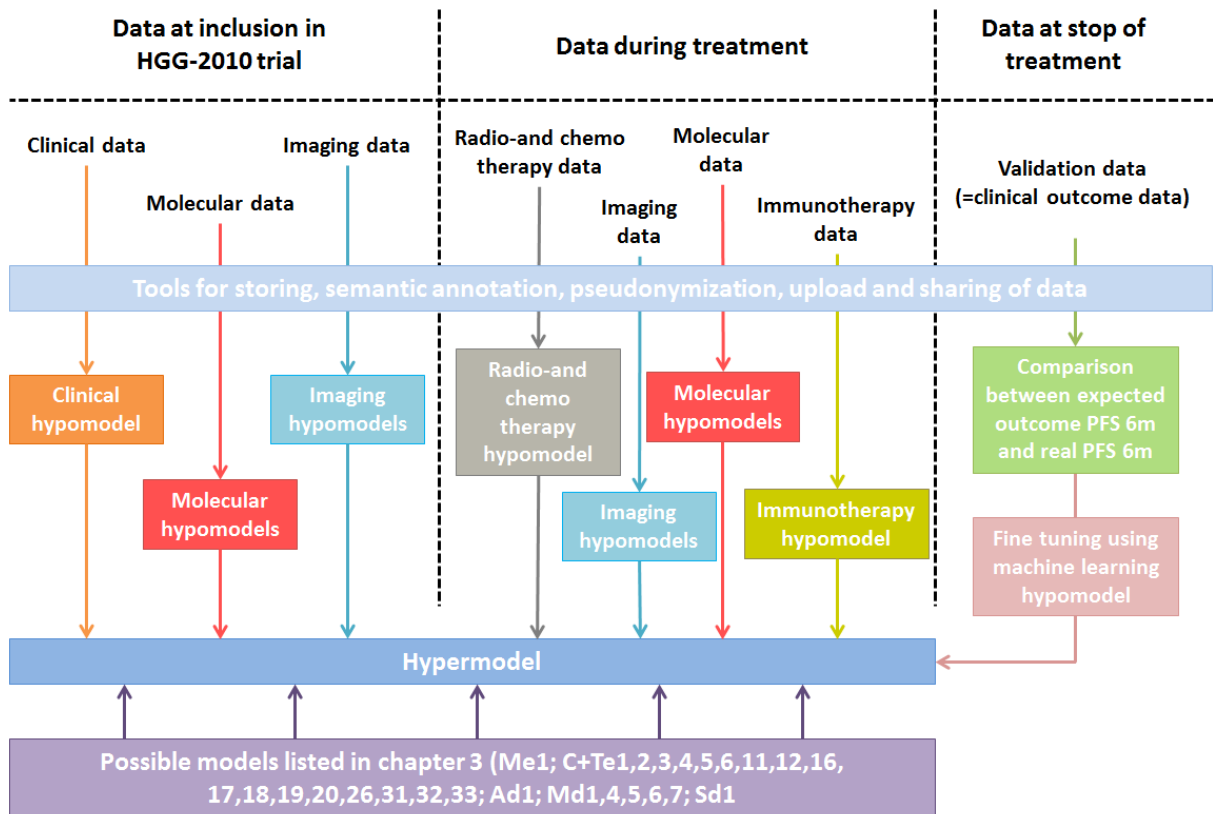


Fig. 6.2: Schematic view of the glioblastoma scenario described by the linkage of hypomodels composing the glioblastoma hypermodel

6.4.1 Data sharing and integration

All of the data described above need to be anonymized or pseudonymized and semantic annotated before uploading and storage at the CHIC platform for sharing, integration and usage. All the necessary tools and models to do so are described earlier in this deliverable.

KU Leuven will store all data in an in-house managed FileMaker database. From this database the data will be exported to the CHIC platform according to the legal framework of CHIC. Imaging data are stored on a DICOM server. These data need post-processing using tools developed within the CHIC project.

6.4.2 Clinical scenario

The clinical scenario will be translated into the clinical hypomodel. The RPA and the extent of resection are the most important clinical data related to outcome.

6.4.3 Imaging scenario

The imaging scenario consists of two parts:

In the inclusion phase: Imaging data of the tumor and its environment will be investigated (cfr above: location, volume of the contrast-enhancement, volume of perilesional oedema, cerebral blood volume in the contrast-enhancing lesions and mean diffusivity in the contrast-enhancing lesions). In this hypomodel will be investigated if these characteristics can predict a good response on DC vaccination.

During treatment: Imaging data collected in the follow-up setting of the study will be investigated in the second imaging hypomodel to investigate if changes in the imaging data can predict the outcome.

6.4.4 Molecular scenario

The molecular hypomodel consists of two parts:

In the inclusion phase: Molecular data of the tumor will be investigated (cfr above: mutational, methylation state, gene expression signature). It will be investigated in this hypomodel which tumors will have a good response on DC vaccination. Furthermore, immunologic data before start of treatment will be collected (before and after radiochemotherapy) to find in a separate hypomodel which immunologic state before start of DC vaccination will predict a good response and outcome.

During treatment: Molecular data of the immune cells will be collected as stated above in the process of immune monitoring. Clustering of multiple data will be performed. In this hypomodel, it will be investigated which changes in the immune system reflex and immunologic and clinical response. This will inform the clinician when to stop, change or intensify DC vaccination, and will give additional monitoring data besides the imaging data.

6.4.5 Radio- and chemotherapy scenario

Radio- and chemotherapy are part of the standard therapy for GBM so their efficacy in the GBM scenario has already been proven. Other models, as described in chapter 3 of this deliverable, can be used in this radio- and chemotherapy hypomodel.

6.4.6 Immunotherapy scenario

The immunotherapy scenario will be translated into the immunotherapy hypomodel. Data that will serve as input for this hypomodel will be specific to the outline of the study as described above. Immune monitoring will probably be of great value to this hypomodel.

6.4.7 Usage of models as listed in chapter 3 of this deliverable

It needs to be investigated if the hypomodels depicted in figure 6.3 and described in chapter 3 can be used in the glioblastoma hypermodel. Plausible linkage between these models with all other hypomodels of the glioblastoma hypermodel will be solved by semantic interoperability.

6.4.1 Validation scenario

The validation scenario will compare the real PFS 6m with the prediction of the hypermodel. This validation hypomodel will send this comparison to the machine learning hypomodel.

6.4.2 Machine learning scenario

The machine learning hypomodel will fine-tune the hypermodel to improve the prediction. The more often the hypermodel is used in different patients the better the prediction will get.

6.5 *Hypermodel for glioblastoma*

The hypermodel for GBM will predict if a single patient, with specific pretreatment, surgical and tumor characteristics will benefit from adding DC vaccination to standard therapy, in terms of PFS at 6 months.

7 Scenarios for Non-Small-Cell Lung Cancer (NSCLC)

7.1 Introduction and description of the scenario

Tumor-specific pathways detected very early after tumor diagnosis will be used to choose the most promising therapy as first line therapy, maintenance or adjuvant therapy. For that purpose a system biology model will be developed based on the transcriptome analysis of up to 100 tumour specimen to get new insights in the biology of NSCLC. This data will form the basis for the bottom-up approach of the in silico model for NSCLC and thus improving the accuracy of the developed in silico Hyper-Multiscale Models. All relevant clinical data, tumor typing according to the current adenocarcinoma classification as well as radiological, macroscopic, quantitative microscopic data, proliferation data and angiogenesis data were retrieved or collected prospectively from lung cancer resection specimens of NSCLC. Genetic profiles of the relevant pathways, miRNA data, and deep sequencing data of at least a limited number of well-defined NSCLCs, will be added for comprehensive analysis. Small biopsy samples of lung cancer, which are often the only tumor tissue available from patients with advanced NSCLC, manual dissection, laser-microdissection, quantitative few cell PCR approaches, DNA sequencing, biochip reverse-phase hybridization, mRNA preamplification and whole genome amplification are available as well as epidemiological and follow-up parameters from the Saarland Tumor Center and will be integrated into the Models for In Silico Oncology in order facilitate the therapy-related clinical decisions.

7.2 Available data and post-processing of data

7.2.1 Available data

There will be retrospective and prospective data available for the Non-Small Cell Lung Cancer (NSCLC) scenario. The retrospective data are data that are collected within the ContraCancrum project. For these data ethical approval is already available (Ethik-Kommission der Ärztekammer des Saarlandes Kenn-Nr.: 104/10 from 19th of August 2013; see also Appendix 2). Prospective data will be collected by the Institute of Pathology of the Saarland University. Ethical approval for the usage of these data within the CHIC needs to be obtained. All data will only be shared and used according to the legal framework of CHIC. Within this framework the data can be regarded as de-facto anonymous data.

The following data will be available for the NSCLC scenario:

Clinical data:

Gender, age, tumor localisation, tumor identification as primary tumor, tumor response to therapy, overall survival.

Pathological data:

Tumor size (in resection specimens), pTNM-Klassifikation, number of tumor-containing biopsies (in biopsy specimens), focus on tumor histotype according to IASLC adenocarcinoma classification proposal 2011, selection of specimens with predominant acinar pattern and predominant solid pattern (representing the largest groups of adenocarcinoma lung cancer subtypes), grading according to ATS/ ERS/ IASLC adenocarcinoma consensus, histological tumor necrosis, Ki67 proliferation data, CD31 angiogenesis data.

Imaging data:

Tumor localisation, tumor size, tumor margins, tumor necrosis.

Molecular data:

In order to ensure clinical relevance, the molecular data will be collected in a way to allow correlation with histological subtypes and / or clinical outcome.

EGFR, KRAS, BRAF, EML4-ALK will be analysed on primary tumor material.

- Epidermal growth factor receptor (EGFR) gene exon 19 and exon 21 status (activating mutation?, wild-type?),
- Kirsten RAS (KRAS) gene exon 2 and exon 3 status (activating mutation?, wild-type?)
- BRAF gene exon 15 (activating mutation?, wild-type?)
- EML4-ALK translocation (yes/ no)

miRNA signatures will be related to the clinical data of lung cancer.

The identified pattern will prospectively be correlated with the findings of the individual patients' prognosis. Ultimately the pattern will help to determine which of the aberrant parameters might be useful to be integrated as a parameter for the molecular hypomodel. For this purpose a focus will be on relevant aberrations and disrupted pathways in the tumor, thus stratifying treatment according to the individual outcome or even finding new drugs targeting disrupted pathways. To this end, it is important to emphasize that the molecular data stem from the same patient as the imaging, the histological and the clinical data.

7.2.2 Post processing of data

Imaging data will be uploaded on the DICOM server.

CT or MR images will be assessed preferentially for the identification of tumor necrosis.

7.2.3 Knowledge about data correlations

Up to now it is well known that therapy-relevant EGFR mutations are found at a rate of about 10% of adenocarcinoma cases in European populations with primary adenocarcinoma of the lung. KRAS mutations can be found in up to 33% of European primary lung adenocarcinomas [67]. Both mutation frequency rates differ considerably from the results in primary lung adenocarcinomas in Asian patients. With respect to outcome large series of the IASLC Lung Cancer Staging Project from 2007 described new stage groupings as the basis for the current TNM classification of lung cancer. Thus tumors >7 cm moved to the T3 category and pleural effusions were categorized as an M descriptor. Beyond the prognostic values of additional pulmonary nodules was reassessed and stage grouping of stage IB, IIA, IIB, IIIA and IIIB were redefined [68]. Tumor grading was recently defined for the most frequent adenocarcinoma subtypes of the ATS/ ERS/ IASLC proposal [69] and tumors with a predominant lepidic pattern were classified as grade 1, tumors with predominant acinar or papillary pattern were graded as grade 2 and tumors with predominant solid or micropapillary pattern were classified as grade 3 [70]. The prognostic applicability of this approach was shown in many specimens of stage I lung adenocarcinomas as well as in combined series of resected and non-resectable lung adenocarcinoma cases. The histologic parameters of vascular invasion, prominent nucleoli and mitotic activity recently turned out to be independently associated with metastatic potential [71]. The immunohistochemical lack of TTF-1 expression in adenocarcinomas was found to be an independent predictor of disease recurrence in intermediate-grade tumors [72].

7.3 Granular dissection of the scenario

The granularity of the scenario is based on the available data. 100 cases of the most frequent adenocarcinoma subtypes will be analyzed.

7.3.1 Data sharing and integration

All data will be pseudoanonymized and stored at the CHIC platform for sharing, integration and usage. Up to now roughly 50% of the clinical and molecular data could be raised.

7.3.2 Clinical scenario

The clinical scenario considers the most recent global updates of lung cancer classification, lung cancer staging and lung adenocarcinoma grading, as suggested by the ATS/ ERS/ IASLC consortium. They contributed considerably new knowledge to the field of lung cancer.

7.3.3 Imaging scenario

The imaging analyses focus mainly on CT- and MRI-reports with special evaluation of the clinical tumor size and the extension of tumor necrosis. Additionally tumor margins will be analyzed.

7.3.4 Molecular scenario

The molecular scenario will be the most challenging topic of analysis as its clinical impact might change during the course of the CHIC project due to data from ongoing trials. Up to now the survival prolongation of inoperable cases (stage IIIb and stage IV) with lung adenocarcinomas is well-documented in Asian and European populations. The detection of activating oncogenic mutations of the EGFR pathway [73] and the analysis of the EML4-ALK translocation status [74] are currently considered as the most important molecular parameters. Beyond, especially due to the considerably higher frequency of KRAS-mutations in lung cancer cases of European origin as compared to Asian cases, it is expected that the influence of KRAS wild-type or KRAS activating point mutations on survival and recurrence status will soon have stronger influence on therapy selection at least in patients with metastasis.

7.3.5 Drug selection scenario

The scientists of this part of the WP cannot primarily influence drug selection, as it is based not only on the morphological, imaging and molecular data but also clinical factors. Nevertheless the types of first line, second line and third line therapies performed will be recorded and considered within the outcome evaluation.

7.3.6 Validation scenario

All pathoanatomical procedures as well as histopathological procedures and immunohistological analyses are established in consultant-supervised laboratories and were/ will be evaluated by experienced anatomical pathologists. The validation of the molecular tests performed is achieved by recent participation in nation-wide laboratory quality control tests i.e. for EGFR-, KRAS- and BRAF-molecular analysis. For predictive purposes new cases of primary lung cancer will be selected after the hypomodel is established.

7.3.7 Machine learning scenario

This scenario will not be primarily established in the current part of project.

7.4 Hypermodel for NSCLC

The NSCLC hypermodel will focus on the both most frequent types of adenocarcinoma of the lung: the adenocarcinoma with predominant acinar pattern and the adenocarcinoma with predominant solid pattern. Various basic clusters of processes (biomechanisms) will be modelled at the cell/ tissue level in appropriate hypomodels

- Tumor cell cycling
- Biomechanics (e.g. tumour expansion and shrinkage)
- Tumor-host interaction (e.g. angiogenesis)
- Metabolic potential spatial distribution across the tumors

At the molecular level hypomodels for the following major clusters of hypomodels will be developed:

- for therapy-related oncogene mutations
- for miRNA expression data as analyzed by histotype of pulmonary adenocarcinoma and
- for estimators of the cell kill probability during chemotherapy and radiotherapy based on both statistics and pathway analysis

8 Scenarios for prostate cancer

8.1 Introduction and description of the scenario

The main question of our investigation is related to the management of the biochemical recurrences that sometimes follow the surgical/radiotherapy radical approach of the prostate cancer (see Fig. 8.1).

As a matter of fact, this scenario is the most dramatic one both for the patient and for the clinician, who faces the problem with salvage therapies and/or hormonal therapy (Androgen Deprivation Therapy) but often doesn't know enough about timing, dosage and success probability of such actions.

Modelling the natural evolution of the pathology and/or the effects of the therapies maybe extremely useful provided the models are properly validated on robust clinical data.

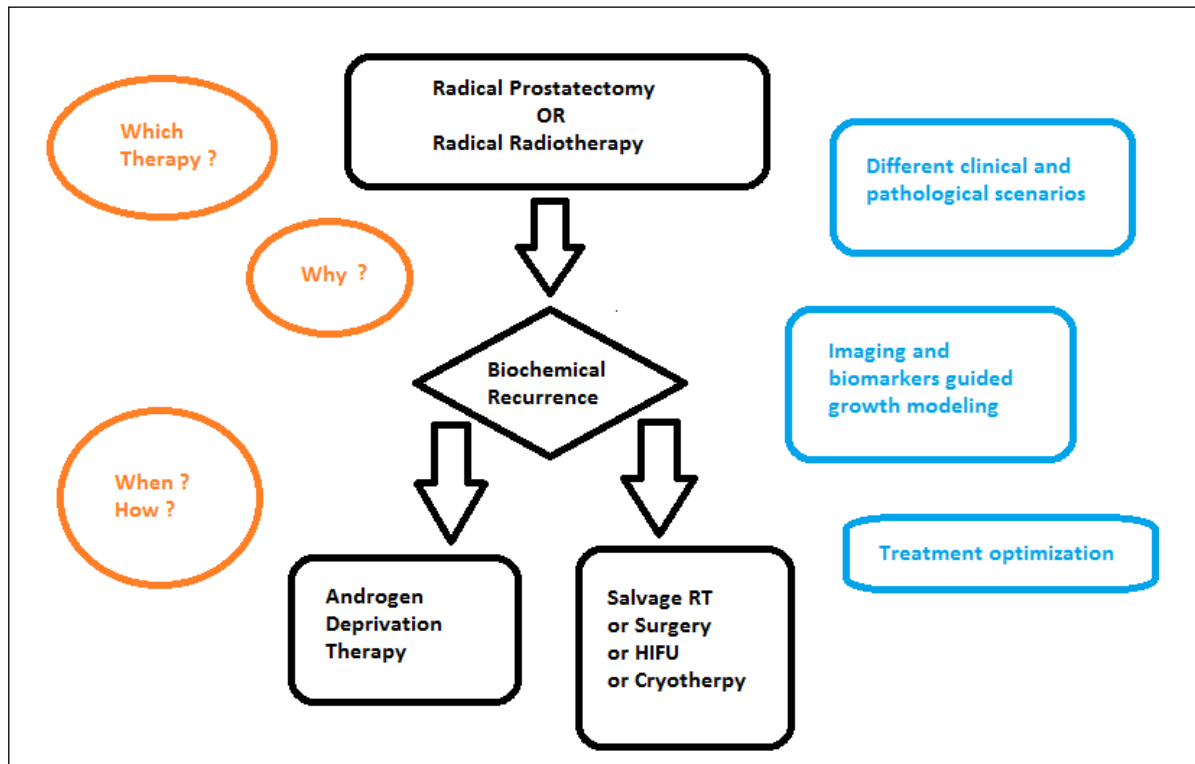


Fig. 8.1 – Rationale of prostate cancer studies.

A great extent of “hidden” knowledge is potentially available querying properly the clinical data from patients affected by the same disease. However there are many issues, from a practical (data are often on paper, such as medical records, in untidy and often incomplete form), ethical and, especially, methodological point of view.

Large data collections are normally interrogated using more or less complicated statistical models, in order to get information from a more or less homogeneous population, or to build nomograms and/or practical indications about therapies. Much less often they are used to properly validate mathematical models founded on biological assumptions, and to estimate with great accuracy the values of biologically relevant parameters.

In the framework of the European ICT Project CHIC focused on the building of a common repository for data and models in the field of human cancer, the activity of each research group is challenged by a number of requirements:

- data should be representative (similar in pertinence, accuracy, provenience, without bias in selection and treatment);
- data should be properly pseudo-anonymized to be shared among groups in different countries, with possibly different legal issues;
- data should be collected in a database easily included into larger or more structured ones;
- the database size and structure are selected in order to be able to host also diagnostic images and metadata, provisionally available from further perspective studies or analyses;
- data should be easily queried, using different statistical tools and different data mining approaches;
- data need to be protected against involuntary or voluntary hacking;
- data should be easily usable to validate models proposed by researchers, using different software and requiring different input formats.

In this context the prostate cancer group would specify three primary goals:

- 1) To fill in a huge database about prostate cancer in an homogeneous cohort (Italian Piedmont region population) with thousands of patients and about a hundred multi-scale fields, including clinical, serological, pathological, molecular and radiological data;
- 2) For the retrospective studies to develop a statistical model about reliable correlations between prognosis and risk factors, several of them already present in the existent formulas and some of them, like PSA doubling time, collected specifically and extensively by the present study;
- 3) For the perspective studies to develop mathematical models, more deterministic than the previous ones, taking into consideration, beyond the classical risk parameters, molecular markers and tumor volume, density, cellular burden and dynamics of growth estimated through imaging and molecular biology assays.

8.2 Available data and post-processing of data

8.2.1 Available data

In order to assure a good data representativeness we selected two specific prostate cancer patient cohorts: radical prostatectomy and radical radiotherapy (RT).

The patients, except a few, are treated in the geographical Italian region of Piedmont.

Two observational retrospective studies, named EUREKA-1 and EUREKA-2 with reference to surgical and RT studies respectively, were explicitly authorized last July 2013 by the Ethical committee of the IRCCS Candiolo, lead institution of the clinical studies.

A table of the clinical centres involved in the EUREKA-1 and EUREKA-2 studies is given below.

EUREKA-1 (Radical Prostatectomy)		EUREKA-2 (Radical Radiotherapy)	
Participating Hospital	Town	Participating Hospital	Town
Ospedale Molinette University	Torino	IRCCS	Candiolo
San Luigi Gonzaga University	Orbassano	Ospedale Maggiore University	Novara
Ospedale Maggiore University	Novara	San Luigi Gonzaga University	Orbassano
Ospedale San Giovanni Bosco	Torino	Ospedale Civile	Ivrea
Ospedale Santa Croce	Cuneo	Ospedale degli Infermi	Biella
Ospedale Regionale	Aosta	Ospedale Cardinal Massaia	Asti
Ospedale Gradenigo	Torino	Istituto Europeo di Oncologia	Milano
Ospedale Cardinal Massaia	Asti	Osp. Santa Chiara University	Pisa
Ospedale Civile / ASL Torino 4	Ivrea / Cirié		
Ospedale Santissima Trinità	Borgomanero		
Ospedale Maria Vittoria	Torino		
Ospedale Mauriziano	Torino		

A common database platform, consisting in some tens of parameters recorded before and after treatment and recoverable either from paper or electronic clinical records, was devised. Depending on the available licenses and operator skills databases are filed using MS-Excel or MS-Access.

All data will only be shared and used according to the legal framework of CHIC. Within this framework the data can be regarded as de-facto anonymous data. Each patient record is consecutively numbered and only the collecting center owns the 'key' connecting such number and the patient name.

More details on the clinical studies are given:

EUREKA-1 is a retrospective study on prostatectomysed patients, approved by Ethical Committee July 9th, 2013 (see Fig. 1), data collection started August 1st, 2013 and pertains to: anamnesis, diagnosis, biopsy, staging, radical prostatectomy and adjuvant therapies, pathology, clinical and serological follow-up, toxicity. Number of patients to be accrued: between 4000 and 4750.

EUREKA-2 is a retrospective study on irradiated patients, approved by Ethical Committee July 9th, 2013, data collection started August 1st, 2013 (see Appendix 2) and pertains to: anamnesis, diagnosis, biopsy, staging, radiotherapy technique and adjuvant therapies, clinical and serological follow-up, toxicity. Number of patients to be accrued: between 3500 and 4000.

In the following Tables (8.1, 8.2 and 8.3) details about the Prostate Tumor Staging and the Eureka1 and Eureka2 studies are given.

Table 8.1: Prostate cancer TNM staging

Primary Tumor categories

T1: Tumor not felt with a digital rectal exam (DRE) or seen with imaging such as transrectal ultrasound.

- **T1a:** Cancer is found incidentally (by accident) during a transurethral resection of the prostate (TURP) that was done for benign prostatic hyperplasia (BPH). Cancer is in no more than 5% of the tissue removed.
- **T1b:** Cancer is found during a TURP but is in more than 5% of the tissue removed.
- **T1c:** Cancer is found by needle biopsy that was done because of an increased PSA.

T2: Tumor felt with a DRE or seen with imaging such as transrectal ultrasound, but it still appears to be confined to the prostate gland.

- **T2a:** The cancer is in one half or less of only one side (left or right) of your prostate.
- **T2b:** The cancer is in more than half of only one side (left or right) of your prostate.
- **T2c:** The cancer is in both sides of your prostate.

T3: The cancer has begun to grow and spread outside your prostate and may have spread into the seminal vesicles.

- **T3a:** The cancer extends outside the prostate but not to the seminal vesicles.
- **T3b:** The cancer has spread to the seminal vesicles.

T4: The cancer has grown into tissues next to your prostate (other than the seminal vesicles), such as the urethral sphincter, the rectum, the bladder, and/or the wall of the pelvis.

N categories

N categories describe whether the cancer has spread to nearby (regional) lymph nodes.

NX: Nearby lymph nodes were not assessed.

N0: The cancer has not spread to any nearby lymph nodes.

N1: The cancer has spread to one or more nearby lymph nodes in the pelvis.

M categories

M0: The cancer has not spread past nearby lymph nodes.

M1: The cancer has spread beyond the nearby lymph nodes.

- **M1a:** The cancer has spread to distant (outside of the pelvis) lymph nodes.
- **M1b:** The cancer has spread to the bones.
- **M1c:** The cancer has spread to other organs such as lungs, liver, or brain (with or without spread to the bones).

Table 8.2: EUREKA-1 Data

ID Data	ID Number, Date of birth
Anamnesis and diagnosis	Familiarity for Prostate Cancer, ethnicity, number of biopsies executed, flogosis and precancerosis at biopsy, PCA-3 dosage, number of total and positive cores, core surface affected by tumor in %, bioptic monolateral versus bilateral tumor, pre-surgery PSA velocity
Staging	Initial PSA, clinical-radiological TNM staging, bioptic primary secondary and total Gleason Score, free-PSA, pro-PSA, Chromogranin-A dosage, Staging by Bone Scintigraphy, CT, MR with endorectal coil and choline-PET
Therapies	Date of Radical Prostatectomy, RP Type (open versus laparoscopic versus robotic and radical versus nerve-sparing), lymphadenectomy yes/no, Surgical center experience, neo-adjuvant and adjuvant androgen deprivation therapy data, RT adjuvant or salvage intent and technical data, first therapy after relapse and its date
Pathology	Pathologic primary secondary and total Gleason Score, pathologic T and N staging, Margin, ECE and Seminal vesicles status, number of total cropped nodes and metastatic ones, peri-neural and vascular invasion, HGPIN positivity
Toxicity	Urinary incontinence and erectile impotence
Follow-up	Last FU date, Biochemical relapse and its date, Clinical-Radiological Relapse and its date, site of relapse, death, cause of death and its date, first exam showing the macroscopic progression and its date, at least 4 PSA values after radical prostatectomy and their dates

Table 8.3: EUREKA-2 Data

ID Data	ID Number, Date of birth
Anamnesis and diagnosis	Familiarity for Prostate Cancer, ethnicity, ECOG Performance Status, Diabetes and Cardiovascular Diseases anamnesis, flogosis and precancerosis at biopsy, PCA-3 dosage, number of total and positive cores, core surface affected by tumor in %, pre-RT PSA velocity
Staging	Initial PSA, clinical-radiological TNM staging, bioptic primary secondary and total Gleason Score, free-PSA, pro-PSA, Chromogranin-A dosage, Staging by Bone Scintigraphy, CT, MR with endorectal coil, endorectal-echography and choline-PET
Therapies	RT start and end-dates, RT technique (3DCRT or IMRT), IGRT yes/no and IGRT type, RT center experience, Radiation Dose to primary tumor and its fractionation, pelvic irradiation data, rectum and bladder set-up protocols, doses to bladder and rectum, neo-adjuvant concomitant and adjuvant androgen deprivation therapy data, first therapy after relapse and its date
Toxicity	Acute and Chronic Genito-Urinary and Gastro-Intestinal Toxicities

Follow-up	Last FU date, Biochemical relapse and its date, Clinical-Radiological Relapse and its date, site of relapse, death, cause of death and its date, first exam showing the macroscopic progression and its date, at least 6 PSA values after radical RT and dates
-----------	--

8.2.2 Post processing of data

Data and DICOM images will be unpacked and transferred to a general database and stocked into a dedicated server physically situated in a room at UNITO.

The server is equipped with software for statistical analysis (SAS) and modeling (MatLab) purchased with academic licenses. The database structure can be dynamically resized when new data come from the clinical centers, and the statistical routines automatically updated.

8.2.3 Knowledge about data correlations

Simple statistical tables, graphs and formulas able to correlate clinical data with outcome and classify patients by risk of relapse after therapy with a concordance index between 70 and 75 % already exist in prostate cancer: the most famous are Partin Tables [75], Roach Formulas [76], Kattan nomogram [77], CAPRA-Score [78] and GPSM nomogram [79]. Besides the utility of combined therapies summing up surgery, radiotherapy and hormone-therapy has been shown several times in literature [80], [81]; the usefulness to check PSA dynamics after first-line treatment and to sum up its temporal evolution into parameters like PSA doubling time has been studied by [82], [83], [84], [85], [86] (see references).

8.3 Granular dissection of the scenario

8.3.1 Data sharing and integration

Data uploading to the CHIC platform for sharing, integrating and usage is a necessity. Data will be easily transferred to the common European database. The modeling features will be developed on a MatLab software platform, and will easily include already existing or future models.

8.3.2 Clinical scenario

The clinical scenario focuses on the traditional clues of cancer extension and aggressiveness: TNM staging, Gleason score, PSA value at diagnosis, biopsy cores' data and classical pathological parameters such as surgical margin status, capsular involvement, perineural and vascular invasion. Besides anamnestic data (such as familiarity for prostate cancer, ethnicity, main concomitant diseases), clinical and serological follow-up and toxicities are recorded.

In particular, we foresee two perspective clinical studies:

EUREKA-3 prospective study on irradiated patients, already written, to be submitted to the Ethical Committee in February 2014: thorough data about anamnesis, biopsy, staging, radiotherapy plans and hormone therapy schedule, clinical and serological follow-up, toxicity. Creation of an Imaging Data Bank to archive pictures and files coming from MRI, CT, PET and radiotherapy planning systems. Number of patients to be accrued: approximately 650.

EUREKA-4 prospective study on prostatectomised patients, protocol to be written: thorough data about anamnesis, biopsy, staging, surgery and adjuvant therapies, pathology and molecular biomarkers, clinical and serological follow-up, toxicity. Creation of a Tissue Bio-Bank to store and later on study molecular biomarkers and their prognostic value. Number of patients to be accrued: approximately 550.

8.3.3 Imaging scenario

Imaging data include mainly scintigraphy and CT reports for retrospective studies and MRI and CT-PET images for prospective ones. In fact MRI and PET-CT functional imaging are nowadays the golden standards to stage primary tumors and lymph nodes and to drive more conservative and personalized therapies [87], [88], [89], [90].

MRI sequences will include both anatomical T2-weighted scans and functional DCE and DWI ones. Besides in EUREKA-3 radiotherapy plans (both images and physical data) will be available too.

8.3.4 Molecular scenario

Molecular bio-markers like micro-RNA, expression mRNA and proteins are thought to disclose each cancer phenotype, aggressiveness, and sensibility to medical and radiation therapies. Some examples of biomarkers already studied in basic research and small cohorts of patients and ready for more extensive clinical applications may be E-Cadherin, Chromogranin, ki-67, bcl-2 (see references: [91], [92], [93], [94], [95], [96], [97], [98], [99], [100], [101]).

Molecular scenario will be developed in the prospective studies and will focus in several groups of markers:

- a) proliferation markers, such as Ki-67, bcl-2 and p53
- b) hormone-like molecules, like chromogranin
- c) cancer-stroma interaction proteins, like cadherin-E, metallo-proteinases and neo-vascularization markers, looking for clues of invasion and metastatization potential

8.3.5 Drug selection scenario

We'll consider the drug selection scenario in its extended meaning as therapy selection scenario including not only the drugs, mainly hormone-depriving drugs used in this setting, but also radiotherapy and surgery. For what concerns surgery the prostatectomy may be radical or nerve-sparing, open-space or laparoscopic or robotic, with or without lymphadenectomy. RT technique may be 3DCRT or IMRT with/without IGRT, with or without prophylactic pelvic irradiation and the dose may vary consistently (from 72 to more than 80 Gy). Regarding hormone therapy the choice of the drug, its dosage, lasting and continuity of assumption differ significantly, mainly according to the risk of relapse and the patient response.

8.3.6 Validation scenario

Final results from the perspective studies will allow a population-based validation based on software, which will drive the clinical therapeutic decision.

8.3.7 Machine learning scenario

Software available in the first step to physicians participating to the CHIC project, and thereafter to the whole scientific community.

8.4 Hypermodel for prostate cancer

The modelling features will be developed on the MatLab software platform.

According to the general structure of the CHIC project, models will be designed according to an horizontal and a vertical scheme.

i) horizontal structure (scenarios)

Clinical data will be dynamically stratified and organized as homogeneous clusters characterized by a range of values of a number of parameters that are assumed to be significant for prognosis according to previous nomogram-based studies.

Within each non-empty cluster the natural history of recurrence following prostatectomy or radical RT will be monitored based on the PSA values collected in the follow-up of the patients not further treated.

Data will be modelled according to a growth law which generalizes the Gompertz law with “growth spurts” (see references: [102], [103], [104], [105]) and estimates a set of parameters related to tumor duplication time and carrying capacity during each developmental phase (expressed as time at spurts mean ± SD).

$$\Delta y_m(t) = G(t_m, \sigma_m, t) y_{0m} \exp\left\{\left(\frac{a_m}{\beta_m}\right) [\exp(\beta_m(t - t_m)) - 1]\right\}, \quad (1)$$

In Eq. 1 parameter a is the growth rate, β represents a retardation factor, which may be defined as $\beta = -a_0/z_\infty$, where z_∞ is the asymptotic value of $z(t)$ and is related to the carrying capacity of the system, y_{0m} is the amplitude of the spurt at $t = t_m$, and $G(t_m, \sigma_m, t)$ is the Gauss cumulative function with average value t_m and standard deviation σ_m , defined by:

$$G(t_m, \sigma_m, t) = \frac{1}{\sqrt{2\pi}} \int_{-\infty}^t e^{-\frac{(\tau - t_m)^2}{2\sigma_m^2}} d\tau \quad (2)$$

A special case of the Gauss cumulative function is the Heaviside function that can be used when tumor growth is very rapid.

$$H(t_m, t) = G(t_m, 0, t) = \begin{cases} 0 & \text{if } t \leq t_m; \\ 1 & \text{if } t > t_m. \end{cases} \quad (3)$$

A set of situations of clinical interest will be selected for further validation, both on the experimental (perspective data collection) and the modelling point of view.

ii) *Vertical structure (granularity)*

For the selected scenarios a structured model will be developed based on the following steps:

- the actual tumor extension and temporal evolution will be validated in a small number of patients belonging to a given scenario by mean of accurate imaging of the tumor by functional MRI;
- according to the timing of the growth spurts, pertinent biomarkers (e.g. miRNA) will be identified and collected in a selected subset of patients, in order to focus the biological mechanisms at work and share the results with the modeller partners involved with the mathematical simulations at the microscopic level;
- the response to the therapies will be modelled based on follow-up data either sequel to the primary therapy (surgery or radiotherapy) or to a second-line one (e.g. hormone-therapy or salvage RT).

9 A brief outline of the hypermodels for nephroblastoma, lung cancer and glioblastoma multiforme to be developed by CHIC

In the following section a high level outline of the three hypermodels to be developed by CHIC for the cancer types of nephroblastoma (Wilms tumour), lung cancer and glioblastoma multiforme is provided. These three models will constitute the core of the corresponding hypermodel based CHIC Oncosimulators to be developed. A detailed description of the approaches will be provided in the deliverables of workpackage 6 starting with D6.2.

Nephroblastoma and lung cancer cases

The biocomplexity level (spatial scale) of reference i.e. the biocomplexity level to which all biological processes modelled will *finally* refer will be the cell/tissue level. Other levels such as the atomic level, the molecular level and the body system level (in which e.g. pharmacokinetics is modelled) will also be addressed and the corresponding processes will be modelled in order to perturb the values of a number of cell/tissue level parameters. Such perturbations will be based on the individual multiscale data of the patient. Obviously the patient individual data will also be exploited in order to estimate the initial values of several cell/tissue level parameters.

The following basic clusters of processes (biomechanisms) will be modelled at the **cell/tissue level** by developing appropriate hypomodels (i.e. component models)

1. Tumour cell cycling (either for free tumour growth or for tumour treatment)
2. Biomechanics (e.g. tumour expansion and shrinkage)
3. Tumour-host interaction (e.g. angiogenesis-neovasculature, immune system response)
4. Metabolic potential spatial distribution across the tumour

The hypomodels or their combinations will operate on a *hypermatrix of the status of the anatomic region of interest* [106] and lead to changes of certain aspects of the status. The precise way in which these operations are to take place, generally in an iterative way, will be indicated by a special program called the *orchestrator*.

As an example of biomechanism modelling, Fig. 9.1 shows a possible cytokinetic diagram to serve as a basis for the modelling of tumour cell cycling. Thus this model may constitute the “tumour cell cycling” hypomodel.

At the **molecular level** hypomodels for the following major clusters of hypomodels will be developed:

For the case of nephroblastoma: estimators of the nephroblastoma histology based on miRNA expression data. Both statistics based molecular biomarkers and molecular pathway based estimators will be addressed. It is noted that tumour histology determines cell kill probability, being a cellular level parameter, during chemotherapy.

For the case of lung cancer: estimators of the cell kill probability during chemotherapy and radiotherapy based on both statistics and pathway analysis will be developed.

All molecular level hypomodels will in some way address pertinent “hallmarks of cancer” [2]

At the **atomic level** for the case of lung cancer, hypomodels based on the simulation of drug-protein interactions using molecular dynamics will serve as perturbators of a number of molecular level parameters.

At the **body system level** for both nephroblastoma and lung cancer, hypomodels for the pharmacokinetics of the drugs administered will be developed.

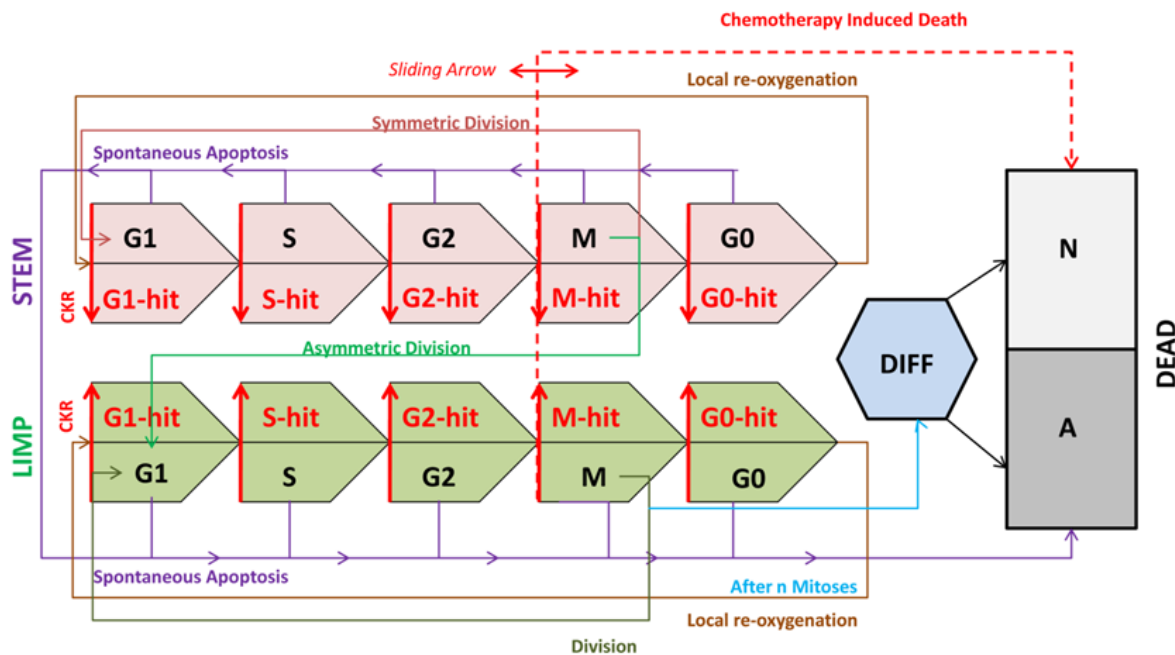


Fig. 9.1 A generic cytokinetic model for chemotherapy treatment. LIMP: Limited Mitotic Potential cell. DIFF: terminally differentiated cell. G1: Gap 1 phase. S: DNA synthesis phase. G2: Gap 2 phase. M: Mitosis. G0: dormant phase. N: necrosis. A: apoptosis. Hit: cell lethally hit by chemotherapy. CKR: Cell Kill Rate. The arrow indicating chemotherapy-induced death is a sliding arrow, with position dependent on the drug pharmacodynamics.

Glioblastoma multiforme cases

Since the cases of glioblastoma multiforme to be considered involve a highly complex combination of experimental immunotherapy with chemotherapy and radiotherapy, the modelling approach will consist of the following two stages.

In the first stage a model based on machine learning techniques such as neural networks and Bayes filters will be developed, trained and validated. This is expected to lead to the identification of those clinical, imaging and laboratory measurements that play a major role in the treatment outcome.

In the second stage, a mechanistic hypermodel based on the analysis of the previously identified most crucial measurements will be developed. The type of the measurements will dictate the nature and the structure of the corresponding hypomodels to be developed. The model development process will be quite similar to the one proposed for the nephroblastoma and lung cancer cases.

All three cancer types

In all hypermodels imaging, histological, molecular, clinical and treatment data will be exploited for all phases of model development, clinical adaptation and clinical validation. It is noted, however, that in the case of nephroblastoma histological data corresponding to time points only after the completion of the chemotherapeutic treatment and the following surgical excision of the tumour will be made available.

Regarding the mathematical approaches adopted, a mixture of discrete mathematics (e.g. discrete event simulation and the Monte Carlo technique) and continuous mathematics (e.g. ordinary and partial differential equations) will be used.

References [107], [108], [109], [110], [111], [112], [113], [114], [115], [116], [117] provide *background* information on a number of the hypomodeling approaches to be adopted.

10 Strategy of the CHIC project from the clinical perspective: Bridging clinical features to molecular mechanisms

This paragraph outlines the strategy of the CHIC project from the clinical perspective. It describes core elements of a generic oncology research **platform** that combines clinical image analysis with molecular- and cell-biology studies. These studies involve assaying, analytic and modelling steps. Specifically, this platform will focus on identifying the relationship between:

- (i) The variability of blood perfusion (**BP**) and cell density (**CD**) determined by tumour MRI image post-processing⁵,
- (ii) Molecular mechanisms (**MMs**) underlying such variability,
- (iii) Molecular mechanisms of treatment response on cellular level (**MM-TR**) and
- (iv) Clinical, pharmacological and pathological data.

In particular, the aim of this platform is to reproduce, through simulation, the frequency distribution of BP-CD pairs observed in the tumour image.

The proposed platform will consist of a pipeline of clinical, experimental and modelling procedural steps. The first step is to generate a **clinical dataset** that belongs to a **cohort** of cancer patients.

The **inclusion criteria** for the above cohort are that:

- (a) The patients are diagnosed with the same type of tumour;
- (b) The pre- and post-treatment tumour images are acquired via the same type of machine;
- (c) The tumour image data is post-processed via the same software, using the same settings, to calculate pre-defined indices for BP and CD for every pixel that belongs to the tumour;
- (d) Tissue for molecular readouts is acquired and assayed via the same protocol;
- (e) The patients undergo the same type of treatment

Therefore, the resultant clinical dataset will consist of (i) pixel-associated BP and CD indices, as well as (ii) molecular assay results relevant to the biology of the tumour. Machine learning-based methods that study the relationship between molecular readouts and clinical features can be carried out at this stage to identify clinically relevant biomarkers.

The pipeline will proceed with the analytic and modelling steps. This stage of the pipeline will take as input the above clinical dataset and carry out the following:

- 1) The molecular assay results [*with particular emphasis on biomarkers that have been identified*] will be mapped onto a dataset of MMs, such as (i) normal/pathological molecular pathways⁶, as well as (ii) drug ADME and mechanisms of action
- 2) Pre-existing or newly-developed mechanistic models that describe the above molecular pathways [taking into account parameter settings for both tumour-free and diseased tissue] will be linked to generic models that study (i) blood vessel development, (ii) cell division, (iii) tissue biomechanics, (iv) the resultant spatial organization of cells [*i.e.* tissue architecture, in response to (i) & (iii)], and (v) the overall tumour response to treatment;
- 3) A cell-based modelling infrastructure is used to instantiate (i) a population of [tumour-free and pre- / post-treatment diseased] tissue spaces representing MRI pixel volumes, such that

⁵ The following image processing open source tool is available:

<http://www.mitk.org/DiffusionImaging>

⁶ *e.g.* in nephroblastoma, for instance, blood-derived microRNA data will be analysed by the GeneTrail procedure (<http://genetrail.bioinf.uni-sb.de/>) (Molecular mechanisms) to determine which pathways are over-represented.

- each tissue space has (ii) a population of appropriately-parameterised cell-based models constructed in step 2;
- 4) The above models are run to produce frequency distributions of pixel-associated BP-CD pairs for tumour-free and pre- / post-treatment diseased tissue;
 - 5) The results of the above step are compared to the distributions from the clinical dataset.

A graphical outline of this strategy is given in figure 10.1.

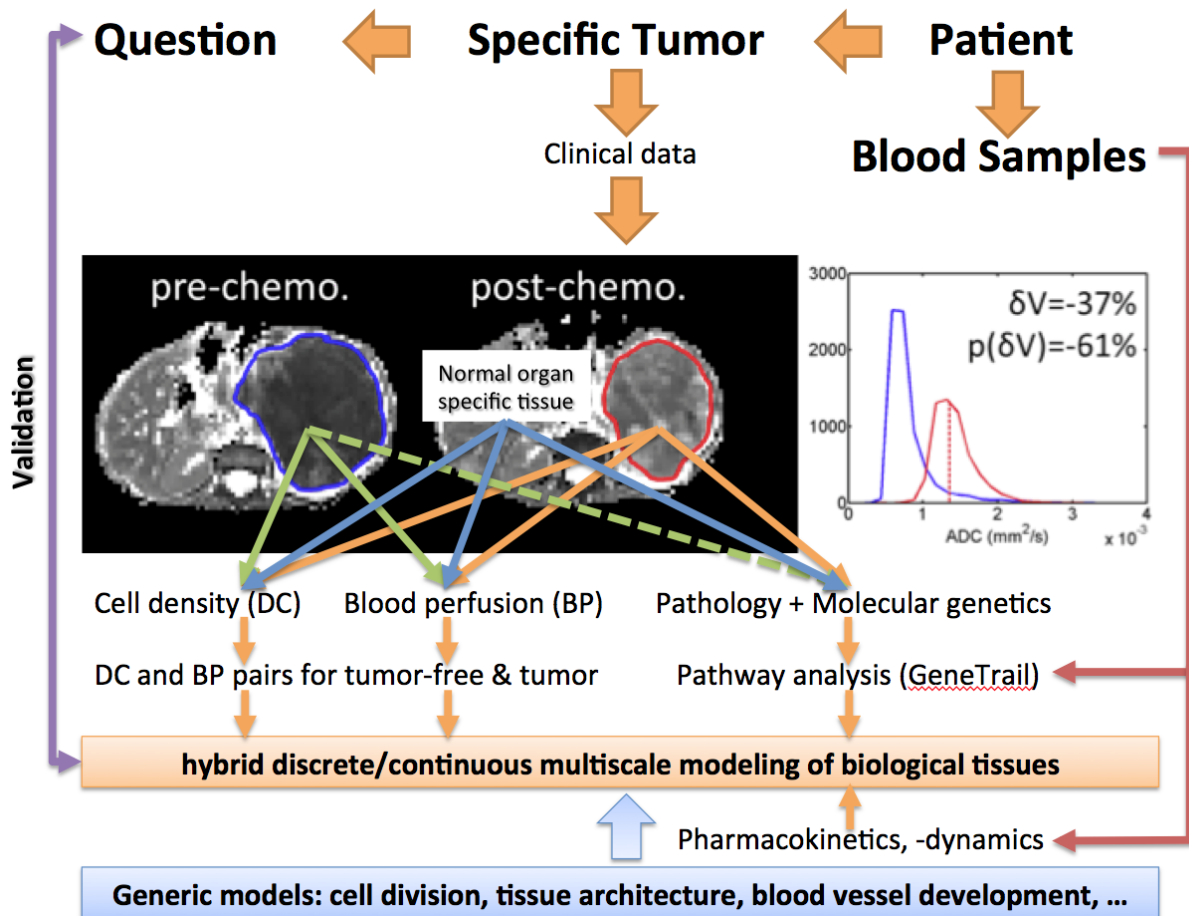


Fig. 10.1: A generic outline of the CHIC strategy from the clinical standpoint

11 Conclusion

This deliverable deals with the scenario based user needs and requirements and outlines the strategy of CHIC. Scenarios for nephroblastoma, glioblastoma, Non-small cell lung cancer and prostate cancer are described as the basis of the hypermodels to be developed. These scenarios are dissected into granular components and translated into use cases for hypomodels. From a technological perspective the project is based on the three layers, multiscale biology, engineering and Software. Most important for the architecture is the modularity of the system. All developed software, tools and services will be as granular and modular as possible and provide standardized, open interfaces and functionality descriptions, so that a user can easily build new models as a composition of existing granular tools. Such an approach needs to standardize interfaces between different tools and tools and data. A description of such specifications will be done, that allows different research groups how to standardize their data and what are preconditions to run such composed models.

We are facing on one side a bottom-up approach coming from biology and a top-down approach coming from the clinical side. To combine both approaches in one model we start to model both approaches by interacting with each others to define which data can be provided by executing models from the bottom-up approach that might get input data for the top-down approach. Therefore the development of the architecture for CHIC needs to take interoperability issues into account. A categorization of models into four different levels (technical, basic, domain unspecific, domain specific and hypermodel specific) will guarantee the reuse of hypomodels in hypermodels in different domains.

It is agreed that for each of the cancer domains one single question will be answered by a hypermodel that will be developed composed of different models including hypermodels themselves. The steps during the developmental process are clearly defined and start from the description of a scenario to answer a clinical relevant question. It ends with the validation of the hypermodel with prospective data. This is done in iterative process involving all partners of CHIC. A general outline of the strategy is given in chapter 4 of this deliverable.

In Appendix 3 relevant cancer models are listed and ranked according to their relevance for CHIC hypermodels. All these models are categorized according to different scales: the atomic, molecular, cellular and body scale. In addition tools are needed that serve as component models and fulfil necessary functionalities needed in general for (hyper-)models. These are IT tools that define the architecture, security tools like pseudonymization and/or anonymization tools and tools dealing with semantic interoperability. These tools are needed for each (hyper-)model and they will be generalized and reusable for all developed (hyper-)models within the CHIC project. Last but not least the question of standardization of interfaces will be addressed to simplify the linkage of component models to build a hypermodel.

For the most relevant cancer domains addressed in the CHIC project the hypermodels are described in detail in chapters 5 to 8. A brief outline of the hypermodels for nephroblastoma, lung cancer and glioblastoma multiforme to be developed by CHIC is given in chapter 9. Chapter 10 summarizes the overall strategy of the CHIC platform.

12 References

- [1] Hanahan D, Weinberg RA: The hallmarks of cancer. *Cell* 100:57–70, 2000
- [2] Hanahan D, Weinberg RA: Hallmarks of cancer: the next generation. *Cell* 144:646–674, 2011
- [3] Hainaut P, Plymoth A: Targeting the hallmarks of cancer: towards a rational approach to next-generation cancer therapy. *Curr Opin Oncol* 25:50–51, 2013
- [4] Vujanic GM, Sandstedt B, Harms D, Kelsey A, Leuschner I, de Kraker J; SIOP Nephroblastoma Scientific Committee: Revised International Society of Paediatric Oncology (SIOP) working classification of renal tumors of childhood. *Med Pediatr Oncol* 38:79–82, 2002
- [5] Huff V: Wilms' tumours: about tumour suppressor genes, an oncogene and a chameleon gene. *NRC* 11:111–121, 2011
- [6] Rivera MN et al.: An X chromosome gene, WTX, is commonly inactivated in Wilms tumor. *Science* 315:642–645, 2007
- [7] Hastie ND: The genetics of Wilms' tumor; a case of disrupted development. *Ann Rev Genet* 1994; 28: 523–58, 1994
- [8] Pelletier J, Bruening W, Kashtan CE, et al.: Germline mutations in the Wilms' tumor suppressor gene are associated with abnormal urogenital development in Denys-Drash syndrome. *Cell* 67: 437–47
- [9] Barbaux S, Niaudet P, Gubler, MC et al.: Donor splice-site mutations in WT1 are responsible for Frasier syndrome. *Nature Genet* 17: 467–470, 1997
- [10] Pritchard-Jones K: Molecular genetic pathways to Wilms' tumour. *Crit Rev Oncog* 1997; 8: 1–27
- [11] Huff V: Wilms tumor genetics. *Am J Med Genet* 79: 260–267, 1998
- [12] Schumacher V, Schneider S, Figg A et al.: Correlation of germ-line mutations and two-hit inactivation WT1 gene with Wilms' tumors of stromal-predominant histology. *Proc Natl Acad Sci USA* 94: 3972–3977, 1997
- [13] Brown KW, Malik KT: The molecular biology of Wilms tumour. *Expert Rev Mol Med* 2001:1-16, 2001
- [14] Zin R, Murch A, Charles A: Pathology, genetics and cytogenetics of Wilms' tumour. *Pathology*. 43:302-312, 2011
- [15] EnScott RH, Stiller CA, Walker L, Rahman N: Syndromes and constitutional chromosomal abnormalities associated with Wilms tumour. *J Med Genet* 43:705-715, 2006
- [16] Rahman N, Arbour L, Tonin P et al.: Evidence for a familial Wilms' tumour gene (FWT1) on chromosome 17q12-q211. *Nat Genet* 13: 461–463, 1996
- [17] Rapley EA, Barfoot R, Bonaiti-Pellie C et al.: Evidence for susceptibility genes to familial Wilms' tumor in addition to WT1, FWT1 and FWT2. *Br J Cancer* 83:177–183, 2000
- [18] Turnbull C, Perdeaux E, David Pernet et al.: A genome-wide association study identifies susceptibility loci for Wilms tumor. *Nature Genetics* 44:681-684, 2012
- [19] Scott RH, Stiller CA, Walker L, Rahman N.: Syndromes and constitutional chromosomal abnormalities associated with Wilms tumour. *J Med Genet* 43:705-715, 2006
- [20] Huff V: Genotype/phenotype correlations in Wilms' tumor. *Med Pediatr Oncol* 27:408-414, 1996

-
- [21] Arai E, Wakai-Ushijima S, Fujimoto H et al.: Genome-wide DNA methylation profiles in renal tumors of various histological subtypes and non-tumorous renal tissues. *Pathobiology* 78:1-9, 2011
- [22] Morris MR, Ricketts CJ, Gentle D et al.: Genome-wide methylation analysis identifies epigenetically inactivated candidate tumour suppressor genes in renal cell carcinoma. *Oncogene* 30:1390-1401, 2011
- [23] Purdue MP, Johansson M, Zelenika D et al.: Genome-wide association study of renal cell carcinoma identifies two susceptibility loci on 2p21 and 11q13.3. *Nat Genet* 43:60-65, 2011
- [24] Chen M, Ye Y, Yang H, Tamboli et al.: Genome-wide profiling of chromosomal alterations in renal cell carcinoma using high-density single nucleotide polymorphism arrays. *Int J Cancer* 125:2342-2348, 2009
- [25] Varela I, Tarpey P, Raine K et al.: Exome sequencing identifies frequent mutation of the SWI/SNF complex gene PBRM1 in renal carcinoma. *Nature* 469:539-542, 2011
- [26] Keller A, Leidinger P, Bauer A et al. Toward the blood-born miRNome of human diseases. *Nature methods*, 8:841-843, 2011
- [27] Schmitt J, Backes C, Nourkami-Tutdibi N et al. Treatment independent miRNA signature in blood of Wilms tumor patients. *BMC Genomics* 13:379, 2012
- [28] Schmitt J, Heisel S, Keller A, et al. Multicenter study identified molecular blood-born protein signatures for Wilms Tumor. *Int J Cancer* 131:673-682, 2012
- [29] Leidinger P, Keller A, Backes C, Huwer H, Meese, E. MicroRNA expression changes after lung cancer resection: a follow-up study. *RNA Biol* 9:900-910, 2012
- [30] Benjamini Y, Hochberg Y. Controlling the False Discovery Rate: A Practical and Powerful Approach to Multiple Testing. *J R Statist Soc B* 57: 289–300, 1995
- [31] Guyon I, E.A. 2003. An Introduction to Variable and Feature Selection. *Journal of Machine Learning Research*: 1157-1182.
- [32] Lu M, Shi B, Wang J, Cao Q, Cui Q. TAM: a method for enrichment and depletion analysis of a microRNA category in a list of microRNAs. *BMC Bioinformatics* 2010;11:419.
- [33] Backes C, Keller A, Kuentzer J, Kneissl B, Comtesse N, et al. (2007) GeneTrail--advanced gene set enrichment analysis. *Nucleic Acids Res* 35: W186-192.
- [34] Keller A, Backes C, Al-Awadhi M, Gerasch A, Küntzer J, Kohlbacher O, Kaufmann M, Lenhof HP. GeneTrailExpress: a web-based pipeline for the statistical evaluation of microarray experiments. *BMC Bioinformatics*. 2008 Dec 22;9:552
- [35] Ruslan D, Graf N, Karatzanis I, Stenzhorn H, Manikis GC, Sakkalis V, Stamatakos GS, Marias K: Clinical Evaluation of DoctorEye Platform in Nephroblastoma. In G. Stamatakos and D. Dionysiou (Eds): *Proc. 2012 5th Int. Adv. Res. Workshop on In Silico Oncology and Cancer Investigation – The TUMOR Project Workshop (IARWISOCI)*, Athens, Greece, Oct.22-23, 2012 (<http://www.5th-iarwisoci.iccs.ntua.gr>), pp.39-42. ISBN: 978-618-80348-0-8 (open-access version)
- [36] Johansson JO: Measuring homogeneity of planar point-patterns by using kurtosis. *Pattern Recognition Letters* 21:1149-1156, 2000
- [37] Szafer A, Zhong J, Anderson AW, Gore JC. Diffusion-weighted imaging in tissues: theoretical models. *NMR Biomed* 8:289–296, 1995
- [38] Einarsdóttir H, Karlsson M, Wejde J, Bauer HC. Diffusion-weighted MRI of soft tissue tumours. *Eur Radiol* 14:959–963, 2004
-

-
- [39] Owens CM, Brisse HJ, Olsen ØE, Begent J, Smets AM: Bilateral disease and new trends in Wilms tumour. *Pediatr Radiol* 38:30–39, 2008
- [40] Humphries PD, Sebire NJ, Siegel MJ, Olsen ØE Tumors in pediatric patients at diffusion-weighted MR imaging: apparent diffusion coefficient and tumor cellularity. *Radiology* 245:848-854, 2007
- [41] Graf N: Nephroblastom (Wilms-Tumor): In: *Hiddemann W, Huber H, Bartram CR, (Hrsg): Die Onkologie, Teil 2, Springer-Verlag, ISBN 3-540-64648-5, S. 1677-1696, 2004*
- [42] Estlin EJ, Graf N: Renal Tumors. p193-215, 2010. In: *Pediatric Hematology and Oncology: Scientific Principles and Clinical Practice*. Edward Estlin (Editor), Richard Gilbertson (Editor), Rob Wynn (Editor). ISBN: 978-1-4051-5350-8
- [43] Graf N, Bergeron C: Wilms and other renal tumors. In: *Stevens MCG, Caron HN, Biondi A. Cancer in children. 6th edition. Oxford University Press 2012. ISBN 978-0-19-959941-7, S. 312-327*
- [44] Wan SZ, Coveney PV, Flower DR: Peptide recognition by the T cell receptor: comparison of binding free energies from thermodynamic integration, Poisson-Boltzmann and linear interaction energy approximations. *Philosophical Transactions of the Royal Society A-Mathematical Physical and Engineering Sciences* 363, 2037-2053, 2005
- [45] Liu Y, Agrawal NJ, Radhakrishnan R: A flexible-protein molecular docking study of the binding of ruthenium complex compounds to PIM1, GSK-3 β , and CDK2/Cyclin A protein kinases. *J Mol Model*, 2011, DOI 10.1007/s00894-012-1555-4
- [46] Park JH, Liu Y, Lemmon MA, Radhakrishnan R: Erlotinib binds both inactive and active conformations of the EGFR tyrosine kinase domain. *Biochem J* 448:417-423, 2012
- [47] Stupp R, Mason WP, van den Bent MJ, et al. Radiotherapy plus concomitant and adjuvant temozolomide for glioblastoma. *N. Engl. J. Med.* 2005;352(10):987–96
- [48] Ardon H et al. Integration of autologous dendritic cell-based immunotherapy in the standard of care treatment for patients with newly diagnosed glioblastoma: results of the HGG-2006 phase I/II trial. *Cancer Immunol. Immunother.* 2012;61(11):2033–44
- [49] Phillips HS, Kharbanda S, Chen R, et al. Molecular subclasses of high-grade glioma predict prognosis, delineate a pattern of disease progression, and resemble stages in neurogenesis. *Cancer Cell.* 2006;9(3):157–73
- [50] Verhaak RGW, Hoadley K a, Purdom E, et al. Integrated genomic analysis identifies clinically relevant subtypes of glioblastoma characterized by abnormalities in PDGFRA, IDH1, EGFR, and NF1. *Cancer Cell.* 2010;17(1):98–110
- [51] Sturm D et al, Hotspot mutations in H3F3A and IDH1 define distinct epigenetic and biological subgroups of glioblastoma. *Cancer Cell.* 2012;22(4):425–37
- [52] Prins RM et al. Gene expression profile correlates with T cell infiltration and relative survival in glioblastoma patients vaccinated with dendritic cell immunotherapy. *Clin. Dev. Immunol.* 2011;17(6):1603–1615
- [53] Mirimanoff R-O et al. Radiotherapy and temozolomide for newly diagnosed glioblastoma: recursive partitioning analysis of the EORTC 26981/22981-NCIC CE3 phase III randomized trial. *J. Clin. Oncol.* 2006;24(16):2563–9)
- [54] Radford MM. A rapid and sensitive method for the quantitation of microgram quantities of protein utilizing the principle of protein-dye binding. *Anal Biochem* 1976; 72:248-54
-

-
- [55] Fadul CE et al. Immune response in patients with newly diagnosed glioblastoma multiforme treated with intranodal autologous tumor lysate-dendritic cell vaccination after radiation chemotherapy. *J. Immunother.* 2011;34(4):382–389
- [56] Wolff JE, Daumling E, Dirksen A, Dabrock A, Hartmann M, Jurgens H. [Munster Heidelberg Abilities Scale—a measuring instrument for global comparison of illness sequelae]. *Klin Padiatr* 1996; 208(5):294-8
- [57] Aaronson NK, Ahmedzai S, Bergman B et al. The European Organization for Research and Treatment of Cancer QLQC30: a quality-of-life instrument for use in international clinical trials in oncology. *J Natl Cancer Inst* 1993; 85(5):365-76
- [58] Osoba D, Aaronson N, Zee B, Sprangers M, te Velde A. Modification of the EORTC QLQ-C30 (version 2.0) based on content validity and reliability testing in large samples of patients with cancer. The Study Group on Quality of Life of the EORTC and the Symptom Control and Quality of Life Committees of the NCI of Canada Clinical Trials Group. *Qual Life Res* 1997; 6(2):103-8
- [59] Osoba D, Aaronson NK, Muller M et al. The development and psychometric validation of a brain cancer quality- of-life questionnaire for use in combination with general cancer- specific questionnaires. *Qual Life Res* 1996; 5(1):139-50
- [60] Osoba D, Aaronson NK, Muller M et al. Effect of neurological dysfunction on health-related quality of life in patients with high-grade glioma. *J Neurooncol* 1997; 34(3):263-78
- [61] Dummer W, Niethammer AG, Baccala R, et al. T cell homeostatic proliferation elicits effective antitumor autoimmunity. *J. Clin. Invest.* 2002;110(2):157–159
- [62] Zierler KL (1965) Equations for measuring blood flow by external monitoring of radioisotopes. *Circulation Research* 16: 309–321
- [63] Stejskal EO, Tanner JE. Spin Diffusion Measurements: Spin echoes in the presence of a time-dependent field gradient. *Journal of Chemical Physics* 1965 Jan 1;42(1):288-92
- [64] Wen PY, Macdonald DR, Reardon DA, et al. Updated response assessment criteria for high-grade gliomas: response assessment in Neuro-Oncology Working Group. *J Clin Oncol* 2010;28(11):1963-1972
- [65] Lacerda S, Law M. Magnetic resonance perfusion and permeability imaging in brain tumors. *Neuroimaging Clin N Am.* 2009 Nov;19(4):527-57
- [66] Jain R, Poisson L, Narang J, Gutman D, Scarpace L, Hwang SN, Holder C, Wintermark M, Colen RR, Kirby J, Freymann J, Brat DJ, Jaffe C, Mikkelsen T. Genomic mapping and survival prediction in glioblastoma: molecular subclassification strengthened by hemodynamic imaging biomarkers. *Radiology.* 2013 Apr;267(1):212-20
- [67] Smits AJ, Kummer JA, Hinrichs JW, Herder GJ, Scheidel-Jacobse KC, Jiwa NM, Ruijter TE, Nooijen PT, Looijen-Salamon MG, Ligtenberg MJ, Thunnissen FB, Heideman DA, de Weger RA, Vink A. EGFR and KRAS mutations in lung carcinomas in the Dutch population: increased EGFR mutation frequency in malignant pleural effusion of lung adenocarcinoma. *Cell Oncol (Dordr).* 2012;35(3):189-96
- [68] Goldstraw P, Crowley J, Chansky K, Giroux DJ, Groome PA, Rami-Porta R, Postmus PE, Rusch V, Sobin L; International Association for the Study of Lung Cancer International Staging Committee; Participating Institutions. The IASLC Lung Cancer Staging Project: proposals for the revision of the TNM stage groupings in the forthcoming (seventh) edition of the TNM Classification of malignant tumours. *J Thorac Oncol.* 2007 Aug;2(8):706-14. Erratum in: *J Thorac Oncol.* 2007;2(10):985
-

- [69] Travis WD, Brambilla E, Noguchi M, Nicholson AG, Geisinger KR, Yatabe Y, Beer DG, Powell CA, Riely GJ, Van Schil PE, Garg K, Austin JH, Asamura H, Rusch VW, Hirsch FR, Scagliotti G, Mitsudomi T, Huber RM, Ishikawa Y, Jett J, Sanchez-Cespedes M, Sculier JP, Takahashi T, Tsuboi M, Vansteenkiste J, Wistuba I, Yang PC, Aberle D, Brambilla C, Flieder D, Franklin W, Gazdar A, Gould M, Hasleton P, Henderson D, Johnson B, Johnson D, Kerr K, Kuriyama K, Lee JS, Miller VA, Petersen I, Roggli V, Rosell R, Saijo N, Thunnissen E, Tsao M, Yankelewitz D. International association for the study of lung cancer/american thoracic society/european respiratory society international multidisciplinary classification of lung adenocarcinoma. *J Thorac Oncol*. 2011;6(2):244-85.
- [70] Sica G, Yoshizawa A, Sima CS, Azzoli CG, Downey RJ, Rusch VW, Travis WD, Moreira AL. A grading system of lung adenocarcinomas based on histologic pattern is predictive of disease recurrence in stage I tumors. *Am J Surg Pathol*. 2010;34(8):1155-62
- [71] Xu L, Tavora F, Burke A. Histologic features associated with metastatic potential in invasive adenocarcinomas of the lung. *Am J Surg Pathol*. 2013;37(7):1100-8
- [72] Kadota K, Nitadori J, Sarkaria IS, Sima CS, Jia X, Yoshizawa A, Rusch VW, Travis WD, Adusumilli PS. Thyroid transcription factor-1 expression is an independent predictor of recurrence and correlates with the IASLC/ATS/ERS histologic classification in patients with stage I lung adenocarcinoma. *Cancer*. 2013;119(5):931-8
- [73] Rosell R, Carcereny E, Gervais R, Vergnenegre A, Massuti B, Felip E, Palmero R, Garcia-Gomez R, Pallares C, Sanchez JM, Porta R, Cobo M, Garrido P, Longo F, Moran T, Insa A, De Marinis F, Corre R, Bover I, Illiano A, Dansin E, de Castro J, Milella M, Reguart N, Altavilla G, Jimenez U, Provencio M, Moreno MA, Terrasa J, Muñoz-Langa J, Valdivia J, Isla D, Domine M, Molinier O, Mazieres J, Baize N, Garcia-Campelo R, Robinet G, Rodriguez-Abreu D, Lopez-Vivanco G, Gebbia V, Ferrera-Delgado L, Bombaron P, Bernabe R, Bearz A, Artal A, Cortesi E, Rolfo C, Sanchez-Ronco M, Drozdowskyj A, Queralt C, de Aguirre I, Ramirez JL, Sanchez JJ, Molina MA, Taron M, Paz-Ares L; Spanish Lung Cancer Group in collaboration with Groupe Français de Pneumo-Cancérologie and Associazione Italiana Oncologia Toracica. Erlotinib versus standard chemotherapy as first-line treatment for European patients with advanced EGFR mutation-positive non-small-cell lung cancer (EURTAC): a multicentre, open-label, randomised phase 3 trial. *Lancet Oncol*. 2012;13(3):239-46
- [74] Thunnissen E, Bubendorf L, Dietel M, Elmberger G, Kerr K, Lopez-Rios F, Moch H, Olszewski W, Pauwels P, Penault-Llorca F, Rossi G. EML4-ALK testing in non-small cell carcinomas of the lung: a review with recommendations. *Virchows Arch*. 2012;461(3):245-57
- [75] Eifler JB, Feng Z, Lin BM, Partin MT, Humphreys EB, Han M, Epstein JI, Walsh PC, Trock BJ and Partin AW, An updated prostate cancer staging nomogram (Partin tables) based on cases from 2006 to 2011, *BJU* 2012; 111: 22-29
- [76] Abdollah F, Cozzarini C, Suardi N, Gallina A, Capitanio U, Bianchi M, Tutolo M, Salonia A, La Macchia M, Di Muzio N, Rigatti P, Montorsi F and Briganti A, Indications for pelvic nodal treatment in prostate cancer should change. Validation of the Roach Formula in a large extended nodal dissection series, *Int J Radiation Oncol Biol Phys* 2012; 83: 624-629
- [77] Kattan MW, Wheeler TM and Scardino PT, Postoperative Nomogram for Disease Recurrence after Radical Prostatectomy for Prostate Cancer, *J Clin Oncol* 1999; 17: 1499-1507
- [78] Cooperberg MR, Hilton JF and Carroll PR, The CAPRA-S score: a straightforward tool for improved prediction of outcomes after radical prostatectomy, *Cancer* 2011; 117: 5039–5046
- [79] Houston Thompson R, Blute ML, Slezak JM, Bergstralh EJ and Leibovich BC, Is the GPSM Scoring Algorithm for Patients with Prostate Cancer Valid in the Contemporary Era?, *J Urology* 2007; 178: 459-463

-
- [80] Bolla M, van Poppel H, Collette L, van Cangh P, Vekemans K, Da Pozzo L, de Reijke TM, Verbaeys A, Bosset JF, van Velthoven R, Maréchal JM, Scalliet P, Haustermans K and Piérart M, Postoperative radiotherapy after radical prostatectomy: a randomised controlled trial (EORTC trial 22911), *Lancet* 2005; 366: 572-78
- [81] Nguyen QN, Levy LB, Lee AK, Choi SS, Frank SJ, Pugh TJ, McGuire S, Hoffman K and Kuban DA, Long-Term Outcomes for Men With High-Risk Prostate Cancer Treated Definitively With External Beam Radiotherapy With or Without Androgen Deprivation, *Cancer* 2013; 119: 3265-71
- [82] Dimonte G, Bergstralh EJ, Bolander ME, Karnes RJ and Tindall DJ, Use of Tumor Dynamics to Clarify the Observed Variability Among Biochemical Recurrence Nomograms for Prostate Cancer, *Prostate* 2012; 72: 280-290
- [83] D'Amico AV, Chen MH, Roehl KA and Catalona WJ, Identifying Patients at Risk for Significant Versus Clinically Insignificant Postoperative Prostate-Specific Antigen Failure, *J Clin Oncol* 2005; 23: 4975-4979
- [84] Cannon GM Jr, Walsh PC, Partin AW and Pound CR, Prostate-specific antigen doubling time in the identification of patients at risk for progression after treatment and biochemical recurrence for prostate cancer, *Urology* 2003; 62 (Suppl 6B): 2-8
- [85] Castorina P, Carcò D, Guiot C and Deisboeck TS, Tumor Growth Instability and Its Implications for Chemotherapy, *Cancer Res* 2009; 69: 8507-8515
- [86] Guiot C, Garibaldi E, Gabriele D and Gabriele P, Prostate tumour growth modelled by a statistically -modulated PUN scheme, Advanced research workshop on in silico oncology and cancer investigation - the TUMOR project workshop (IARWISOCI), 2012 5th International
- [87] Wang L, Incremental value of magnetic resonance imaging in the advanced management of prostate cancer, *World J Radiol* 2009; 1: 3-14
- [88] Meijer H, Debats OA, van Lin E, Witjes JA, Kaanders J and Barentsz JO, A retrospective analysis of the prognosis of prostate cancer patients with lymph node involvement on MR lymphography: who might be cured, *Radiation Oncology* 2013; 8: 190
- [89] Rischke HC, Nestle U, Fechter T, Doll C, Volegova-Neher N, Henne K, Scholber J, Knippen S, Kirste S, Grosu AL, and Jilg CA, 3 Tesla multiparametric MRI for GTV-definition of Dominant Intraprostatic Lesions in patients with Prostate Cancer - an interobserver variability study, *Radiation Oncology* 2013; 8: 183
- [90] Marzola MC, Chondrogiannis S, Ferretti A, Grassetto G, Rampin L, Massaro A, Castellucci P, Picchio M, Al-Nahhas A, Colletti PM, Marcolongo A and Rubello D, Role of 18F-Choline PET/CT in Biochemically Relapsed Prostate Cancer After Radical Prostatectomy: Correlation With Trigger PSA, PSA Velocity, PSA Doubling Time, and Metastatic Distribution, *Clinical Nuclear Medicine* 2013; 38: e26-e32
- [91] Martin NE, Mucci LA, Loda M and DePinho RA, Prognostic Determinants in Prostate Cancer, *Cancer* 2011; 17: 429-437
- [92] Cordon-Cardo C, Kotsianti A, Verbel DA, Teverovskiy M, Capodiecì P, Hamann S, Jeffers Y, Clayton M, Elkhettabi F, Khan FM, Sapir M, Bayer-Zubek V, Vengrenyuk Y, Fogarsi S, Saidi O, Reuter VE, Scher HI, Kattan MW, Bianco F Jr, Wheeler TM, Ayala GE, Scardino PT and Donovan MJ, Improved prediction of prostate cancer recurrence through systems pathology, *J Clin Investigation* 2007; 117: 1876-1883
-

-
- [93] Richmond P, Karayiannakis AJ and Akira Nagafuchi, Aberrant E-Cadherin and a-Catenin Expression in Prostate Cancer: Correlation with Patient Survival, *Cancer Res* 1997; 57: 3189-3193
- [94] Berruti A, Mosca A, Porpiglia F, Bollito E, Tucci M, Vana F, Cracco C, Torta M, Russo L, Cappia S, Saini A, Angeli A, Papotti M, Scarpa RM and Dogliotti L, Chromogranin A Expression in Patients With Hormone Naïve Prostate Cancer Predicts the Development of Hormone Refractory Disease, *J Urology* 2007; 178: 838-843
- [95] Miyake H, Muramaki M, Kurahashi T, Takenaka A and Fujisawa M, Expression of potential molecular markers in prostate cancer: Correlation with clinicopathological outcomes in patients undergoing radical prostatectomy, *Urologic Oncology: Seminars and Original Investigations* 2010; 28: 145–151
- [96] Bauer J, Sesterhenn IA, Mostofi FK, McLeod DG, Srivastava S and Moul JW, Elevated levels of apoptosis regulator proteins p53 and bcl-2 are independent prognostic biomarkers in surgically treated clinically localized prostate cancer, *J Urology* 1996; 156: 1511-1516
- [97] Cuzick J, Swanson GP, Fisher G, Brothman AR, Berney DM, Reid JE, Mesher D, Speights VO, Stankiewicz E, Foster CS, Møller H, Scardino P, Warren JD, Parke J, Younuse A, Flake DD II, Wagner S, Gutin A, Lanchbury JS and Stone S, Prognostic value of an RNA expression signature derived from cell cycle proliferation genes for recurrence and death from prostate cancer: A retrospective study in two cohorts, *Lancet Oncol* 2011; 12: 245–255
- [98] Choudhury AD, Eeles R, Freedland SJ, Isaacs WB, Pomerantz MM, Schalken JA, Tammela T and Visakorpi T, The Role of Genetic Markers in the Management of Prostate Cancer, *Eur Urology* 2012; 62: 577-587
- [99] Ding Z, Wu CJ, Chu GC, Xiao Y, Ho D, Zhang J, Perry SR, Labrot ES, Wu X, Lis R, Hoshida Y, Hiller D, Hu B, Jiang S, Zheng H, Stegh AH, Scott KL, Signoretti S, Bardeesy N, Wang YA, Hill D, Golub TR, Stampfer MJ, Wong WH, Loda M, Mucci L, Chin L and DePinho RA, SMAD4-dependent barrier constrains prostate cancer growth and metastatic progression, *Nature* 2011; 470: 269-273
- [100] Martens-Uzunova ES, Jalava SE, Dits NF, van Leenders GJ, Trapman J, Bangma CH, Litman T, Visakorpi T and Jenster G, Diagnostic and prognostic signatures from the small non-coding RNA transcriptome in prostate cancer, *Oncogene* 2012; 31: 978–991
- [101] Tomas D, Ulamec M, Hudolin T, Bulimbasic S, Belicza M and Kruslin B, Myofibroblastic stromal reaction and expression of tenascin-C and laminin in prostate adenocarcinoma, *Prostate Cancer and Prostatic Diseases* 2006; 9: 414–419
- [102] Castorina P, Delsanto PP and Guiot C, Classification scheme for phenomenological universalities in growth problems in physics and other sciences, *Phys Rev Lett* 2007; 98: 209901
- [103] Castorina P, Deisboeck TS, Gabriele P and Guiot C, Growth laws in cancer: implications for radiotherapy, *Radiation Res* 2007; 168: 349-356
- [104] Delsanto PP, Gliozzi A, Iordache DA and Guiot C, Universal features in the laws of growth, *J of Design and Nature and Ecodynamics* 2010; 5: 1-12
- [105] Gliozzi A, Guiot C, Delsanto PP and Iordache DA, A novel approach to the analysis of human growth, *Theoretical Biology and Medical Modelling* 2012; 9: 17
- [106] Stamatakos G "In Silico Oncology Part I: Clinically Oriented Cancer Multilevel Modeling Based on Discrete Event Simulation" In T.Deisboeck and G. Stamatakos Eds " Cancer Multiscale
-

- Modeling," CRC Press, pp. 407-436. Print ISBN: 978-1-4398-1440-6 eBook ISBN: 978-1-4398-1442-0 DOI: 10.1201/b10407-19 Boca Raton, Florida, USA, 2010
- [107] Stamatakos GS, Georgiadi E Ch, Graf N, Kolokotroni EA, and Dionysiou DD, "Exploiting Clinical Trial Data Drastically Narrows the Window of Possible Solutions to the Problem of Clinical Adaptation of a Multiscale Cancer Model", PLOS ONE 6(3), e17594 2011
- [108] G.S.Stamatakos, E.A.Kolokotroni, D.D.Dionysiou, E.Ch.Georgiadi, C.Desmedt. "An advanced discrete state - discrete event multiscale simulation model of the response of a solid tumor to chemotherapy: Mimicking a clinical study." Journal of Theoretical Biology 266, 124-139, 2010
- [109] D.D. Dionysiou, G.S. Stamatakos, D. Gintides, N. Uzunoglu, K. Kyriaki "Critical Parameters Determining Standard Radiotherapy Treatment Outcome for Glioblastoma Multiforme: A Computer Simulation," The Open Biomedical Engineering Journal 2, pp. 43-51, 2008
- [110] N. Graf, A. Hoppe, E. Georgiadi, R. Belleman, C. Desmedt, D. Dionysiou, M. Erdt, J. Jacques, E. Kolokotroni, A. Lunzer, M. Tsiknakis, G. Stamatakos, " In Silico Oncology for Clinical Decision Making in the Context of Nephroblastoma." Klinische Pädiatrie 221, pp.141-149, 2009.
- [111] G.S. Stamatakos, D.D. Dionysiou, E.I. Zacharaki, N.A. Mouravliansky, K.S.Nikita, N.K. & Uzunoglu, "In silico radiation oncology: combining novel simulation algorithms with current visualization techniques," IEEE Proceedings: Special Issue on Bioinformatics: Advances and Challenges , 90(11) , pp. 1764-1777 , 2002
- [112] D.D.Dionysiou, G.S. Stamatakos, N.K.Uzunoglu, K.S.Nikita, A. Marioli, "A Four Dimensional In Vivo Model of Tumour Response to Radiotherapy: Parametric Validation Considering Radiosensitivity, Genetic Profile and Fractionation ," J. Theor. Biol. , 230 , 1-20 , 2004
- [113] G.S.Stamatakos, V.P.Antipas, and N.K. Uzunoglu, "A spatiotemporal, patient individualized simulation model of solid tumor response to chemotherapy in vivo: the paradigm of glioblastoma multiforme treated by temozolomide ," IEEE Transactions on Biomedical Engineering , 53(8) , pp. 1467-1477 , 2006
- [114] G.S.Stamatakos, D.D.Dionysiou, N.M.Graf, N.A.Sofra, C.Desmedt, A.Hoppe, N.Uzunoglu, M.Tsiknakis , "The Oncosimulator: a multilevel, clinically oriented simulation system of tumor growth and organism response to therapeutic schemes. Towards the clinical evaluation of in silico oncology," in Proceedings of the 29th Annual International Conference of the IEEE EMBS Cite Internationale, August 23-26, SuB07.1:pp. 6628-6631 , Lyon, France , 2007
- [115] E.A. Kolokotroni, D.D. Dionysiou, N.K. Uzunoglu, G.S. Stamatakos, "Studying the growth kinetics of untreated clinical tumors by using an advanced discrete simulation model", Mathematical and Computer Modelling," 54, pp. 1989-2006, 2011
- [116] Georgiadi ECh, Dionysiou DD, Graf N, Stamatakos GS, "Towards in silico oncology: adapting a four dimensional nephroblastoma treatment model to a clinical trial case based on multi-method sensitivity analysis." Comput Biol Med. 2012 Nov;42(11):1064-78
- [117] Giatili, S and G. Stamatakos, "A detailed numerical treatment of the boundary conditions imposed by the skull on a diffusion–reaction model of glioma tumor growth. Clinical validation aspects," Applied Mathematics and Computation 218 (2012) 8779–8799.

Appendix 1 – Abbreviations and acronyms

<i>3DCRT</i>	3D Conformal Radiation Therapy
<i>ADC</i>	Apparent Diffusion Coefficient
<i>ATRA</i>	All-trans-retinoic acid
<i>BAC</i>	Binding Affinity Calculator
<i>BBB</i>	Blood-Brain Barrier
<i>BP</i>	Blood perfusion
<i>CD</i>	Cell density
<i>CDISC-ODM</i>	Clinical Data Interchange Standards Consortium - Operational Data Model
<i>CT</i>	Computerized Tomography
<i>CTLA-4</i>	Cytotoxic T-Lymphocyte Antigen 4
<i>DCE</i>	Dynamic Contrast Enhanced
<i>DC_(i/m)</i>	(Immature/Mature) Dendritic Cell(s)
<i>DCE-MRI</i>	Dynamic Contrast-Enhanced - Magnetic Resonance Imaging
<i>DCm-HGG-L</i>	mature Dendritic Cells loaded with Lysate from the High Grade Glioma
<i>dMRI</i>	Diffusion weighted Magnetic Resonance Imaging
<i>DSC-MRI</i>	Dynamic Susceptibility Contrast - Magnetic Resonance Imaging
<i>DWI</i>	Diffusion weighted imaging
<i>ECE</i>	Extra-Capsular Extension
<i>EORTC</i>	European Organisation for Research and Treatment of Cancer
<i>FACS</i>	Fluorescence-Activated Cell Sorting
<i>FLAIR</i>	FLuid Attenuated Inversion Recovery
<i>FMH</i>	Fertigkeitenskala Münster Heidelberg
<i>GARP</i>	Glycoprotein A Repetitions Predominant
<i>GBM</i>	Glioblastoma Multiforme
<i>GCP</i>	Good Clinical Practice
<i>GE-EPI</i>	Grade Echo – Echo-Planar Imaging
<i>HGG(-L)</i>	(Lysate of) High Grade Glioma
<i>HGPIN</i>	High-Grade Prostate Intra-epithelial neoplasia

<i>IGRT</i>	Image Guided Radiation Therapy
<i>IDH1</i>	Isocitrate DeHydrogenase 1
<i>IFNγ</i>	Interferon gamma
<i>IMRT</i>	Intensity Modulated Radiation Therapy
<i>KPS</i>	Karnofsky Performance Scale
<i>KWS</i>	'Klinisch Werk Station' Clinical Working Station
<i>LIE</i>	Linear interaction energy
<i>LOH</i>	Loss of heterozygosity
<i>LOI</i>	Loss of imprinting
<i>MD</i>	Molecular dynamics
<i>MGMT</i>	Methyl-Guanine Methyl-Transferase
<i>MM</i>	Molecular mechanisms or molecular mechanics
<i>MMSE</i>	Mini-Mental State Examination
<i>MM-TR</i>	Molecular mechanisms of treatment response
<i>MRI</i>	Magnetic Resonance Imaging
<i>NK(T)-cells</i>	Natural Killer (T)-cells
<i>NSCLC</i>	Non-Small-Cell-Lung-Cancer
<i>ObTiMA</i>	Ontology based Trial Management Application
<i>PBMC</i>	Peripheral Blood Mononuclear Cell(s)
<i>PBSA</i>	Poisson-Boltzmann surface area
<i>PET</i>	Positron Emission Tomography
<i>PFS (6m)</i>	Progression Free Survival (at 6 months)
<i>PSA</i>	Prostatic Specific Antigen
<i>qPCR</i>	quantitative Polymerase Chain Reaction
<i>RP</i>	Radical Prostatectomy
<i>RPA</i>	Recursive Partitioning Analysis
<i>RPC</i>	Remote Procedure Call
<i>RT</i>	Radiation Therapy
<i>SaaS</i>	Software as a Service
<i>SOA</i>	Service Oriented Architecture

<i>SOAP</i>	Simple Object Access Protocol
<i>STITCH</i>	Search tool for interactions of chemicals
<i>TI</i>	Thermodynamic integration
<i>Treg-cells</i>	Regulatory T-cells
<i>TSG</i>	Tumor suppressor gene
<i>TTD</i>	Therapeutic Target Database
<i>TTP</i>	Trusted Third Party
<i>UDDI</i>	Universal Description, Discovery and Integration
<i>URI</i>	Uniform resource identifier
<i>WAGR</i>	Wilms Tumor, Aniridia, Urogenital malformations, Retardation
<i>WHO</i>	World Health Organisation
<i>WSDL</i>	Web Services Description Language

Appendix 2 – Ethical Approvals

Nephroblastoma and Non-Small Cell Lung Cancer Scenario

Ärztchamber des Saarlandes · Postfach 10 02 62 · 66002 Saarbrücken
Ethik-Kommission

Herrn Professor
Dr. med. N. Graf
Direktor der Klinik für Pädiatrische
Onkologie und Hämatologie
Kliniken für Kinder- und Jugendmedizin
Universitätsklinikum des Saarlandes
66421 Homburg

Ärztchamber
des Saarlandes
Körperschaft
des öffentlichen Rechts



Ethik-Kommission

Geschäftsstelle

Hafenstr. 25
66111 Saarbrücken
Telefon Durchwahl (06 81) 40 03 - 378
Telefax (06 81) 40 03 - 394
E-Mail: ethikkommission@aeksaar.de
Internet: www.aerztekammer-saarland.de

Unser Zeichen:

Ihr Schreiben vom:

Ihr Zeichen:

Datum:

19. Aug. 2013

**Retrospektive Nutzung der pseudonymisierten Daten in den Forschungsprojekten
CHIC und MyHealthAvatar**

Unsere Kenn-Nr.: 104/10 (*bitte stets angeben!*)

Sehr geehrter Herr Graf!

lieber Herr Graf,

In Ihrem Schreiben vom 09. August 2013 bitten Sie um die retrospektive Nutzung pseudonymisierter Daten aus den vorausgegangenen Forschungsprojekten CHIC und MyHealthAvatar. Außerdem werden Daten der SIOF Wilmstumorstudie benutzt sowie bisher anonymisierte Daten aus dem Homburger Krankenhausinformationssystem.

Die Ethik-Kommission der Ärztekammer des Saarlandes ist mit diesem Vorgehen und der Nutzung aus den vorliegenden Forschungsprojekten einverstanden.

Mit freundlichen Grüßen

Dr. H. Schieffer

San.-Rat Prof. Dr. Schieffer

Die Ethik-Kommission bei der Ärztekammer des Saarlandes ist unter Beachtung der internationalen Richtlinien der ICH, GCP u. der 12. Novelle AMG tätig, nach Landesrecht (Saarländisches Heilberufekammergesetz, § 5 Abs. 1) anerkannt und beim Bundesinstitut für Arzneimittel und Medizinprodukte gem. § 22 des Medizinproduktegesetzes sowie beim Bundesamt für Strahlenschutz nach § 92 der Strahlenschutzverordnung und nach § 28g der Röntgenverordnung registriert.

Commerzbank Saarbrücken
Kto.-Nr. 53 89 200
BLZ 590 400 00

Dt. Apotheker- und Ärztebank Saarbrücken
Kto.-Nr. 0 001 926 209
BLZ 590 906 26

Postbank Saarbrücken
Kto.-Nr. 95 15 666
BLZ 590 100 66

Bank 1 Saar Saarbrücken
Kto.-Nr. 157 5007
BLZ 581 900 00

Glioblastoma Scenario

Not available yet

Prostate Cancer Scenario



FONDAZIONE PIEMONTESE
PER LA RICERCA SUL CANCRO
ONLUS

COMITATO ETICO

Candiolo, 9 luglio 2013

Dott. Pietro Gabriele
Responsabile U.O.A.
di Radioterapia
IRCC CANDIOLO

OGGETTO: Valutazione “Studio osservazionale retrospettivo multicentrico per la definizione di modelli prognostici sul cancro prostatico in pazienti operati – European multicentric Retrospective Study evaluating prognostic factors on prostate K (Cancer) in prostatectomysed patients “ – EUREKA-1

Le comunico che nella seduta dell’8 luglio 2013 il Comitato Etico dell’Istituto, esaminato e discusso il protocollo in oggetto, ha espresso **parere favorevole**.

Si fa presente che:

La sperimentazione va condotta nel rispetto della normativa vigente e dei regolamenti dell’istituzione presso la quale deve essere svolta, secondo i principi etici fissati nella Dichiarazione di Helsinki e della buona pratica clinica (D.M.S. 15.07.1997).

Si fa, inoltre, presente che lo sperimentatore ha l’obbligo di comunicare la data di inizio della sperimentazione.

Il responsabile della sperimentazione ha l’obbligo di riferire immediatamente al Comitato Etico indipendente:

- le eventuali variazioni del protocollo;
- tutte le reazioni avverse da farmaci soprattutto se serie ed inattese;

segue



Indirizzo Strada Provinciale 142, Km 3.95, 10060 Candiolo (TO) **T** 011.9933.380 - **F** 011.9933.389 **c/c Postale** 410100 - **C. F.** 97519070011 **UniCredit IBAN** IT 64 T 02008 01154 000008780163 - **Intesa Sanpaolo IBAN** IT 07 0 03069 01000 100000516980 - **web** www.fprconlus.it - **e-mail** fprc@fprconlus.it

CONSIGLIO DIRETTIVO: Presidente Allegra Agnelli. **Vice Presidenti** Carlo Acutis, Maria Vaccari Scassa. **Consigliere Delegato** Giampiero Gabotto. **Consiglieri** Marco Boglione, Bruno Ceretto, Paolo Maria Comoglio, Giuseppe Della Porta, Gianluca Ferrero, Gianluigi Gabetti, Giuseppe Gilardi, Maria Elena Giraudo Rayneri, Eugenio Lancellotta, Antonio Maria Marocco, Aldo Ottavio, Carlo Pacciani, Lodovico Passerin d’Entrèves, Patrizia Re Rebaudengo Sandretto, Silvio Saffirio, Piero Sierra. **Direttore Scientifico dell’Istituto di Candiolo** Paolo Maria Comoglio. **REVISORI DEI CONTI: Presidente** Giacomo Zunino. **Componenti** Mario Boldi, Lionello Jona Celesia.

Riconoscimento della Regione Piemonte: D.G.R. 22/07/1986 n° 3-6673 - Iscrizione anagrafe Onlus prot. n. 9882440 del 19/06/1998



FONDAZIONE PIEMONTESE
PER LA RICERCA SUL CANCRO
ONLUS

COMITATO ETICO

Candiolo, 9 luglio 2013

Dott. Pietro Gabriele
Responsabile U.O.A.
di Radioterapia
IRCC CANDIOLO

OGGETTO: **Valutazione** “Studio osservazionale retrospettivo multicentrico per la definizione di modelli prognostici sul cancro prostatico in pazienti radio trattati” EUREKA-2

Le comunico che nella seduta dell'8 luglio 2013 il Comitato Etico dell'Istituto, esaminato e discusso il protocollo in oggetto, ha espresso **parere favorevole**.

Si fa presente che:

La sperimentazione va condotta nel rispetto della normativa vigente e dei regolamenti dell'istituzione presso la quale deve essere svolta, secondo i principi etici fissati nella Dichiarazione di Helsinki e della buona pratica clinica (D.M.S. 15.07.1997).

Si fa, inoltre, presente che lo sperimentatore ha l'obbligo di comunicare la data di inizio della sperimentazione.

Il responsabile della sperimentazione ha l'obbligo di riferire immediatamente al Comitato Etico indipendente:

- le eventuali variazioni del protocollo;
- tutte le reazioni avverse da farmaci soprattutto se serie ed inattese;

segue



Indirizzo Strada Provinciale 142, Km 3.95, 10060 Candiolo (TO) **T** 011.9933.380 - **F** 011.9933.389 **c/c Postale** 410100 - **C. F.** 97519070011 **UniCredit**
IBAN IT 64 T 02008 01154 000008780163 - **Intesa Sanpaolo** **IBAN** IT 07 0 03069 01000 100000516980 - **web** www.fprconlus.it - **e-mail** fprc@fprconlus.it

CONSIGLIO DIRETTIVO: **Presidente** Allegra Agnelli. **Vice Presidenti** Carlo Acutis, Maria Vaccari Scassa. **Consigliere Delegato** Giampiero Gabotto. **Consiglieri** Marco Boglione, Bruno Ceretto, Paolo Maria Comoglio, Giuseppe Della Porta, Gianluca Ferrero, Gianluigi Gabetti, Giuseppe Gilardi, Maria Elena Giraudo Rayneri, Eugenio Lancellotta, ~~Antonio Maria Marocco~~, Aldo Ottavis, Carlo Pacciani, Lodovico Passerin d'Entrèves, Patrizia Re Rebaudengo Sandretto, Silvio Saffirio, Piero Sierra. **Direttore Scientifico dell'Istituto di Candiolo** Paolo Maria Comoglio. **REVISORI DEI CONTI:** **Presidente** Giacomo Zunino. **Componenti** Mario Boidi, Lionello Jona Celesia.

Riconoscimento della Regione Piemonte: D.G.R. 22/07/1986 n° 3-6673 - Iscrizione anagrafe Onlus prot. n. 9882440 del 19/06/1998

Appendix 3 - Representative cancer models spanning all major spatiotemporal scales of biological complexity

Cancer models that do exist

In the following table all collected cancer models that do exist are listed. The colour in the first row indicates the clinical relevance of the model. Three different categories are defined:

1. Implement in first phase as test case (highly relevant)
2. Implement later in the project (relevant)
3. Implement only if time permits (less relevant)

Category 1 is indicated in green, 2 in yellow and 3 not highlighted.

Model information						
Model number	Reference partner	Model title	Brief model description	Biological scale	Core mathematical methods utilized	References
ATOMIC SCALE (MAINLY) - CODE "A"						
Ae1.	UPENN	Molecular Dynamics of clinical mutations in oncogenic receptors	All-atom molecular dynamics simulations are performed and analyzed for 30 mutations found in neuroblastoma patients to determine potential of kinase activation	ATOMIC	NAMD molecular dynamics package VMD molecular visualization package carma molecular dynamics analysis package	http://www.ks.uiuc.edu/Research/namd/ http://www.ks.uiuc.edu/Research/vmd/ http://utopia.duth.gr/~glykos/Carma.html
Ae2.	UPENN	Autodock	AutoDock is a suite of automated docking tools. It is designed to predict how small molecules, such as substrates or drug candidates, bind to a receptor of known 3D structure. http://autodock.scripps.edu	ATOMIC	Computational Small Molecule Docking Algorithm. Generates a score that attempts to distinguish between molecules binding ability, as well as their optimal placement in the binding pocket.	J.Computational Chemistry 2009, 16: 2785-91. J.Computational Chemistry, 28: 1145-1152.
Ae3.	UPENN	Glide	Glide offers the full spectrum of speed and accuracy from high-throughput virtual screening of millions of compounds to extremely accurate binding mode predictions, providing consistently high enrichment at every level.	ATOMIC	Computational Small Molecule Docking Algorithm. Generates a score that attempts to distinguish between molecules binding ability, as well as	J. Med. Chem., 2006, 49, 6177–6196 J. Med. Chem., 2004, 47, 1750–1759 J. Med. Chem., 2004, 47, 1739–1749

			http://www.schrodinger.com/productpage/14/5/		their optimal placement in the binding pocket.	
Ae4.	UPENN	Shape Signatures	Computer-aided ligand- and receptor-based drug design.	ATOMIC	Ray-tracing to explore the volume enclosed by a ligand molecule, or the volume exterior to the active site of a protein. Probability distributions are derived from the ray-trace, and can be based solely on the geometry of the reflecting ray, or may include joint dependence on properties, such as the molecular electrostatic potential, computed over the surface.	J Med Chem. 2003 Dec 18;46(26):5674-90
MOLECULAR SCALE (MAINLY) - CODE "M"						
Me1.	UOXF	Cell cycle model	ODE model of cell cycle at subcellular level; focus on influence of local oxygen concentration on cell cycle progression; distinguish between normal and cancer cells	MOLECULAR		
Me2.	UOXF	Wnt signalling pathway	Ode model for wnt signalling pathway at subcellular level; model accounts for competition for beta-catenin between nucleus and cell membrane.	MOLECULAR		Van Leeuwen et al (2007). J Theor Biol, 247: 77-102

CELL AND TISSUE SCALE (MAINLY) - CODE "C+T"						
C+Te1.	ICCS	Untreated Tumor Growth. Spatial code	<p>The model simulates the spatiotemporal growth of untreated clinical tumors. It is based on the consideration of a discrete time and space stochastic cellular automaton, representing the tumor region. More specifically, the tumor region can be considered as a grid of "geometrical cells" (GCs, the elementary volume of the grid). Each GC corresponds to a cluster of heterogeneous cells found in various states. Specific rules regulate the transition between these states, as well as cell movement throughout the tumor volume; the aim is a realistic, conformal to the initial shape of the tumor, simulation of spatial evolution. The adopted cytokinetic model incorporates the biological mechanisms of cell cycling, quiescence, differentiation and loss. Stem, LIMP, DIFF, apoptotic and necrotic cells represent the distinct cell categories of the model. More specifically, tumor sustenance is attributed to the presence of a cell population that exhibits stem cell like properties. Specifically, cancer stem cells have the ability to preserve their own population, as well as give birth to cells of limited mitotic potential (LIMP cells) that follow the path towards terminal differentiation (DIFF cells). A proliferating tumor cell (stem or LIMP) passes through the successive cell cycle phases. Phases within or out of the</p>	CELL AND TISSUE	Based on discrete time and space stochastic cellular automata	<p>Eleni A. Kolokotroni, Dimitra D. Dionysiou, Nikolaos K. Uzunoglu, Georgios S. Stamatakos, Studying the growth kinetics of untreated clinical tumors by using an advanced discrete simulation model, Mathematical and Computer Modelling, volume 54, issues 9–10, pages 1989-2006, November 2011. DOI:10.1016/j.mcm.2011.05.007.</p> <p>G. S. Stamatakos, E. Ch. Georgiadi, N. Graf, E. A. Kolokotroni, and D. D. Dionysiou, "Exploiting Clinical Trial Data Drastically Narrows the Window of Possible Solutions to the Problem of Clinical Adaptation of a Multiscale Cancer Model", PLoS ONE 6(3), e17594, 2011</p> <p>"D.D.Dionysiou, G.S. Stamatakos, N.K.Uzunoglu, K.S.Nikita, A. Marioli, "A Four Dimensional In Vivo Model of Tumour Response to Radiotherapy: Parametric Validation Considering Radiosensitivity, Genetic Profile and Fractionation," Journal of Theoretical Biology , 230 , 1-20 , 2004"</p>

			<p>cell cycle (G1, S, G2, M, G0) constitute different states in which cells may be found. After the completion of mitosis a fraction of newborn cells will enter the dormant phase, whereas the rest will continue to cycle. Transition to quiescence (dormant, G0, phase) and “awakening” of dormant cells are regulated by local metabolic conditions. All cell categories may die through spontaneous apoptosis. However, for dormant and differentiated cells necrosis is the main cell loss mechanism caused by inadequate nutrients’ and oxygen supply.</p>			
C+Te2.	ICCS	Untreated Tumor Growth. Non Spatial code	<p>The non-spatial model constitutes a variation/simplification of the previous model (ICCS-NTUA-ISOG-Untreated Tumor Growth. Spatial code). Its crucial new features consist in a. omitting the simulation of the spatial evolution of the tumor and b. considering more compartments that the proliferating cells can be found. The omission of the simulation of the three dimensional expansion of the tumor allows a more realistic modeling of the cell cycle, in terms of available computational resources. The exclusion of the spatial evolution of the tumor does not affect the temporal evolution of the various cancerous cell categories and the total cell population. Subsequently, the time course</p>	CELL AND TISSUE	Based on discrete cellular automata	<p>Eleni A. Kolokotroni, Dimitra D. Dionysiou, Nikolaos K. Uzunoglu, Georgios S. Stamatakos, Studying the growth kinetics of untreated clinical tumors by using an advanced discrete simulation model, Mathematical and Computer Modelling, volume 54, issues 9–10, pages 1989-2006, November 2011. DOI:10.1016/j.mcm.2011.05.007.</p> <p>G. S. Stamatakos, E. Ch. Georgiadi, N. Graf, E. A. Kolokotroni, and D. D. Dionysiou, "Exploiting Clinical Trial Data Drastically Narrows the Window of Possible Solutions to the Problem of Clinical Adaptation of a Multiscale Cancer Model", PLoS ONE 6(3), e17594, 2011</p>

			of the tumor volume can be easily derived assuming typical cell densities, e.g. 10^9 biological cells/cm ³ (Steel, 1997). In the non-spatial model the cycling and dormant cancerous cells are distributed in a number of classes/compartments that equals the duration of the relevant phase (see paragraph 1.2). Each compartment corresponds to an hour-long interval.			D.D.Dionysiou, G.S. Stamatakos, N.K.Uzunoglu, K.S.Nikita, A. Marioli , “A Four Dimensional In Vivo Model of Tumour Response to Radiotherapy: Parametric Validation Considering Radiosensitivity, Genetic Profile and Fractionation,” Journal of Theoretical Biology , 230 , 1-20 , 2004
C+Te3.	ICCS	Single Agent Chemotherapy. Spatial code	<p>The model simulates the spatiotemporal response of clinical tumors to chemotherapeutic treatment. It is based on the consideration of a discrete time and space stochastic cellular automaton, representing the tumor region. More specifically, the tumor region can be considered as a grid of “geometrical cells” (GCs, the elementary volume of the grid). Each GC corresponds to a cluster of heterogeneous cells found in various states. Specific rules regulate the transition between these states, as well as cell movement throughout the tumor volume; the aim is a realistic, conformal to the initial shape of the tumor, simulation of spatial evolution.</p> <p>Free Growth: The adopted cytokinetic model incorporates the biological mechanisms of cell cycling, quiescence, differentiation and loss. Stem, LIMP, DIFF, apoptotic and necrotic cells represent the distinct cell categories of the model. More specifically, tumor sustenance is</p>	CELL AND TISSUE	Based on discrete time and space stochastic cellular automata	G.S. Stamatakos, E.A. Kolokotroni, D.D. Dionysiou, E.Ch. Georgiadi, C. Desmedt, An advanced discrete state - discrete event multiscale simulation model of the response of a solid tumor to chemotherapy: Mimicking a clinical study, Journal of Theoretical Biology volume 266, issue 1, pages 124-139, September 2010. DOI:10.1016/j.jtbi.2010.05.019.

		<p>attributed to the presence of a cell population that exhibits stem cell like properties. Specifically, cancer stem cells have the ability to preserve their own population, as well as give birth to cells of limited mitotic potential (LIMP cells) that follow the path towards terminal differentiation (DIFF cells). A proliferating tumor cell (stem or LIMP) passes through the successive cell cycle phases. Phases within or out of the cell cycle (G1, S, G2, M, G0) constitute different states in which cells may be found. After the completion of mitosis a fraction of newborn cells will enter the dormant phase, whereas the rest will continue to cycle. Transition to quiescence (dormant, G0, phase) and “awakening” of dormant cells are regulated by local metabolic conditions. All cell categories may die through spontaneous apoptosis. However, for dormant and differentiated cells necrosis is the main cell loss mechanism caused by inadequate nutrients’ and oxygen supply.</p> <p>Treatment: The model addresses the case of cell-cycle non-specific chemotherapeutic agents. When a tumor is chemotherapeutically treated, a fraction of cancerous proliferating cells are lethally hit by the drug. These cells enter a rudimentary cell cycle that leads to apoptotic death through a cell cycle phase</p>		
--	--	--	--	--

			depending each time on the specific chemotherapeutic agent. In the simulation model the case of drugs that primarily inhibit the DNA synthesis and lead to apoptotic death at the end of the S phase is addressed. The effect of the drug is considered instantaneous at the time of its administration.			
C+Te4.	ICCS	Single Agent Chemotherapy. Non Spatial code	The non-spatial model constitutes a variation/simplification of the previous model (ICCS-NTUA-ISOG- Single Agent Chemotherapy. Spatial code). Its crucial new features consist in a. omitting the simulation of the spatial evolution of the tumor and b. considering more compartments that the proliferating cells can be found. The omission of the simulation of the three dimensional expansion of the tumor, in the case of free growth, or shrinkage, in the case of therapy, allows a more realistic modeling of the cell cycle, in terms of available computational resources. The exclusion of the spatial evolution of the tumor does not affect the temporal evolution of the various cancerous cell categories and the total cell population. Subsequently, the time course of the tumor volume can be easily derived assuming typical cell densities, e.g. 10^9 biological cells/cm ³ (Steel, 1997). In the non-spatial model the cycling and dormant cancerous cells are distributed in a number of	CELL AND TISSUE	Based on discrete cellular automata	G.S. Stamatakos, E.A. Kolokotroni, D.D. Dionysiou, E.Ch. Georgiadi, C. Desmedt, An advanced discrete state - discrete event multiscale simulation model of the response of a solid tumor to chemotherapy: Mimicking a clinical study, Journal of Theoretical Biology volume 266, issue 1, pages 124-139, September 2010. DOI:10.1016/j.jtbi.2010.05.019.

			classes/compartments that equals the duration of the relevant phase (see paragraph 1.2). Each compartment corresponds to an hour-long interval.			
C+Te5.	ICCS	Radiotherapy. Spatial code	<p>The model simulates the spatiotemporal response of clinical tumors to chemotherapeutic treatment. It is based on the consideration of a discrete time and space stochastic cellular automaton, representing the tumor region. More specifically, the tumor region can be considered as a grid of “geometrical cells” (GCs, the elementary volume of the grid). Each GC corresponds to a cluster of heterogeneous cells found in various states. Specific rules regulate the transition between these states, as well as cell movement throughout the tumor volume; the aim is a realistic, conformal to the initial shape of the tumor, simulation of spatial evolution.</p> <p>Free Growth: The adopted cytokinetic model incorporates the biological mechanisms of cell cycling, quiescence, differentiation and loss. Stem, LIMP, DIFF, apoptotic and necrotic cells represent the distinct cell categories of the model. More specifically, tumor sustenance is attributed to the presence of a cell population that exhibits stem cell like properties. Specifically, cancer stem cells have the ability to preserve their own</p>	CELL AND TISSUE	Based on discrete time and space stochastic cellular automata	<p>G.S. Stamatakos, E.A. Kolokotroni, D.D. Dionysiou, E.Ch. Georgiadi, C. Desmedt, An advanced discrete state - discrete event multiscale simulation model of the response of a solid tumor to chemotherapy: Mimicking a clinical study, <i>Journal of Theoretical Biology</i> volume 266, issue 1, pages 124-139, September 2010. DOI:10.1016/j.jtbi.2010.05.019.</p> <p>D.D. Dionysiou, G.S. Stamatakos, D. Gintides, N. Uzunoglu, K. Kyriaki, “Critical Parameters Determining Standard Radiotherapy Treatment Outcome for Glioblastoma Multiforme: A Computer Simulation,” <i>The Open Biomedical Engineering Journal</i> 2, 43-51, 2008</p> <p>G.S. Stamatakos, D.D. Dionysiou, E.I. Zacharaki, N.A. Mouravliansky, K.S.Nikita, N.K. Uzunoglu, “In silico radiation oncology: combining novel simulation algorithms with current visualization techniques,” <i>Proceedings of the IEEE, Special Issue on Bioinformatics: Advances and Challenges</i></p>

			<p>population, as well as give birth to cells of limited mitotic potential (LIMP cells) that follow the path towards terminal differentiation (DIFF cells). A proliferating tumor cell (stem or LIMP) passes through the successive cell cycle phases. Phases within or out of the cell cycle (G1, S, G2, M, G0) constitute different states in which cells may be found. After the completion of mitosis a fraction of newborn cells will enter the dormant phase, whereas the rest will continue to cycle. Transition to quiescence (dormant, G0, phase) and “awakening” of dormant cells are regulated by local metabolic conditions. All cell categories may die through spontaneous apoptosis. However, for dormant and differentiated cells necrosis is the main cell loss mechanism caused by inadequate nutrients’ and oxygen supply.</p> <p>Treatment: In the case of radiation therapy lethally damaged cells die through a radiation-induced mitotic necrotic mechanism. These cells enter a rudimentary cell cycle and die after undergoing a few mitotic divisions. The probability of cells to be hit by irradiation depends primarily on the phase they reside. Cell killing by irradiation is described by the Linear Quadratic or LQ Model.</p>			, 90(11) , 1764-1777 , 2002
C+Te6.	ICCS	Radiotherapy. Non Spatial	The non-spatial model constitutes a variation/simplification of the previous model (ICCS-NTUA-ISOG- Radiotherapy.	CELL AND TISSUE	Based on discrete cellular automata	G.S. Stamatakos, E.A. Kolokotroni, D.D. Dionysiou, E.Ch. Georgiadi, C. Desmedt, An advanced discrete state - discrete

		code	<p>Spatial code). Its crucial new features consist in a. omitting the simulation of the spatial evolution of the tumor and b. considering more compartments that the proliferating cells can be found. The omission of the simulation of the three dimensional expansion of the tumor, in the case of free growth, or shrinkage, in the case of therapy, allows a more realistic modeling of the cell cycle, in terms of available computational resources. The exclusion of the spatial evolution of the tumor does not affect the temporal evolution of the various cancerous cell categories and the total cell population. Subsequently, the time course of the tumor volume can be easily derived assuming typical cell densities, e.g. 10^9 biological cells/cm³ (Steel, 1997). In the non-spatial model the cycling and dormant cancerous cells are distributed in a number of classes/compartments that equals the duration of the relevant phase (see paragraph 1.2). Each compartment corresponds to an hour-long interval.</p>			<p>event multiscale simulation model of the response of a solid tumor to chemotherapy: Mimicking a clinical study, Journal of Theoretical Biology volume 266, issue 1, pages 124-139, September 2010. DOI:10.1016/j.jtbi.2010.05.019.</p> <p>D.D. Dionysiou, G.S. Stamatakos, D. Gintides, N. Uzunoglu, K. Kyriaki, “ Critical Parameters Determining Standard Radiotherapy Treatment Outcome for Glioblastoma Multiforme: A Computer Simulation,” The Open Biomedical Engineering Journal 2, 43-51, 2008</p> <p>G.S. Stamatakos, D.D. Dionysiou, E.I. Zacharaki, N.A. Mouravliansky, K.S.Nikita, N.K. Uzunoglu , “In silico radiation oncology: combining novel simulation algorithms with current visualization techniques,” Proceedings of the IEEE, Special Issue on Bioinformatics: Advances and Challenges , 90(11) , 1764-1777 , 2002</p>
C+Te7.	ICCS	Breast Cancer Therapy: Epirubicin	<p>The model simulates the spatiotemporal response of breast cancer clinical tumors to chemotherapeutic treatment with single agent Epirubicin. It is based on the consideration of a discrete time and space stochastic cellular automaton,</p>	CELL AND TISSUE	Based on discrete time and space stochastic cellular automata	<p>G.S. Stamatakos, E.A. Kolokotroni, D.D. Dionysiou, E.Ch. Georgiadi, C. Desmedt, An advanced discrete state - discrete event multiscale simulation model of the response of a solid tumor to chemotherapy: Mimicking a clinical</p>

		<p>representing the tumor region. More specifically, the tumor region can be considered as a grid of “geometrical cells” (GCs, the elementary volume of the grid). Each GC corresponds to a cluster of heterogeneous cells found in various states. Specific rules regulate the transition between these states, as well as cell movement throughout the tumor volume; the aim is a realistic, conformal to the initial shape of the tumor, simulation of spatial evolution.</p> <p>Free Growth: The adopted cytokinetic model incorporates the biological mechanisms of cell cycling, quiescence, differentiation and loss. Stem, LIMP, DIFF, apoptotic and necrotic cells represent the distinct cell categories of the model. More specifically, tumor sustenance is attributed to the presence of a cell population that exhibits stem cell like properties. Specifically, cancer stem cells have the ability to preserve their own population, as well as give birth to cells of limited mitotic potential (LIMP cells) that follow the path towards terminal differentiation (DIFF cells). A proliferating tumor cell (stem or LIMP) passes through the successive cell cycle phases. Phases within or out of the cell cycle (G1, S, G2, M, G0) constitute different states in which cells may be found. After the completion</p>		<p>study, Journal of Theoretical Biology volume 266, issue 1, pages 124-139, September 2010. DOI:10.1016/j.jtbi.2010.05.019.</p> <p>Eleni A. Kolokotroni, Dimitra D. Dionysiou, Nikolaos K. Uzunoglu, Georgios S. Stamatakos, Studying the growth kinetics of untreated clinical tumors by using an advanced discrete simulation model, Mathematical and Computer Modelling, volume 54, issues 9–10, pages 1989-2006, November 2011. DOI:10.1016/j.mcm.2011.05.007.</p>
--	--	---	--	---

			<p>of mitosis a fraction of newborn cells will enter the dormant phase, whereas the rest will continue to cycle. Transition to quiescence (dormant, G0, phase) and “awakening” of dormant cells are regulated by local metabolic conditions. All cell categories may die through spontaneous apoptosis. However, for dormant and differentiated cells necrosis is the main cell loss mechanism caused by inadequate nutrients’ and oxygen supply.</p> <p>Treatment: The model addresses the case of Epirubicin agent. When a tumor is chemotherapeutically treated, a fraction of cancerous proliferating cells are lethally hit by the drug. These cells enter a rudimentary cell cycle that leads to apoptotic death through a cell cycle phase depending each time on the specific chemotherapeutic agent. In the simulation model the case of Epirubicin agent that primarily inhibits the DNA synthesis and lead to apoptotic death at the end of the S phase is addressed. The effect of the drug is considered instantaneous at the time of its administration.</p>			
C+Te8.	ICCS	Lung Cancer Therapy: Cisplatin and Docetaxel	The model simulates the spatiotemporal response of lung cancer to combination chemotherapy treatment with the regimens Cisplatin and Docetaxel. In accordance to clinical practice the cisplatin/docetaxel regimen is given as a	CELL AND TISSUE	Based on discrete time and space stochastic cellular automata	G. S.Stamatakos, E. Kolokotroni, D. Dionysiou, C. Veith, Yoo-Jin Kim, A. Franz, K. Marias, J. Sabczynski, R. Bohle, N.Graf, “In Silico Oncology: Exploiting Clinical Studies to Clinically Adapt and Validate Multiscale Oncosimulators,”

		<p>three-week cycle and is administrated usually three times. On the first day of each cycle the patient is given both the docetaxel and cisplatin.</p> <p>It is based on the consideration of a discrete time and space stochastic cellular automaton, representing the tumor region. More specifically, the tumor region can be considered as a grid of “geometrical cells” (GCs, the elementary volume of the grid). Each GC corresponds to a cluster of heterogeneous cells found in various states. Specific rules regulate the transition between these states, as well as cell movement throughout the tumor volume; the aim is a realistic, conformal to the initial shape of the tumor, simulation of spatial evolution.</p> <p>Free Growth: The adopted cytokinetic model incorporates the biological mechanisms of cell cycling, quiescence, differentiation and loss. Stem, LIMP, DIFF, apoptotic and necrotic cells represent the distinct cell categories of the model. More specifically, tumor sustenance is attributed to the presence of a cell population that exhibits stem cell like properties. Specifically, cancer stem cells have the ability to preserve their own population, as well as give birth to cells of limited mitotic potential (LIMP cells) that</p>		<p>accepted in Proc. EMBC 2013 (35th Annual International Conference of the IEEE Engineering in Medicine and Biology Society, Osaka, Japan)</p> <p>Eleni A. Kolokotroni, Dimitra D. Dionysiou, Nikolaos K. Uzunoglu, Georgios S. Stamatakos, Studying the growth kinetics of untreated clinical tumors by using an advanced discrete simulation model, Mathematical and Computer Modelling, volume 54, issues 9–10, pages 1989-2006, November 2011. DOI:10.1016/j.mcm.2011.05.007.</p>
--	--	--	--	--

			<p>follow the path towards terminal differentiation (DIFF cells). A proliferating tumor cell (stem or LIMP) passes through the successive cell cycle phases. Phases within or out of the cell cycle (G1, S, G2, M, G0) constitute different states in which cells may be found. After the completion of mitosis a fraction of newborn cells will enter the dormant phase, whereas the rest will continue to cycle. Transition to quiescence (dormant, G0, phase) and “awakening” of dormant cells are regulated by local metabolic conditions. All cell categories may die through spontaneous apoptosis. However, for dormant and differentiated cells necrosis is the main cell loss mechanism caused by inadequate nutrients’ and oxygen supply.</p> <p>Treatment: When a tumor is chemotherapeutically treated, a fraction of cancerous proliferating cells are lethally hit by the drug. These cells enter a rudimentary cell cycle that leads to apoptotic death through a cell cycle phase depending each time on the specific chemotherapeutic agent. The effect of the drug is considered instantaneous at the time of its administration.</p>			
C+Te9.	ICCS	Lung Cancer Therapy:	The model simulates the spatiotemporal response of lung cancer to combination chemotherapy treatment with the	CELL AND TISSUE	Based on discrete time and space stochastic	G. S.Stamatakis, E. Kolokotroni, D. Dionysiou, C. Veith, Yoo-Jin Kim, A. Franz, K. Marias, J. Sabczynski, R. Bohle,

		<p>Cisplatin and Gemcitabine</p>	<p>regimens Cisplatin and Gemcitabine. In accordance to clinical practice the cisplatin/ gemcitabine regimen is given as a three-week cycle and is administrated usually two or three times. On the first day of treatment the patient is given both the gemcitabine and cisplatin. On the same day of the following week (day eight) only gemcitabine is adminstrated.</p> <p>It is based on the consideration of a discrete time and space stochastic cellular automaton, representing the tumor region. More specifically, the tumor region can be considered as a grid of “geometrical cells” (GCs, the elementary volume of the grid). Each GC corresponds to a cluster of heterogeneous cells found in various states. Specific rules regulate the transition between these states, as well as cell movement throughout the tumor volume; the aim is a realistic, conformal to the initial shape of the tumor, simulation of spatial evolution.</p> <p>Free Growth: The adopted cytokinetic model incorporates the biological mechanisms of cell cycling, quiescence, differentiation and loss. Stem, LIMP, DIFF, apoptotic and necrotic cells represent the distinct cell categories of the model. More specifically, tumor sustenance is attributed to the presence of a cell</p>		<p>cellular automata</p>	<p>N.Graf, “In Silico Oncology: Exploiting Clinical Studies to Clinically Adapt and Validate Multiscale Oncosimulators,” accepted in Proc. EMBC 2013 (35th Annual International Conference of the IEEE Engineering in Medicine and Biology Society, Osaka, Japan)</p> <p>Eleni A. Kolokotroni, Dimitra D. Dionysiou, Nikolaos K. Uzunoglu, Georgios S. Stamatakos, Studying the growth kinetics of untreated clinical tumors by using an advanced discrete simulation model, Mathematical and Computer Modelling, volume 54, issues 9–10, pages 1989-2006, November 2011. DOI:10.1016/j.mcm.2011.05.007.</p>
--	--	----------------------------------	---	--	--------------------------	--

		<p>population that exhibits stem cell like properties. Specifically, cancer stem cells have the ability to preserve their own population, as well as give birth to cells of limited mitotic potential (LIMP cells) that follow the path towards terminal differentiation (DIFF cells). A proliferating tumor cell (stem or LIMP) passes through the successive cell cycle phases. Phases within or out of the cell cycle (G1, S, G2, M, G0) constitute different states in which cells may be found. After the completion of mitosis a fraction of newborn cells will enter the dormant phase, whereas the rest will continue to cycle. Transition to quiescence (dormant, G0, phase) and “awakening” of dormant cells are regulated by local metabolic conditions. All cell categories may die through spontaneous apoptosis. However, for dormant and differentiated cells necrosis is the main cell loss mechanism caused by inadequate nutrients’ and oxygen supply.</p> <p>Treatment: When a tumor is chemotherapeutically treated, a fraction of cancerous proliferating cells are lethally hit by the drug. These cells enter a rudimentary cell cycle that leads to apoptotic death through a cell cycle phase depending each time on the specific chemotherapeutic agent. The effect of the drug is considered instantaneous at the time of its administration.</p>			
--	--	--	--	--	--

<p>C+Te10.</p>	<p>ICCS</p>	<p>Lung Cancer Therapy: Cisplatin and Vinorelbine</p>	<p>The model simulates the spatiotemporal response of lung cancer to combination chemotherapy treatment with the regimens Cisplatin and Vinorelbine. In accordance to clinical practice the cisplatin/vinorelbine regimen is given as a three-week cycle and is administrated usually two or three times. On the first day of treatment the patient is given both the vinorelbine and cisplatin. On the same day of the following week (day eight) only vinorelbine is administrated.</p> <p>It is based on the consideration of a discrete time and space stochastic cellular automaton, representing the tumor region. More specifically, the tumor region can be considered as a grid of “geometrical cells” (GCs, the elementary volume of the grid). Each GC corresponds to a cluster of heterogeneous cells found in various states. Specific rules regulate the transition between these states, as well as cell movement throughout the tumor volume; the aim is a realistic, conformal to the initial shape of the tumor, simulation of spatial evolution.</p> <p>Free Growth: The adopted cytokinetic model incorporates the biological mechanisms of cell cycling, quiescence, differentiation and loss. Stem, LIMP, DIFF, apoptotic and necrotic cells represent the</p>	<p>CELL AND TISSUE</p>	<p>Based on discrete time and space stochastic cellular automata</p>	<p>G. S.Stamatakos, E. Kolokotroni, D. Dionysiou, C. Veith, Yoo-Jin Kim, A. Franz, K. Marias, J. Sabczynski, R. Bohle, N.Graf, “In Silico Oncology: Exploiting Clinical Studies to Clinically Adapt and Validate Multiscale Oncosimulators,” accepted in Proc. EMBC 2013 (35th Annual International Conference of the IEEE Engineering in Medicine and Biology Society, Osaka, Japan)</p> <p>Eleni A. Kolokotroni, Dimitra D. Dionysiou, Nikolaos K. Uzunoglu, Georgios S. Stamatakos, Studying the growth kinetics of untreated clinical tumors by using an advanced discrete simulation model, Mathematical and Computer Modelling, volume 54, issues 9–10, pages 1989-2006, November 2011. DOI:10.1016/j.mcm.2011.05.007.</p> <p>K. Marias, D. Dionysiou, V. Sakkalis, N. Graf, R.M. Bohle, P.V. Coveney, S. Wan, A. Folarin, P. Bóchler, M. Reyes, G. Clapworthy, E. Liu, J. Sabczynski, T. Bily, A. Roniotis, M. Tsiknakis, E. Kolokotroni, S. Giatili, C. Veith, E. Messe, H. Stenzhorn, Yoo-Jin Kim, S. Zasada, A.N. Haidar, C. May, S. Bauer, T. Wang, Y. Zhao, M. Karasek, R. Grewer, A. Franz, G. Stamatakos, Clinically driven design of multi-scale cancer models: the ContraCancrum project paradigm,</p>
----------------	-------------	---	--	------------------------	--	--

		<p>distinct cell categories of the model. More specifically, tumor sustenance is attributed to the presence of a cell population that exhibits stem cell like properties. Specifically, cancer stem cells have the ability to preserve their own population, as well as give birth to cells of limited mitotic potential (LIMP cells) that follow the path towards terminal differentiation (DIFF cells). A proliferating tumor cell (stem or LIMP) passes through the successive cell cycle phases. Phases within or out of the cell cycle (G1, S, G2, M, G0) constitute different states in which cells may be found. After the completion of mitosis a fraction of newborn cells will enter the dormant phase, whereas the rest will continue to cycle. Transition to quiescence (dormant, G0, phase) and “awakening” of dormant cells are regulated by local metabolic conditions. All cell categories may die through spontaneous apoptosis. However, for dormant and differentiated cells necrosis is the main cell loss mechanism caused by inadequate nutrients’ and oxygen supply.</p> <p>Treatment: When a tumor is chemotherapeutically treated, a fraction of cancerous proliferating cells are lethally hit by the drug. These cells enter a rudimentary cell cycle that leads to apoptotic death through a cell cycle phase depending each time on the specific chemotherapeutic agent. The effect of the drug is considered instantaneous at the</p>		<p>Interface Focus volume 1, number 3, pages 450–461, June 2011. DOI:10.1098/rsfs.2010.0037.</p>
--	--	---	--	--

			time of its administration.			
C+Te11.	ICCS	NTUA-ISOG-Glioblastoma Therapy: Temozolomide and Radiation	<p>The model simulates the spatiotemporal response of glioblastoma multiforme to combined modality treatment using radiation and chemotherapy with temozolomide agent. It is based on the consideration of a discrete time and space stochastic cellular automaton, representing the tumor region. More specifically, the tumor region can be considered as a grid of “geometrical cells” (GCs, the elementary volume of the grid). Each GC corresponds to a cluster of heterogeneous cells found in various states. Specific rules regulate the transition between these states, as well as cell movement throughout the tumor volume; the aim is a realistic, conformal to the initial shape of the tumor, simulation of spatial evolution.</p> <p>Free Growth: The adopted cytokinetic model incorporates the biological mechanisms of cell cycling, quiescence, differentiation and loss. Stem, LIMP, DIFF, apoptotic and necrotic cells represent the distinct cell categories of the model. More specifically, tumor sustenance is attributed to the presence of a cell population that exhibits stem cell like</p>	CELL AND TISSUE	Based on discrete time and space stochastic cellular automata	<p>G.S.Stamatakis, V.P.Antipas, and N.K. Uzunoglu , “A spatiotemporal, patient individualized simulation model of solid tumor response to chemotherapy in vivo: the paradigm of glioblastoma multiforme treated by temozolomide,” IEEE Transactions on Biomedical Engineering , 53(8) , 1467-1477 , 2006</p> <p>Eleni A. Kolokotroni, Dimitra D. Dionysiou, Nikolaos K. Uzunoglu, Georgios S. Stamatakis, Studying the growth kinetics of untreated clinical tumors by using an advanced discrete simulation model, Mathematical and Computer Modelling, volume 54, issues 9–10, pages 1989-2006, November 2011. DOI:10.1016/j.mcm.2011.05.007.</p> <p>K. Marias, D. Dionysiou, V. Sakkalis, N. Graf, R.M. Bohle, P.V. Coveney, S. Wan, A. Folarin, P. Bóchler, M. Reyes, G. Clapworthy, E. Liu, J. Sabczynski, T. Bily, A. Roniotis, M. Tsiknakis, E. Kolokotroni, S. Giatili, C. Veith, E. Messe, H. Stenzhorn, Yoo-Jin Kim, S. Zasada, A.N. Haidar, C. May, S. Bauer, T. Wang, Y. Zhao, M. Karasek, R. Grewer, A. Franz, G. Stamatakis, Clinically driven design</p>

		<p>properties. Specifically, cancer stem cells have the ability to preserve their own population, as well as give birth to cells of limited mitotic potential (LIMP cells) that follow the path towards terminal differentiation (DIFF cells). A proliferating tumor cell (stem or LIMP) passes through the successive cell cycle phases. Phases within or out of the cell cycle (G1, S, G2, M, G0) constitute different states in which cells may be found. After the completion of mitosis a fraction of newborn cells will enter the dormant phase, whereas the rest will continue to cycle. Transition to quiescence (dormant, G0, phase) and “awakening” of dormant cells are regulated by local metabolic conditions. All cell categories may die through spontaneous apoptosis. However, for dormant and differentiated cells necrosis is the main cell loss mechanism caused by inadequate nutrients’ and oxygen supply.</p> <p>Treatment: The model addresses the case of temozolomide chemotherapeutic agent. When a tumor is chemotherapeutically treated, a fraction of cancerous proliferating cells are lethally hit by the drug. These cells enter a rudimentary cell cycle that leads to apoptotic death through a cell cycle phase depending each time on the specific chemotherapeutic agent. The effect of the</p>		<p>of multi-scale cancer models: the ContraCancrum project paradigm, Interface Focus volume 1, number 3, pages 450–461, June 2011. DOI:10.1098/rsfs.2010.0037.</p>
--	--	---	--	--

			<p>drug is considered instantaneous at the time of its administration.</p> <p>In the case of radiation therapy, lethally damaged cells die through a radiation-induced mitotic necrotic mechanism after undergoing a few mitotic divisions. The probability of cells to be hit by irradiation depends primarily on the phase they reside.</p>			
C+Te12.	ICCS	Free Growth of homogeneous solid tumors simulation model	A four-dimensional discrete simulation model of solid homogeneous tumor free growth.	CELL AND TISSUE	Hybrid method (primarily discrete event based).	<p>E.C.Georgiadi, D.D.Dionysiou, N.Graf, G.Stamatakos, "Towards In Silico Oncology: Adapting a Four Dimensional Nephroblastoma Treatment Model to a Clinical Trial Case Based on Multi-Method Sensitivity Analysis.", <i>Comput Biol Med.</i> 2012 Nov;42(11):1064-78. doi: 10.1016/j.compbimed.2012.08.008. Epub 2012 Oct 10</p> <p>N. Graf, A. Hoppe , E. Georgiadi, R. Belleman, C. Desmedt, D. Dionysiou, M. Erdt , J. Jacques, E. Kolokotroni, A. Lunzer, M. Tsiknakis and G. Stamatakos, " "In Silico Oncology" for Clinical Decision Making in the Context of Nephroblastoma. [Die Bedeutung von ‚in silico Onkologie` zur klinischen Entscheidungsfindung am Beispiel des Nephroblastoms],” <i>Klin. Paediatr. (Klinische Paediatric)</i> 221, 141-149, 2009</p> <p>Eleni Ch. Georgiadi, Dimitra D.</p>

						<p>Tumour Response to Radiotherapy: Parametric Validation Considering Radiosensitivity, Genetic Profile and Fractionation,” Journal of Theoretical Biology , 230 , 1-20 , 2004</p> <p>G.S. Stamatakos, D.D. Dionysiou, E.I. Zacharaki, N.A. Mouravliansky, K.S.Nikita, N.K. Uzunoglu , “In silico radiation oncology: combining novel simulation algorithms with current visualization techniques,” Proceedings of the IEEE, Special Issue on Bioinformatics: Advances and Challenges , 90(11) , 1764-1777 , 2002</p>
C+Te13.	ICCS	Actinomycin Chemotherapy Simulation model	A generic four-dimensional simulation model of tumor response to actinomycin chemotherapy. The model is based on the consideration of a discrete time and space stochastic cellular automata.	CELL AND TISSUE	Hybrid method (primarily discrete event based).	<p>E.C.Georgiadi, D.D.Dionysiou, N.Graf, G.Stamatakos, "Towards In Silico Oncology: Adapting a Four Dimensional Nephroblastoma Treatment Model to a Clinical Trial Case Based on Multi-Method Sensitivity Analysis.", Comput Biol Med. 2012 Nov;42(11):1064-78. doi: 10.1016/j.compbiomed.2012.08.008. Epub 2012 Oct 10</p> <p>G.S. Stamatakos, E.C. Georgiadi, N. Graf, E.A. Kolokotroni, D.D. Dionysiou, Exploiting Clinical Trial Data Drastically Narrows the Window of Possible Solutions to the Problem of Clinical Adaptation of a Multiscale Cancer Model, Plos One, 6 (2011).</p>

					<p>N. Graf, A. Hoppe , E. Georgiadi, R. Belleman, C. Desmedt, D. Dionysiou, M. Erdt , J. Jacques, E. Kolokotroni, A. Lunzer, M. Tsiknakis and G. Stamatakos, “ "In Silico Oncology" for Clinical Decision Making in the Context of Nephroblastoma. [Die Bedeutung von ,in silico Onkologie` zur klinischen Entscheidungsfindung am Beispiel des Nephroblastoms],” Klin. Paediatr. (Klinische Paediatric) 221, 141-149, 2009</p> <p>Eleni Ch. Georgiadi, Dimitra D. Dionysiou, Norbert Graf and Georgios S. Stamatakos, “Modeling nephroblastoma treatment response cases with in-silico scenarios”, 10/2012; In proceeding of: 2012 5 th Int. Adv. Res. Workshop on In Silico Oncology and Cancer Investigation – The TUMOR Project Workshop (IARWISOCI), At Athens, Greece, Volume: ISBN: 978-618-80348-0-8 (open-access version) , www.5th-iarwisoci.iccs.ntua.gr, Edited by G. Stamatakos and D. Dionysiou, pages 35-28.</p> <p>E. Ch. Georgiadi, G. S. Stamatakos, N. M. Graf, E. A. Kolokotroni, D. D. Dionysiou, A. Hoppe, N. K. Uzunoglu, "Multilevel Cancer Modeling in the Clinical</p>
--	--	--	--	--	--

						<p>Environment: Simulating the Behavior of Wilms Tumor in the Context of the SIOP 2001/GPOH Clinical Trial and the ACGT Project," Proc. 8th IEEE International Conference on Bioinformatics and Bioengineering (BIBE 2008), Athens, Greece, 8-10 Oct. 2008. IEEE Catalog Number: CFP08266, ISBN: 978-1-4244-2845-8, Library of Congress: 2008907441, Paper No. BE-2.1.2, length: 8 pages (in electronic format). 2008</p> <p>D.D.Dionysiou, G.S. Stamatakos, N.K.Uzunoglu, K.S.Nikita, A. Marioli , "A Four Dimensional In Vivo Model of Tumour Response to Radiotherapy: Parametric Validation Considering Radiosensitivity, Genetic Profile and Fractionation," Journal of Theoretical Biology , 230 , 1-20 , 2004</p> <p>G.S. Stamatakos, D.D. Dionysiou, E.I. Zacharaki, N.A. Mouravliansky, K.S.Nikita, N.K. Uzunoglu , "In silico radiation oncology: combining novel simulation algorithms with current visualization techniques," Proceedings of the IEEE, Special Issue on Bioinformatics: Advances and Challenges , 90(11) , 1764-1777 , 2002</p>
C+Te14.	ICCS	Vincristine Chemotherapy	A generic four-dimensional simulation model of tumor response to vincristine chemotherapy. The model is based on the	CELL AND TISSUE	Hybrid method (primarily discrete event based).	E.C.Georgiadi, D.D.Dionysiou, N.Graf, G.Stamatakos, "Towards In Silico Oncology: Adapting a Four Dimensional

	Simulation model	consideration of a discrete time and space stochastic cellular automata.		<p>Nephroblastoma Treatment Model to a Clinical Trial Case Based on Multi-Method Sensitivity Analysis.", <i>Comput Biol Med.</i> 2012 Nov;42(11):1064-78. doi: 10.1016/j.compbiomed.2012.08.008. Epub 2012 Oct 10</p> <p>G.S. Stamatakos, E.C. Georgiadi, N. Graf, E.A. Kolokotroni, D.D. Dionysiou, Exploiting Clinical Trial Data Drastically Narrows the Window of Possible Solutions to the Problem of Clinical Adaptation of a Multiscale Cancer Model, <i>Plos One</i>, 6 (2011).</p> <p>N. Graf, A. Hoppe , E. Georgiadi, R. Belleman, C. Desmedt, D. Dionysiou, M. Erdt , J. Jacques, E. Kolokotroni, A. Lunzer, M. Tsiknakis and G. Stamatakos, " "In Silico Oncology" for Clinical Decision Making in the Context of Nephroblastoma. [Die Bedeutung von ,in silico Onkologie` zur klinischen Entscheidungsfindung am Beispiel des Nephroblastoms],” <i>Klin. Paediatr. (Klinische Paediatric)</i> 221, 141-149, 2009</p> <p>Eleni Ch. Georgiadi, Dimitra D. Dionysiou, Norbert Graf and Georgios S. Stamatakos, "Modeling nephroblastoma treatment response cases with in-silico</p>
--	------------------	--	--	--

						<p>scenarios”, 10/2012; In proceeding of: 2012 5 th Int. Adv. Res. Workshop on In Silico Oncology and Cancer Investigation – The TUMOR Project Workshop (IARWISOCI), At Athens, Greece, Volume: ISBN: 978-618-80348-0-8 (open-access version) , www.5th-iarwisoci.iccs.ntua.gr, Edited by G. Stamatakos and D. Dionysiou, pages 35-28.</p> <p>E. Ch. Georgiadi, G. S. Stamatakos, N. M. Graf, E. A. Kolokotroni, D. D. Dionysiou, A. Hoppe, N. K. Uzunoglu, "Multilevel Cancer Modeling in the Clinical Environment: Simulating the Behavior of Wilms Tumor in the Context of the SIOP 2001/GPOH Clinical Trial and the ACGT Project," Proc. 8th IEEE International Conference on Bioinformatics and Bioengineering (BIBE 2008), Athens, Greece, 8-10 Oct. 2008. IEEE Catalog Number: CFP08266, ISBN: 978-1-4244-2845-8, Library of Congress: 2008907441, Paper No. BE-2.1.2, length: 8 pages (in electronic format). 2008</p> <p>D.D.Dionysiou, G.S. Stamatakos, N.K.Uzunoglu, K.S.Nikita, A. Marioli, “A Four Dimensional In Vivo Model of Tumour Response to Radiotherapy: Parametric Validation Considering Radiosensitivity, Genetic Profile and Fractionation,” Journal of Theoretical Biology , 230 , 1-20 , 2004</p>
--	--	--	--	--	--	--

C+Te15.	ICCS	Actinomycin-Vincristine Combined Chemotherapy Simulation model	A generic four-dimensional simulation model of tumor response to combined therapy of vincristine and actinomycin. The model is based on the consideration of a discrete time and space stochastic cellular automata	CELL AND TISSUE	Hybrid method (primarily discrete event based).	<p>E.C.Georgiadi, D.D.Dionysiou, N.Graf, G.Stamatakos, "Towards In Silico Oncology: Adapting a Four Dimensional Nephroblastoma Treatment Model to a Clinical Trial Case Based on Multi-Method Sensitivity Analysis.", Comput Biol Med. 2012 Nov;42(11):1064-78. doi: 10.1016/j.compbimed.2012.08.008. Epub 2012 Oct 10</p> <p>G.S. Stamatakos, E.C. Georgiadi, N. Graf, E.A. Kolokotroni, D.D. Dionysiou, Exploiting Clinical Trial Data Drastically Narrows the Window of Possible Solutions to the Problem of Clinical Adaptation of a Multiscale Cancer Model, Plos One, 6 (2011).</p> <p>N. Graf, A. Hoppe , E. Georgiadi, R. Belleman, C. Desmedt, D. Dionysiou, M. Erdt , J. Jacques, E. Kolokotroni, A. Lunzer, M. Tsiknakis and G. Stamatakos, " "In Silico Oncology" for Clinical Decision Making in the Context of Nephroblastoma. [Die Bedeutung von ,in silico Onkologie` zur klinischen Entscheidungsfindung am Beispiel des Nephroblastoms],” Klin. Paediatr. (Klinische Paediatric) 221, 141-149, 2009</p> <p>Eleni Ch. Georgiadi, Dimitra D. Dionysiou, Norbert Graf and Georgios S. Stamatakos, "Modeling nephroblastoma treatment response cases with in-silico</p>
---------	------	--	---	-----------------	---	---

						<p>scenarios”, 10/2012; In proceeding of: 2012 5 th Int. Adv. Res. Workshop on In Silico Oncology and Cancer Investigation – The TUMOR Project Workshop (IARWISOCI), At Athens, Greece, Volume: ISBN: 978-618-80348-0-8 (open-access version) , www.5th-iarwisoci.iccs.ntua.gr, Edited by G. Stamatakos and D. Dionysiou, pages 35-28.</p> <p>E. Ch. Georgiadi, G. S. Stamatakos, N. M. Graf, E. A. Kolokotroni, D. D. Dionysiou, A. Hoppe, N. K. Uzunoglu, "Multilevel Cancer Modeling in the Clinical Environment: Simulating the Behavior of Wilms Tumor in the Context of the SIOP 2001/GPOH Clinical Trial and the ACGT Project," Proc. 8th IEEE International Conference on Bioinformatics and Bioengineering (BIBE 2008), Athens, Greece, 8-10 Oct. 2008. IEEE Catalog Number: CFP08266, ISBN: 978-1-4244-2845-8, Library of Congress: 2008907441, Paper No. BE-2.1.2, length: 8 pages (in electronic format). 2008</p> <p>D.D.Dionysiou, G.S. Stamatakos, N.K.Uzunoglu, K.S.Nikita, A. Marioli, “A Four Dimensional In Vivo Model of Tumour Response to Radiotherapy: Parametric Validation Considering Radiosensitivity, Genetic Profile and Fractionation,” Journal of Theoretical Biology , 230 , 1-20 , 2004</p>
--	--	--	--	--	--	--

						G.S. Stamatakos, D.D. Dionysiou, E.I. Zacharaki, N.A. Mouravliansky, K.S.Nikita, N.K. Uzunoglu , “In silico radiation oncology: combining novel simulation algorithms with current visualization techniques,” Proceedings of the IEEE, Special Issue on Bioinformatics: Advances and Challenges , 90(11) , 1764-1777 , 2002
C+Te16.	UOXF	Angiogenesis	PDE model for tumour angiogenesis	CELL AND TISSUE		Byrne and Chaplain (1995). Bull Math Biol, 57: 461-486
C+Te17.	UOXF	Angiogenesis and vasculogenesis	ODE model that investigates how contribution from angiogenesis and vasculogenesis changes during tumour growth	CELL AND TISSUE		
C+Te18.	UOXF	Avascular tumour growth and chemotherapy	PDE model that investigates how interplay between vascular remodelling and tumour growth and resulting spatio-temporal dynamics influence tumour’s response to chemotherapy	CELL AND TISSUE		Stamper, Owen, Maini and Byrne (2009). Biol Direct 5: 27
C+Te19.	UOXF	Vascular tumour growth	PDE model of vascular tumour growth based on the theory of mixtures	CELL AND TISSUE		Hubbard and Byrne (2013). J theor Biol 316: 70-89
C+Te20.	ICCS	Untreated vascular tumour growth	This model describes the interplay between pathological angiogenesis and solid tumour growth.	CELL AND TISSUE	Ordinary Differential Equations	P. Hahnfeldt, D. Panigrahy, J. Folkman and L. Hlatky, “Tumour development under angiogenic signaling: A dynamical theory of tumour growth, treatment response and postvascular dormancy”, Cancer Res., vol. 59, pp. 4770-4775,

						<p>1999.</p> <p>J. Poleszczuk, M. Bodnar, U. Foryś, "New approach to modelling of antiangiogenic treatment on the basis of Hahnfeldt et al. model", Math Biosci Eng., vol. 8, no. 2, pp. 591-603, April. 2011</p> <p>Argyri, K.D.; Dionysiou, D.D.; Stamatakos, G.S., "Modeling the interplay between pathological angiogenesis and solid tumor growth: The anti-angiogenic treatment effect," Advanced Research Workshop on In Silico Oncology and Cancer Investigation - The TUMOR Project Workshop (IARWISOCI), 2012 5th International , vol., no., pp.1,4, 22-23 Oct. 2012</p>
C+Te21.	ICCS	Vascular tumour growth under bevacizumab monotherapy	This model describes the response of a solid tumour to bevacizumab monotherapy	CELL AND TISSUE	Ordinary Differential Equations	<p>J. Poleszczuk, M. Bodnar, U. Foryś, "New approach to modelling of antiangiogenic treatment on the basis of Hahnfeldt et al. model", Math Biosci Eng., vol. 8, no. 2, pp. 591-603, April. 2011</p> <p>Argyri, K.D.; Dionysiou, D.D.; Stamatakos, G.S., "Modeling the interplay between pathological angiogenesis and solid tumor growth: The anti-angiogenic treatment effect," Advanced Research Workshop on In Silico Oncology and Cancer Investigation - The TUMOR Project Workshop (IARWISOCI), 2012 5th International , vol., no., pp.1,4, 22-23 Oct. 2012</p>

C+Te22.	ICCS	Time-course of bevacizumab concentration in plasma	This model describes the time-course of bevacizumab concentration in plasma	CELL AND TISSUE	Ordinary Differential Equations	Bertrand J, Mentré F. Mathematical Expressions of the Pharmacokinetic and Pharmacodynamic Models implemented in the MONOLIX software (http://www.monolix.org). 2008
C+Te23.	ICCS	Bevacizumab concentration in plasma in a given time-point	Given a specific time-point, this model computes the concentration of bevacizumab in plasma	CELL AND TISSUE	Ordinary Differential Equations	Bertrand J, Mentré F. Mathematical Expressions of the Pharmacokinetic and Pharmacodynamic Models implemented in the MONOLIX software (http://www.monolix.org). 2008
C+Te24.	ICCS	Time-course of vinorelbine concentration in plasma	This model describes the time-course of vinorelbine concentration in plasma	CELL AND TISSUE	Ordinary Differential Equations	Bertrand J, Mentré F. Mathematical Expressions of the Pharmacokinetic and Pharmacodynamic Models implemented in the MONOLIX software (http://www.monolix.org). 2008
C+Te25.	ICCS	Vinorelbine concentration in plasma in a given time-point	Given a specific time-point, this model computes the concentration of vinorelbine in plasma	CELL AND TISSUE	Ordinary Differential Equations	Bertrand J, Mentré F. Mathematical Expressions of the Pharmacokinetic and Pharmacodynamic Models implemented in the MONOLIX software (http://www.monolix.org). 2008
C+Te26.	ICCS	Diffusion-Reaction Based	The purpose of the model is to demonstrate in real time the spatiotemporal predictions of the	CELL AND TISSUE	Exploitation of the Generic Diffusion Phenomenon, Partial	Stavroula G. Giatili, Georgios S. Stamatakos , “A detailed numerical treatment of the boundary conditions

		<p>Glioblastom a multiforme (GBM) Invasion and Response to Treatment Model with Boundary Conditions</p>	<p>continuous mathematics based Oncosimulator built around a multiscale model of the evolution of a highly diffusive solid tumor. The modelling approach is based on the numerical solution for a homogeneous approximation of the diffusive growth of gliomas and in particular glioblastoma multiforme (GBM). According to the diffusion based approach the tumor is considered a spatiotemporal distribution of continuous cell density which follows the general diffusion law. The crucial component is the numerical handling of the adiabatic Neumann boundary conditions since the physical processes is taking place in the vicinity of the anatomic boundaries imposed by the of the skull.</p>		<p>Differential Equations (PDEs), Finite Difference Time Domain Numerical Method (FDTD), Crank Nicolson Method, Non - Stationary Iterative Conjugate Gradient Method, Neumann Boundaries, A Novel Numerical Treatment of the Neumann Boundary Conditions.</p>	<p>imposed by the skull on a diffusion– reaction model of glioma tumor growth. Clinical validation aspects.” Applied Mathematics and Computation 05/2012; 218(17):8779-8799.</p> <p>(Georgios S. Stamatakos, Stavroula Giatili, “In Silico Oncology: a Novel and Explicit Numerical Treatment of the Neumann Boundary Conditions Imposed by the Skull on a Multiscale Diffusion- Reaction Model of Glioblastoma Growth. Clinical Validation Aspects.”Proc. VPH2012 Integrative Approaches to Computational Biomedicine, A VPH NoE Conference www.vph-noe.eu/vph2012, London, UK; 09/2012</p> <p>S.Giatili, G.Stamatakos, “The Continuous Mathematics Based Glioblastoma Oncosimulator: Application of an Explicit Three Dimensional Numerical Treatment of the Skull-Glioblastoma Neumann Boundary Condition on Real Anatomical Data.” Proc. 2012 5th Int. Adv. Res. Workshop on In Silico Oncology and Cancer Investigation – The TUMOR Project Workshop, Athens, Greece; http://www.5th-iarwisoci.iccs.ntua.gr</p>
C+Te27.	UNITO	Phenomenological universality	Series expansion Un of the solution of the growth equation: exact solutions of UO	CELL AND TISSUE	Analytical	P. Castorina, P.P. Delsanto, C. Guiot, "Classification scheme for phenomenological universalities in

		in cancer growth	,U1 and U2			<p>growth problems in physics and other sciences.", Phys Rev Lett 96,188701 (2006).</p> <p>Delsanto PP, Gliozzi A, Iordache DA, Guiot C. Universal features in the laws of growth. J of Design & Nature and Ecodynamics, 2010, 5 (4): 1-12.</p> <p>Guiot C., Delsanto PP., Gliozzi A. Computer simulation and modelling in oncology: methods and applications. In: Modelling in Medicine and Biology VIII, Ed. C.A. Brebbia, Witpress, Southampton, 2009, Pages. 267-275. WIT Transactions on Biomedicine and Health, 13.</p>
C+Te28.	UNITO	Cancer growth & radiotherapy	Comparison between the predictions of U1 and U2 in different clinical schedules	CELL AND TISSUE	Analytical, numeric	P. Castorina, T.S. Deisboeck, P. Gabriele, C Guiot, "Growth laws in cancer: implications for radiotherapy", Radiation Res ,168:349-356,2007.
C+Te29.	UNITO	Multipassag e tumor growth	U1 application to tumor regrowth	CELL AND TISSUE		Gliozzi AS, Guiot C, Delsanto PP (2009), "A New Computational Tool for the Phenomenological Analysis of Multipassage Tumor Growth Curves. ", PLoS ONE 4(4): e5358. doi:10.1371/journal.pone.0005358
C+Te30.	UNITO	Cancer growth and chemotherapy	U1 & U2 predictions for chemotherapy dosage	CELL AND TISSUE		Castorina P., Carcò D., Guiot C., TS Deisboeck, "Tumor growth instability and its implications for chemotherapy", Cancer Res. 2009 Nov 1;69(21):8507-15, Epub 2009 Oct 27.

C+Te31.	FORTH	PIHNA-ECM-LQ	<p>The PIHNA-ECM-LQ mathematical model describes the vascular and invasive phases of tumor growth considering the complex interactions between cancer cells and the host-tissue microenvironment. Specifically, the tumor microenvironment consists of the vasculature that provides oxygen to cancer cells, tumor-induced angiogenic factors (e.g., VEGF) as well as the macromolecules of the extracellular matrix (ECM) and matrix degrading enzymes (e.g., Matrix Metalloproteinases), which degrade the ECM locally. Depending on oxygen supply, cancer cells can be proliferative, hypoxic or necrotic. Furthermore, cancer cell populations can invade the surrounding tissue driven by chemotaxis towards higher oxygen or haptotaxis towards higher ECM concentrations. The model can also accommodate the effect of radiotherapy on cancer population, which is based on the Linear Quadratic Model (LQ) approximation.</p>	CELL AND TISSUE	Deterministic approach consisting of a system of coupled reaction-diffusion equations	<p>K. R. Swanson, et al., "Quantifying the role of angiogenesis in malignant progression of gliomas: In Silico modeling integrates imaging and histology," <i>Cancer Res</i>, vol. 71, pp. 7366-7375, 2011</p> <p>P. Hinow, et al., "A spatial model of tumor-host interaction: application of chemotherapy," <i>Math Biosci Eng</i>, vol. 6, no. 3, pp. 521-46, 2009</p> <p>A. Roniotis, et al., "Solving the PIHNA model while accounting for radiotherapy," 5th Int. Adv. Research Workshop on In Silico Oncology and Cancer Investigation (IARWISOCI 2012), Oct 22-23, Athens, Greece, 2012</p>
C+Te32.	FORTH	Cell-level tumor invasion	<p>This mathematical model describes tumor growth invasion at cell-level linking genotypes with phenotypes and their interactions with the extracellular space. Specifically, cells are discrete entities that follow specific rules in response to their</p>	CELL AND TISSUE	Cellular automata linked with a system of partial differential equations of reaction-diffusion type.	<p>A.R.A. Anderson, "A hybrid mathematical model of solid tumour invasion: the importance of cell adhesion," <i>Math. Med. Biol</i>, 2005.</p> <p>G. Tzedakis, et al., "Hybrid Model for</p>

			microenvironment and in accordance to their genotype-phenotype characteristics while the components of the extracellular space are treated as continuous variables.			Tumor Spheroids with Intratumoral Oxygen Supply Heterogeneity," 5th Int. Adv. Research Workshop on In Silico Oncology and Cancer Investigation (IARWISOCI 2012), Oct 22-23, Athens, Greece, 2012
C+Te33.	UBERN	Brain Biomechanics	Calculates strain/stresses in the brain tissues	CELL AND TISSUE	Finite Element Analysis	PMID: 21740923

Cancer models that do not exist

In the following table all cancer models are listed that need to be developed according to the recommendation of the technical partners. The colour in the first row indicates the clinical relevance of the model. Three different categories are defined as in section 3.1.1:

1. Implement in first phase as test case (highly relevant)
2. Implement later in the project (relevant)
3. Implement only if time permits (less relevant)

Category 1 is indicated in green, 2 in yellow and 3 not highlighted.

Model information			
MODEL NUMBER	Reference partner	Model title	Brief model description
ATOMIC SCALE (MAINLY) - CODE "A"			
Ad1.	UPENN	Bioinformatics analysis of somatic cancer mutations	This model seeks to classify cancer mutations as driver or passenger using machine learning
MOLECULAR SCALE (MAINLY) - CODE "M"			
Md1.	UPENN	Modelling signal transduction in cancer signalling pathways.	Signal transduction in the signalling pathways will be studied using a set of coupled ode/pde equations. The code will be primarily written MATLAB with the information about the network provided using the SMBL framework.
Md2.	UPENN	Modelling endocytosis	We use phenomenological model based numerical modelling to understand the process of endocytosis in membranes. For this purpose we will be using a custom code based on Dynamically triangulated Monte Carlo, written in Fortran and C++.
Md3.	ICCS	Molecular models formulated in General SBML	The General Case of an SBML model
Md4.	ICCS	Differentially Expressed Genes	A Statistical Model that identifies the differentially expressed genes between two phenotypes (e.g. patient groups)

Md5.	ICCS	Differentially Expressed Pathways	A Statistical Model that identifies the differentially expressed pathways between two phenotypes (e.g. patient groups)
Md6.	ICCS	Phenotype Prediction Based on Gene Expression	
Md7.	ICCS	Drug Sensitivity Prediction based on Gene Expression	
Md8.	ICCS	A molecular pathway based model of the cell cycle [for the case of Acute Lymphoblastic Leukemia (ALL)]	A kinetic Systems Biology oriented model that simulates the biochemical dynamics of the G1 phase of the cell cycle in precursor-B ALL cells.
CELL SCALE (MAINLY) - CODE "C"			
Cd1.	ICCS (code developer)	Radiation cell killing	The models aims at estimating the cell killing by irradiation based on the Linear Quadratic or LQ Model
Cd2.	ICCS	Epirubicin pharmacodynamics	The model simulates epirubicin pharmacodynamics assuming an exponential law
BODY SYSTEM SCALE (MAINLY) - CODE "S"			
Sd1.	ICCS	Epirubicin pharmacokinetics	The model simulates epirubicin pharmacokinetics assuming a three compartment open model with elimination from the central compartment
Sd2.	ICCS	Prednisolone PK parameters regression model	A regression model that describes the relationship between un-bound Prednisolone PK parameters and patient covariates.
Sd3.	ICCS	Oral Prednisone PK model	A model that simulates the Pharmacokinetics of orally administrated Prednisone